MODELING OF VOLATILE ORGANIC COMPOUNDS EMISSIONS AND SINKS FROM BUILDING MATERIALS

Hongyu Huang

A Thesis

in

The Department

of

Building, Civil and Environmental Engineering

Presented in Partial Fulfillment of the Requirements
for the Degree of Doctor of Philosophy (Building Studies) at
Concordia University
Montreal, Quebec, Canada

February 2003

ABSTRACT

Modeling of Volatile Organic Compounds Emissions and Sinks from Building Materials

Hongyu Huang, Ph.D.
Concordia University, 2003

Volatile Organic Compounds (VOC) emitted from building materials have been recognized as major problems affecting human comfort, health and productivity. Building materials not only are main VOC sources but also are main VOC sinks in buildings. Therefore, accurate modeling of building material VOC emissions and sinks is important for predicting contaminant concentrations, occupant exposures and design of mechanical ventilation systems.

This thesis describes three new modeling approaches to predict building material VOC emissions and sinks. First, a numerical and an analytical VOC emission model have been developed to predict VOC emission rates of a single-layer dry building material and VOC concentrations in a well-mixed room. Second, an integrated IAQ model has been developed to predict VOC emission rates of a multi-layer material, VOC sink rates of a material, VOC concentrations in a well mixed room with both VOC source and sink materials. Third, a zonal model has been integrated with air jet and material VOC emission/sink models to predict the transient VOC distribution in a ventilated room. In addition, a systematic parametric study has been carried out to study the impacts of model input parameters and their interactions on VOC emissions from building materials.

These three models have been validated with available experimental results and/or CFD simulation results. The comparisons with the experimental results and the predictions of the CFD models indicate that there are generally good agreements between the proposed model predictions, the experimental results and the CFD results.

Moreover, these three models have been applied to analyze building material VOC emission/sink behaviors and to examine ventilation system efficiency. Results show that the developed models can provide useful information for building owners or designers in selecting proper building materials, designing efficient ventilation systems and assessing indoor air quality.

ACKNOWLEDGMENTS

I can hardly express my greatest gratitude to my supervisor Dr. F. Haghighat. Without his continuous guidance, encouragements and supports during the course of this work, this thesis would not be finished.

My deepest appreciations go to Mr. Soheil Rastan from Public Works and Government Services Canada for his endless advices and constant encouragements, not only in my work and study, but also in my life.

My sincere appreciations give to my supervising committee, Dr. W. Ghaly, Dr. R. Zmeureanu and Dr. C. Mulligan, for their knowledgeable advices and fruitful discussions regarding the whole thesis and to Dr. E. Wurtz from Université de La Rochelle and Mr. Y. Lin from McGill University for their valuable discussions and selfless assistances concerning the zonal model development.

I would like to extend my appreciations to Dr. Z. Jiang from Flomerics Inc. for doing the CFD simulations and to Dr. X. Yang from University of Miami for providing experimental results.

Special thanks go to Dr. Ian Beausoleil-Morrison from Natural Resources Canada and to Dr. J. Clarke from University of Strathclyde for their assistances in learning ESP-r program and to all my friends and colleagues at Concordia University for their sincere help and good companies throughout these years.

Last, but not least, to my whole family, especially to my parents and my husband, Yuan Wang, for their unconditional love, supports, understanding and encouragements.

TABLE OF CONTENTS

List of Figures ..... **xi**

List of Tables ..... **xvi**

Nomenclature ..... **xvii**

Chapter 1 Introduction **1**

1.1 Indoor air quality 1

1.2 Indoor air pollutants and building materials 2

1.2.1 Volatile Organic Compounds – VOC 3

1.2.2 Building materials as VOC sources 4

1.2.3 Building materials as VOC sinks 6

Chapter 2 Literature Review **7**

2.1 Introduction 7

2.2 Experimental method review 8

2.2.1 Experimental methods and facilities 8

2.2.2 Experimental cost and limitations 10

2.3 Material emission model review 11

2.3.1 Empirical models 12

2.3.2 Physical models 13

2.4 Material sink model review 21

2.4.1 Statistical models 21

2.4.2 Theoretical models 22

2.5 Integrated emission and sink model review 24

2.6 Parameter study review 25

2.7 Conclusions based on literature review 27

2.8 Objectives of the research 31

Chapter 3 Modeling of VOC Emissions from Single-layer Dry Building Materials 33

3.1 Introduction 33

3.2 Emission model development 34

3.2.1 Mass transfer in material 34

3.2.2 Material/air interface 35

3.2.3 Mass transfer in boundary layer 36

3.2.4 Mass balance in a room or chamber 36

3.2.5 Initial and boundary conditions 37

3.3 Solutions 38

3.3.1 Numerical solution 38

3.3.2 Analytical solution 45

3.4 Parameter estimation 50

3.4.1 Mass transfer coefficient in the air, h_m 50

3.4.2 Material/air partition coefficient, k 52

3.4.3 VOC diffusion coefficient of the material, D_m 52

3.4.4 Initial concentration, C_0 52

3.5 Model validation 53

3.5.1 Inter-model validation 53

3.5.2 Validation with experimental results and CFD model 56

3.6 Summary 61

Chapter 4 Building Material VOC Emissions— A Systematic Parametric Study ... 63

4.1 Introduction ... 63

4.2 Numerical model ... 64

4.3 Four-factor simulation design ... 65

4.3.1 Factorial design ... 65

4.3.2 Range of parameters ... 66

4.3.3 Four-factor simulation design ... 67

4.4 Statistical analysis ... 74

4.4.1 The analysis ... 74

4.4.2 Results and discussions ... 78

4.5 Summary ... 82

Chapter 5 An Integrated IAQ Model for Predicting VOC Emissions from Building Materials ... 88

5.1 Introduction ... 88

5.2 Integrated IAQ model development ... 89

5.2.1 Multi-Layer material emission model ... 89

5.2.2 Sink model ... 95

5.2.3 VOC concentration in a room ... 98

5.2.4 Numerical techniques ... 101

5.3 Model validation ... 101

5.4 Multi-layer material VOC emission – source effect ... 106

5.5 Substrate and sink effects ... 109

5.6 Summary ... 115

Chapter 6 An Integrated Zonal Model for Predicting Transient VOC Distribution in a Ventilated Room 117

6.1 Introduction 117

6.2 Zonal model 118

6.2.1 Air mass conservation equations 119

6.2.2 Energy conservation equations 124

6.3 Integrating jet model with zonal model 125

6.3.1 Air jet type 125

6.3.2 Angle of divergence 125

6.3.3 Velocity patterns along the jet axis 126

6.3.4 Velocity profiles of jet 128

6.3.5 Entrainment ratios 129

6.3.6 Jet cells 130

6.4 Integrating material emission/sink model with zonal model 132

6.4.1 Material emission/sink model 132

6.4.2 VOC mass conservation in the air 136

6.5 Solution techniques 136

6.6 Case study 137

6.6.1 Case 1: Natural ventilation 137

6.6.2 Case 2: Natural and forced ventilation 145

6.6.3 Case 3: Forced ventilation with linear air jet 149

6.6.4 Case 4: Forced ventilation with compact jet 157

6.7 Summary 168

Chapter 7 Conclusions and recommendations **171**

7.1 Conclusions 171

7.1.1 Single-layer material emission model 171

7.1.2 Parametric study 172

7.1.3 Integrated IAQ model 173

7.1.4 Integrated Zonal Model 174

7.2 Recommendations 175

References **176**

LIST OF FIGURES

CHAPTER 3

Figure 3-1 Physical configuration of VOC emissions from a single-layer dry building material 34

Figure 3-2 Grid-point cluster 38

Figure 3-3 Material internal and boundary grid points 40

Figure 3-4 Control volume near material bottom 42

Figure 3-5 Control volume near material top surface 43

Figure 3-6 Comparison of decane concentrations in the air 54

Figure 3-7 Comparison of decane emission rates 55

Figure 3-8 Comparison of decane normalized emitted masses 55

Figure 3-9 Comparison of TVOC concentrations (PB1) 57

Figure 3-10 Comparison of hexanal concentrations (PB1) 57

Figure 3-11 Comparison of α-pinene concentrations (PB1) 58

Figure 3-12 Comparison of TVOC concentrations (PB2) 58

Figure 3-13 Comparison of hexanal concentrations (PB2) 59

Figure 3-14 Comparison of α-pinene concentrations (PB2) 59

CHAPTER 4

Figure 4-1 Main effect of the diffusion coefficient (factor A) 79

Figure 4-2 Main effect of the thickness of the material (factor C) 80

Figure 4-3 Interaction effect between the diffusion coefficient and the thickness of the material (A×C) 81

CHAPTER 5

Figure 5-1 Physical configuration of VOC emissions from a multi-layer material..... 90

Figure 5-2 Physical configuration of VOC sinks by a building material 96

Figure 5-3 Physical configuration of the room 98

Figure 5-4 Schematic of the outer and inner chamber assembly (from: Low et al., 1998) 102

Figure 5-5 Comparison of decane emission rates (first 30 hour data) 105

Figure 5-6 Comparison of decane emission rates (full data set) 105

Figure 5-7 Comparison of benzene concentrations in the air 108

Figure 5-8 Comparison of benzene emission rates 109

Figure 5-9 Comparison of benzene normalized emitted masses 109

Figure 5-10 Comparison of decane concentrations in the air (substrate effect) 111

Figure 5-11 Comparison of decane emission rates (substrate effect) 112

Figure 5-12 Comparison of decane concentrations in the air (sink effect) 113

Figure 5-13 Comparison of decane emission rates (sink effect) 114

Figure 5-14 Comparison of normalized emitted masses of decane 114

Figure 5-15 Decane concentration distribution inside the multi-layer material (VF+Glue+Plywood) 115

CHAPTER 6

Figure 6-1 Physical configuration and partition of a room 119

Figure 6-2 Configuration of the horizontal cell interface 121

Figure 6-3 Configuration of the vertical cell interface 122

Figure 6-4 Jet expansion regions 126

Figure 6-5 Configuration of the linear jet (2D) cell 130
Figure 6-6 Configuration of the compact jet (3D) cell 131
Figure 6-7 Comparison of temperature distributions for case 1 138
Figure 6-8 Air flow pattern predicted by the Integrated Zonal Mode for case 1 (grids: 6×3×6) 139
Figure 6-9 Air flow pattern predicted by the POMA model for case 1(grids: 6×1×10) (Haghighat, et al., 2001) 139
Figure 6-10 Air flow pattern predicted by the CFD model for case 1 (grids: 41×51×41) (Jiang, 1998) 140
Figure 6-11 Benzene concentration distribution after 1 hour for case 1 141
Figure 6-12 Benzene concentration distribution after 12 hours for case 1 142
Figure 6-13 Benzene concentration distribution after 24 hours for case 1 142
Figure 6-14 Average benzene concentration in the air for case 1 143
Figure 6-15 Average benzene emission rate for case 1 144
Figure 6-16 Benzene normalized emitted mass for case 1 144
Figure 6-17 Nonane distribution for case 2 (outlet at bottom, 1hour) 147
Figure 6-18 Nonane distribution for case 2 (outlet at top, 1hour) 147
Figure 6-19 Temperature distribution in the middle section of the room for case 2 (outlet at top) 148
Figure 6-20 Comparison of nonane concentrations in the room for case 2 148
Figure 6-21 Comparison of nonane concentrations in the room for case 2 149
Figure 6-22 Geometry of the room with a linear jet 150

Figure 6-23 Air flow pattern predicted by the Integrated Zonal Model for case 3 (grids: 10×3×8)..... 151

Figure 6-24 Air flow pattern predicted by FLOVENT for case 3 (grids: 10×9×8) (Jiang, 2002)..... 151

Figure 6-25 Benzene concentration distribution after 12 hours for case 3 (Y=1.5m).... 153

Figure 6-26 Benzene concentration distribution after 12 hours for case 3 (Z=1.35m)... 153

Figure 6-27 Benzene concentration distribution after 24 hours for case 3 (Y=1.5m).... 154

Figure 6-28 Benzene concentration distribution after 24 hours for case 3 (Z=1.35 m).. 154

Figure 6-29 Average benzene concentration in the air for case 3..... 155

Figure 6-30 Comparison of average benzene emission rates for case 3..... 156

Figure 6-31 Comparison of benzene normalized emitted masses in case 3 157

Figure 6-32 Geometry of the room with a compact jet..... 158

Figure 6-33 Geometry of the diffuser 158

Figure 6-34 Air flow pattern predicted by the Integrated Zonal Model for case 4 (Y=1.5m)..... 160

Figure 6-35 Air flow pattern predicted by FLOVENT for case 4 (Y=1.5m) (Jiang, 2002) 160

Figure 6-36 Air flow pattern predicted by the Integrated Zonal Model for case 4 (X=0.75m)..... 161

Figure 6-37 Air flow pattern predicted by FLOVENT for case 4 (X=0.75m) (Jiang, 2002) 161

Figure 6-38 Air flow pattern predicted by the Integrated Zonal Model for case 4 (X=2.25m)..... 162

Figure 6-39 Air flow pattern predicted by FLOVENT for case 4 (X=2.25m) (Jiang, 2002) 162

Figure 6-40 Toluene concentration distribution after 12 hours for case 4 (Y=1.5m)..... 165

Figure 6-41 Toluene concentration distribution after 12 hours for case 4 (Z=1.18m) ... 165

Figure 6-42 Toluene concentration distribution after 24 hours for case 4 (Y=1.5m)..... 166

Figure 6-43 Toluene concentration distribution after 12 hours for case 4 (Z=1.18m) ... 166

Figure 6-44 Average toluene concentration in the air for case 4 167

Figure 6-45 Average toluene sink rates of walls for case 4 167

Figure 6-46 Average toluene emission rate of the floor for case 4 168

LIST OF TABLES

CHAPTER 1

Table 1-1 Building materials and their health effects. 4

CHAPTER 2

Table 2-1 Source-testing methods 8

CHAPTER 3

Table 3-1 Properties of decane in the carpet 53

Table 3-1 Physical properties of particleboard emissions 56

CHAPTER 4

Table 4-1 Levels of the four parameters 66

Table 4-2 Four-way matrices (ABCD) of the material VOC time $Y_{A_iB_jC_kD_l}$ 84

Table 4-3 Three-way matrices of the sum of material VOC times 85

Table 4-4 Two-way matrices of the sum of material VOC times 86

Table 4-5 Summary of analysis 87

CHAPTER 5

Table 5-1 Experiment and simulation parameters (Temp. =23 ^{0}C). 104

Table 5-2 Simulation parameters of benzene 106

Table 5-3 Simulation parameters of decane 110

CHAPTER 6

Table 6-1 Properties of benzene in the vinyl floor tile 141

Table 6-2 Properties of nonane in the carpet 145

Table 6-3 Properties of benzene in the plywood and vinyl floor tile 152

Table 6-4 Properties of toluene in the plywood and vinyl floor tile 163

NOMENCLATURE

English Letters

a	Neighbor coefficient.
a, b, c, d	Factor levels associated with factor A, B, C, and D.
A_0	Core area or duct area, m^2
A_e	Area of the source material, m^2
A_i	Interface area between cell i and Wall, m^2
A_i	Sum of material VOC time for factor A at level i, s
A_R	Cross-sectional area of confined space normal to jet, m^2
A_s	Area of the sink material, m^2
B	Thickness of the material, m
b_e	Thickness of the multi-layer material, (m).
b_i	Height from the material bottom to the i^{th} layer top surface, m
b_s	Thickness of the sink material, m
B_j	Sum of material VOC time for factor B at level j, s
C_0	VOC initial concentration in the material, $kg_{VOC}/kg_{material}$
C_a	VOC concentration in air, $\mu g/m^3$
C_{a0}	Initial VOC concentration in air, $\mu g/m^3$
C_{aes}	VOC concentration in the near emission material surface air, $\mu g/m^3$
C_{air}	VOC concentration in air, kg_{VOC}/kg_{air}
C_{as}	VOC concentration in the near material surface air, $\mu g/m^3$
C_{ass}	VOC concentration in the near sink material surface air, $\mu g/m^3$

C_d	Coefficient of power law, m/(sPa^n), usually taken as 0.83.
C_{gas}	VOC gas phase concentration in the material, kg_{VOC}/kg_{air}
C_g	VOC concentration in the gas phase, $\mu g/m^3$
C_{in}	VOC concentration in the supply air, $\mu g/m^3$
C_k	Sum of material VOC time for factor C at level k.
C_m	VOC concentration in the material, $\mu g/m^3$
$C_{me,i}$	VOC concentration in the i^{th} layer, $\mu g/m^3$
$C_{me,i+1}$	VOC concentration in the $i+1^{th}$ layer, $\mu g/m^3$
$C_{me,wet}$	VOC concentration in the wet material, $\mu g/m^3$
$C_{me0,i}$	VOC initial concentration in the i^{th} layer, $\mu g/m^3$
$C_{me0,wet}$	Initial VOC concentration in the wet material, $\mu g/m^3$
C_{ms}	VOC concentration at the material surface, $\mu g/m^3$
C_{ms}	VOC concentration in the sink material, $\mu g/m^3$
C_p	Specific heat of air, J/kg K
C_{s0}	Initial VOC concentration in the sink material, $\mu g/m^3$
C_{ad}	VOC adsorbed phase concentration in the material, $kg_{VOC}/kg_{material}$
D_0	Effective or equivalent diameter of stream at discharge for open-end duct or at contracted section, m
D_a	VOC diffusion coefficient in the air, m^2/s
D_e	VOC gas phase diffusion coefficient of the material, m^2/s
D_j	Sum of material VOC time for factor D at level j.
D_m	VOC diffusion coefficient of the material, m^2/s
$D_{me,dry}$	VOC diffusion coefficient of the dried wet material, m^2/s

$D_{me,i}$	VOC diffusion coefficient of the i^{th} layer, m^2/s
$D_{me,i+1}$	VOC diffusion coefficient of the $i+1^{th}$ layer, m^2/s
$D_{me,wet}$	VOC diffusion coefficient of the wet material, m^2/s
$D_{me0,wet}$	Initial VOC diffusion coefficient of the wet material, m^2/s
D_{ms}	VOC diffusion coefficient of the sink material, m^2/s
g	Gravitational acceleration, m^2/s
H	Height, m
h	Height from the bottom of cell i, m
H_0	Width of jet at outlet, m
h_e	Convective mass transfer coefficient over the emission material, m/s
h_m	Convective mass transfer coefficient, m/s
h_s	Convective mass transfer coefficient over the sink material, m/s
h_T	Convective heat transfer coefficient, w/m^2 K
k	Material/air partition coefficient
K	First order decay constant, h^{-1}
K	Centerline velocity constant depending on outlet type and discharge pattern
k_a	Adsorption coefficient, m/h
k_d	Desorption coefficient, 1/h
k_e	Emission material/air partition coefficient
k_s	Sink material/air partition coefficient
L	Material loading factor, m^2/m^3
l	Characteristic length of material, m

L_e	Source-material loading factor, m^2/m^3
L_s	Sink-material loading factor, m^2/m^3
M	VOC mass adsorbed, $\mu g/m^2$
M_a	Air molecular weight, g/mol
$M_{a,i}$	air mass in cell i, kg
$m_{a,ij}$	Air mass flow across cell i and cell j interface, kg/s
m_{sink}	Air mass sink in cell i, kg/s
m_{source}	Air mass source in cell i, kg/s
M_{VOC}	VOC molecular weight, g/mol
$m_{voc,\ sink}$	VOC mass sink in cell i, $\mu g/s$
$m_{voc,ij}$	VOC mass flow across cell i and cell j interface, $\mu g/s$
$m_{voc,source}$	VOC mass source in cell i, $\mu g/s$
N	Air exchange rate,s^{-1}
n	Flow exponent, usually taken as 0.5.
P	Pressure, atm
$P_{i,h}$	Pressure at the height of h in cell i, Pa
$P_{m,i}$	Pressure at the middle of cell i, Pa
P_{ref}	Reference pressure, Pa
ΔP	Pressure difference, Pa
ΔP_{ref}	Reference pressure difference, Pa
$\dot{q}_{a,ij}$	Air flow rate across cell i and cell j interface, kg/m^2s
$\dot{q}_{a,hor}$	Air flow rate across the horizontal cell interface, kg/m^2s

$\dot{q}_{a,0-Z_n}$	Air flow rate below neutral plane, kg/m.s
$\dot{q}_{a,Z_n-H}$	Air flow rate above neutral plane, kg/m.s
$\dot{q}_{a,ver}$	Air flow rate across vertical cell interface, kg/m.s
Q_0	Discharge from outlet, m^3/s
$Q_{T,ij}$	Heat flow rate across cell i and cell j interface, w
$Q_{T,sink}$	Heat energy sink in cell i, w
$Q_{T,source}$	Heat energy source in cell i, w
Q_x	Total volumetric flow rate at distance X from face of outlet, m^3/s
R	Gas constant of air, 287.055 J/kg.K
r	Radial distance of point under consideration from centerline of jet, m
R(t)	VOC emission rate at time t, $\mu g/m^2s$
R_0	VOC emission rate at time zero, $\mu g/m^2s$
$r_{0.5V}$	Radial distance in same cross-sectional plane from axis to point where velocity is one half centerline velocity, m
R_e	VOC emission rate, $\mu g/m^2s$
Re	Reynolds number
R_s	VOC sink rate, $\mu g/m^2s$
S	VOC source term, $\mu g/m^3s$
S_A	Total area of interface A, m^2
Sc	Schmidt number
Sh	Sherwood number
S_{jet}	Jet air flow passing area, m^2

SS	Sum of the squared deviations from the grand mean, usually shortened to sum of squares
SS_T	Total sum of the squared deviations from the grand mean, or the total sum of squares
t	Time, s
Δt	Compute time step, s
T	Absolute temperature, K
T_O	Sum of material VOC time for all the (a)(b)(c)(d) combinations, s
$\Delta T_{,i\text{-}wal}$	Temperature difference between cell i and wall, K
u	Mean air velocity over the material, m/s
V	Actual velocity at point being considered, m/s
V	Volume of the room, m^3
V_0	Average velocity at discharge from outlet, m/s
V_a	Air molar volume, m^3/mol
V_{VOC}	VOC molar volume, cm^3/mol
V_x	Centerline velocity at distance X from outlet, m/s
X	Distance from face of outlet, m
x, y, z	Coordinats
Δx	x-direction width of the control volume, m
δx	x-direction distance between two adjacent grid points
$Y_{A_iB_jC_kD_l}$	Material VOC time for factor A at level i, factor B at level j, factor C at level k, and factor D at level *l*, s
$\overline{Y}$	Marginal mean of material VOC time, s

$\overline{Y}_T$	Grand mean of the material VOC time for all the (a)(b)(c)(d) combinations, s
Δy, δy	Similar to Δx, δx
Z_n	Neutral plane, m
Δz, δz	Similar to Δx, δx

Greek symbols

ν	Kinematic viscosity of the air, m^2/s
ρ	Density of air, kg/m^3
ε	Porosity of the material, m^3/m^3
δ	Boundary layer thickness, m
$\Delta\rho$	Density difference, kg/m^3
ρ_{sol}	Density of material, kg/m^3
ω^2	Ratio of the sum of squared deviation of a factor to the total sum of squared deviation

Subscripts

A, B, C, D	Factor A, factor B, factor C and factor D, respectively
A_i	Factor A at level i
B_j	Factor B at level j
C_k	Factor C at level k
D_l	Factor D at level l

i	Cell i or i^{th} layer
j	Cell j or j^{th} layer
Left, right, bottom, top	Cell at left, right, bottom and top, respectively
P	Currently considered node
W, E, S, N, B, T	Grid node at west, east, south, north, bottom and top, respectively
w, e, s, n, b, t	Interface at west, east, south, north, bottom and top, respectively

Superscripts

0	Old value (at time t) of the variable

Special symbols

×	Interaction

CHAPTER 1 INTRODUCTION

1.1 INDOOR AIR QUALITY

Public interest and concern regarding indoor air quality has grown considerably over the last few years. In cold climates a majority of our time is spent indoors, and indoor air can be three to four times more polluted than outdoor air (ITS, 1996). As energy efficiency has become more important and more synthetic materials are used in buildings and furnishing our homes, the problems associated with indoor air pollution have increased.

One of the main concerns in buildings over the past three decades has been energy efficiency. This has been mainly achieved by increasing insulation levels, improved window technologies, making the building shell more airtight and using more efficient heating systems. As new buildings are more airtight and existing buildings are being 'tightened up' in an effort to reduce energy costs, the natural air leakage in buildings is no longer sufficient to dilute air pollutants. If efficient mechanical ventilation strategies are not used, the Tight Building Syndrome (TBS) would happen.

As modern buildings have been tightened up over the past years, there has been an increase in the amount of synthetic and composite materials used during the construction, renovation and refurnishing of houses. When used, many of these materials introduce new chemical compounds into the building, and when combined with a lack of efficient

ventilation, a multitude of different pollutants can reach concentrations where they become hazardous to the occupant health.

Waxes, paints, polishes, cleansers, air fresheners, fabric protectors, composite materials are all sources of various organic and inorganic chemicals. Health problems such as allergies, respiratory ailments and chemical reactions are all on the rise. In Canada current statistics indicate that 25% of the population has an allergy or chemical sensitivity, while 10% of the adults and 20% of the children have asthma (ITS, 1996).

The control of indoor air pollutants is extremely important because of the long-term detrimental effect they can have on human health. Even at low concentrations, when they produce no noticeable symptoms, many pollutants can cause harm to occupants. Studies so far have shown that long term exposure to even low levels of various chemical contaminants can increase an individual sensitivity to the substance (Berglund 1985). Study also showed that multiple exposure to lower concentration of carcinogens may be even more harmful than exposure to isolated peak concentrations (Holmberg, 1977) and potentially leads to long term health problems.

1.2 INDOOR AIR POLLUTANTS AND BUILDING MATERIALS

There are lots of pollutants in a building which could cause indoor air quality related health problems and sick building syndrome (SBS), such as gases (carbon dioxide, formaldehyde, ozone, radon, combustion gas spillage, VOC etc.), materials (carpets, caulking and sealants, composite wood products, paints etc.), particles (dust, lead, molds, micro-organisms etc), and some consumer products etc.

In all those pollutants, building materials play a major role in determining the indoor air quality due to their larger surface areas and permanent exposure to indoor air. Building materials can release a wide variety of pollutants, especially, the volatile organic compounds (VOC), which could make the quality of indoor air worse than that of outdoor air. Recent studies of VOC emissions in four newly built, unoccupied test houses also demonstrated that building materials are the main source of indoor air pollutants (Yu, et al. 1997, 1998).

1.2.1 Volatile Organic Compounds – VOC

VOC are a broad range of compounds having boiling points from 50 to 260 ^{0}C. These compounds have molecular weights ranging from 50 to 300; exist mainly in the gas phase in the temperature and humidity range found indoors.

Health effects caused by exposure to VOC are diverse. Some compounds are known or suspected carcinogens. Many are odorous. The most common symptoms include: headaches, drowsiness, eye irritation, rashes, respiratory complaints and sinus congestion. In most cases, the concentrations observed indoor are low, often orders of magnitude below occupational limits for exposure to particular compounds. Nonetheless, the large number of compounds present, the uncertainty associated with their interactions and prevalence of reported complaints from building occupants suggests that VOC are an important class of pollutants in the indoor environment.

1.2.2 Building materials as VOC sources

The main building materials and their pollutant sources and health effects are summarized in table 1-1:

Table 1-1 Building materials and their health effects.

Building material name	Main source	Health effect
Carpet	New carpet: over 250 gaseous compounds known to be given off by new carpets, many of them are VOC. Old carpet: host of biological and bio-chemical, carpet dust, sink effect.	Main health risks come from VOC off gassing. General symptoms include: headaches, eye irritation, nausea, drowsiness, skin rashes and respiratory and sinus congestion.
Composite wood materials	The glues and resins used to bind the fibers together can off –gas VOC.	The effects of off-gassing chemical include: headaches, dizziness, eye, nose and throat irritation, vomiting and breathing difficulties.
Paints	Release a variety of potentially harmful compounds into air, including VOC, ammonia and silicates. Solvent based paints are more toxic than non-solvent based paints.	General health problems include: headaches, dizziness, nausea, irritation of the eye, nose and throat and sinus and respiratory congestion.

Table 1-1 Building materials and their health effects (cont'd)

Caulking and sealants		
Acoustical sealant	Used to create an effective air/vapor barrier. It can release VOC into air for a considerable time.	General symptoms include: headaches, eye irritation, nausea, drowsiness, skin rashes and respiratory and sinus congestion.
Acrylic latex	Have a low odor and only release low levels of VOC for a short time.	Main health risks come from VOC off gassing.
Butyl rubber	Used to seal joints and gaps. It is solvent based and can off-gas relatively high levels of VOC.	Off-gas can cause headaches and nausea.
Silicone sealants	Water based silicone can release only small amounts of VOC for a short time. Acid based silicone does off-gas for a short time, usually less than one hour.	Off-gas can cause eye and respiratory irritation in some people.
Urethane foam	It does off-gas HCFC's.	There is no noticeable odor and HCFC's are relatively harmless to people.

Table 1-1 clearly shows that most of the building materials release VOC that have negative health effects to occupants. Usually, users and engineers increase the ventilation rate to dilute the pollution. However, this is not always the proper solution to the indoor air problem. This could cause high-energy consumption and expensive HVAC system investment. Therefore, controlling local source, manufacturing low VOC emission rate

products and selecting efficient ventilation equipments appear to be more promising strategies.

1.2.3 Building materials as VOC sinks

Building materials not only emit VOC but also affect the transport and removal of indoor VOC through sorption (Colombo et al., 1993; Van Der Wal et al., 1998). A building material can act as an adsorbing material when the concentration of a specific VOC compound in the air is higher than that within the material. Material sink effects reduce VOC concentration in a room initially; later, when VOC concentration in the room becomes low, they can re-emit VOC and act as the second source. The adsorbed VOC re-emissions from building materials can elevate room air VOC concentrations. Consequently, building materials can have long-term effects on indoor air quality. Examples of indoor sinks include flooring materials (carpet, vinyl, rugs), wall materials (gypsum board, wallpaper, fabric), ceiling materials (acoustic tiles, sub-floors), insulation materials (fiberglass, rigid foam), and furniture (particleboard, plywood).

Therefore, study of building material VOC emission and sink characteristics is required in predicting contaminant concentrations, occupant exposures and solving indoor air quality problems. Based on the study results, building materials can be ranked by their VOC emission rates and users can select the low VOC emission materials. These will encourage manufacturers to improve product quality and reduce VOC contents in building materials. On the other hand, engineers can set up appropriate ventilation system to efficiently remove VOC from the room.

CHAPTER 2 LITERATURE REVIEW

2.1 INTRODUCTION

Volatile Organic Compounds (VOC) constitute an important class of indoor air pollutants. Various VOC have been associated with certain symptoms of sick building syndrome, multiple chemical sensitivity and other health effects. Building materials, either as structural materials, furnishing or as insulation materials, have been recognized as major VOC sources indoors. Evidence from a variety of investigations and systematic studies suggests that building materials can also affect the transport and removal of indoor VOC through sink process. The long-term effects of building materials on indoor environments have created a demand for accurate characterization of building material VOC emissions and sinks, either through experimental testing or theoretical modeling.

This chapter first reviews the experimental methods and facilities used to study VOC emissions and sinks by building materials. The limitations of the experimental studies have promoted the development of material VOC emission and sink models. The pros and cons of building materials VOC emission and sink models are reviewed also. The emissions of VOC by building materials are dependent on several parameters, such as temperature, relative humidity, air velocity, material properties and VOC type. This chapter also reviews the parameter study. The main achievements as well as the limitations are highlighted and analyzed. Based on this literature review, the objectives of the current research are defined at the end of this chapter.

2.2 EXPERIMENTAL METHOD REVIEW

2.2.1 Experimental methods and facilities

Experimental methods for characterizing sources and sinks indoors have been continuously developing and improving since the early 1980s. In September of 1994 a "Symposium on Methods for Characterizing Indoor Sources and Sinks" was held in Washington, DC to review and discuss the approaches for characterizing emissions and sinks from indoor materials and products. Tichenor (1996) reviewed the types of methods and facilities used by indoor air quality investigators to determine the chemical emissions from indoor materials, as summarized in Table 2-1.

Table 2-1 Source-testing methods

Laboratory studies
• **Extracting and direct analysis:** *Objectives:* ➢ Provide information on material composition. *Procedures:* ➢ Dry material→solvent extraction→gas chromatography (GC) and mass spectrometry (MS) analysis→identify the compounds. ➢ Wet material→ evaporation to dryness or dilution→GC analysis. *Examples:* ➢ Evaluate the composition of carpet samples (Pliel and Whiton, 1990). ➢ Evaluate the composition of paints (Brezinski, 1989). • **Static headspace:** *Objectives:* ➢ Provide information on emission composition. *Procedures:* ➢ Place samples in airtight container→air inside the container analyzed by GC/MS. *Examples:* ➢ Evaluate the emission composition of paints (Zhang, 1996).

Table 2-1 Source-testing methods (cont'd)

Dynamic chamber studies
• **Small chambers** ($\leq 5m^3$)**:** *Objectives:* ➢ Provide emission composition and emission rate data for small size material samples under controlled environmental conditions. *Procedures:* ➢ Place specimen in small chamber→collect air sample from the chamber outlet→analyze air sample by GC. *Examples:* ➢ Evaluate VOC emission rates of indoor materials (Colombo et al., 1991, 1993). • **Large chambers** ($>5m^3$): *Objectives:* ➢ Provide emission composition and emission rate data for large size material samples under controlled environmental conditions. ➢ May be required for evaluating emissions during the application phase of wet materials. *Procedures:* ➢ Place specimen in large chamber→collect air sample from the chamber outlet→analyze air sample by GC. *Examples:* ➢ Measurement of VOC emissions from wood-based panels (Brown, 1999). ➢ Full-scale chamber for material emission study (Zhang et al., 1996, 2002).
Full-scale studies
• **Test house:** *Objectives:* ➢ Provide emission composition and emission rate data under "semi-controlled" environmental conditions. ➢ Validate chamber emission test results. ➢ Provide the opportunity to evaluate the interaction of source emissions with indoor sinks. *Examples:* ➢ Validation of VOC emission model (Sparks et al., 2000[a]). • **Field studies:** *Objectives:* ➢ Provide integrated emission profile of all source and re-emitting sinks under uncontrolled conditions. *Examples:* ➢ Finding VOC source through field study (Tichenor and Sparks, 1996).

As the research on sources advanced, attention was also placed on the material surface sinks. The methods used to evaluate material sink behavior parallel the source characterization methods described above (Tichenor, 1996). Dynamic flow-through chambers can be used to evaluate the sink rates for indoor surfaces. Samples of sink materials are placed in chambers and exposed to known concentrations of pollutants. As with source testing, concentrations versus time data are collected. These data are then analyzed, using appropriate sink models, to determine the mass adsorbed and the sink rates. Test house studies can be used to evaluate the validity of chamber derived sink rates.

2.2.2 Experimental cost and limitations

The experimental cost has discouraged nearly all but the largest product manufacturers from testing their products. The costs have ranged from $1,500 to $3,500 per test for individual product to more than $10,000 for complete workstations in environmental chambers (Bodalal, 1999).

In order to understand the material emission characteristics, experiments should cover all the period from the initial high VOC emission rates to the later low or zero emission rates. For wet materials, it is easy to achieve due to their fast decay emission characteristics. But for dry materials, the emission rate is usually very low and decays very slowly. It could last a few months or years for all VOC totally to be emitted from the material. Because of this, the measurements of entire emission life of dry materials become impractical.

To save money, most experiments for testing building materials are carried out in small-scale chambers. While in a building, both the geometry and the boundary conditions may be different from the test sample. Furthermore, the environment conditions in the building may not be the same as those in the test chamber. Hence, the measured data from an environmental chamber may not be valid in a building.

Even some full-scale studies are used to investigate VOC source and sink behaviors of building materials, unlike chamber studies, precise control of environmental conditions is difficult, especially the air exchange rate. In addition, the interaction of sources and sinks and the outdoor pollutant levels make the full-scale studies very complicated. Moreover, distinguishing the source emissions and sink re-emissions generally is not possible in the field study (Tichenor, 1996).

Therefore, the material emission and sink modeling becomes a more promising strategy for researchers. Appropriate model simulations not only can save lots of money, but also can overcome the limitations of the experiments. Recently, there has been a growing interest in the development of mathematical models to predict the quality of indoor air.

2.3 MATERIAL EMISSION MODEL REVIEW

Building material VOC emission models can be classified as empirical models and physical models. This classification is based on whether or not model parameters have distinct physical meanings.

2.3.1 Empirical models

Most of the empirical emission models were developed in the early 90's. In 1991, Tichenor et al. used the first order decay model to describe wood stain VOC emissions. First order decay model is often deficient in characterizing the tail of the emission curve for rapidly decaying sources (Tichenor et al., 1993). To overcome this deficiency, later researchers added more empirical parameters to the model, such as double exponential decay model (Colombo et al., 1990,1991 1992), two-phase model (Chang and Guo, 1992), the second order decay model (Tichenor, 1995), and the first order decay and diffusion model (Guo et al., 1996). Even though those empirical models distinguish them with their parameters, the core part of those models is:

$$R = R_0 e^{-kt} \tag{2-1}$$

Where:

R: VOC emission rate at time t, $\mu g/m^2 s$

R_0: VOC emission rate at time zero, $\mu g/m^2 s$

K: first order decay constant, h^{-1}

t: time, h

Most of the empirical models were applied to predict the wet materials emissions (the double exponential decay model for dry materials). Empirical models often do a reasonable job for describing the experimental data. They are often easier to handle than physical models as the parameters of empirical models are determined by fitting

experimental data to a predefined model. Because of this, the empirical models have the following inherent drawbacks:

- Each parameter of the empirical models does not have a distinct physical meaning.
- Empirical models cannot interpret the experimental data.
- Nonlinear regression curve fitting might lead to multiple solutions, since more than one parameter are needed to be determined for one set of experimental results (concentration vs. time).
- Model parameters are strongly dependent on each experimental condition, such as air velocity, air exchange rate and relative humidity. Therefore, empirical parameters may not be scaled up for using in actual buildings.

For those reasons, physical modeling approaches based on the mass transfer processes are often applied to study building material VOC emissions.

2.3.2 Physical models

Physical models are based on fundamentals of mass transfer processes (Haghighat and De Bellis, 1998): diffusion within the material as the result of concentration, pressure, or temperature gradients; and surface emissions between the material and the overlying air as a consequence of evaporation, convection and diffusion. Fick's second law is often used to describe the diffusion within the materials.

a) Emission models for wet materials

For wet materials such as paints or wood stains, VOC diffusion coefficients of the

materials are very difficult to determine, and studies showed that the surface emissions usually dominate the emission processes. Therefore, most of the emission models for wet materials are concentrated on VOC transport in the air by ignoring VOC diffusion in the materials and substrates.

Tichenor et al. (1993) did the pioneer work in developing physical models to predict wet material VOC emissions. In this model, the mass transfer mechanisms were controlled by vapor pressure and boundary layer effects, therefore, it was called the VB model. The following assumptions were made in the VB model:

1. For a given product, all freshly applied surfaces have the same VOC equilibrium vapor pressure, C_V (mg/m^3), which is characteristic of that product. In other word, C_V is independent of the amount of coating applied.
2. As the coated surface ages, the vapor pressures of the remaining VOC decrease gradually. If the fresh surface has a VOC vapor pressure C_V and if M_0 (mg/m^2) is the initial, as per unit area of VOC applied, the vapor pressure C_s during the aging period is assumed to be proportional to the remaining mass of VOC, M (mg/m^2).

$$C_s = C_v\left(M/M_0\right) \tag{2-2}$$

3. The average gas phase diffusivity, D_f, of solvent molecules can be represented by the diffusivity of the most abundant component in the solvent mixture.

Based on those assumptions, the emission rate of the wet material becomes:

$$R = -\frac{D_f}{\delta}(C_a - C_s) \qquad (2\text{-}3)$$

Where,

δ: Boundary layer thickness, m

C_a: VOC concentration in bulk air, $\mu g/m^3$

In the VB model, each parameter has clear physical meaning and is independent. The VB model has been widely used for simulating the early stage emissions of wet materials. However, the model assumes mass transfer is only by surface emissions (evaporation and diffusion) and ignores mass transfer by convection and internal diffusion. On the other hand, the mass transfer coefficient, D_f/δ, is a function of the source (via D_f) and the environment (via δ). It is very hard to directly determine the boundary layer thickness due to complex flow pattern in the real building environment. Therefore, later researchers proposed some methods to improve VB model, such as Haghighat and Zhang (1999), by applying boundary layer theory to estimate the gas phase mass transfer coefficient; Sparks et al. (1996) developed a correlation of Nusselt number and Reynolds number to calculate the mass transfer coefficient. Despite such progress, Sparks et al. (2000[b]) added an empirical diffusion model to the improved VB model in order to consider the substrate diffusion.

b) Emission models for dry materials

The physical emission models for dry materials can be classified as one-phase models and multi-phase models. This classification is based on the assumption about VOC phase existing in dry materials.

I. One-phase models

One-phase models treat the dry material as a single homogeneous medium. VOC existing in the material is in a material phase. The dry material is assumed to have a homogeneous diffusivity. VOC mass transfer within the material is through diffusion. One-phase models use Fick's second law to describe the diffusive mass transfer within the materials (Dunn, 1987; Little et al., 1994, 1996; Cox et al., 2000; Yang et al., 1998[a], 2001[d] and Huang and Haghighat, 2002). For one dimension VOC diffusion, it is

$$\frac{\partial C_m}{\partial t} = D_m \frac{\partial^2 C_m}{\partial y^2} \tag{2-4}$$

Where:

C_m: VOC concentration in the material, $\mu g/m^3$

D_m: VOC diffusion coefficient of the material, m^2/s

y: coordinate in which diffusion takes place, m

t, time, s

For example, the diffusion controlled models (Dunn, 1987; Little et al., 1994,1996 and Cox et al., 2000) only considered the internal diffusion and ignored the surface convection process. This simplification may cause models to overestimate VOC emissions at the early stage, when the surface concentration is relatively high. Another main drawback of this diffusion-controlled model is that it assumed VOC concentration in the bulk air was always instantaneously proportional with the VOC concentration at the material surface. This assumption could be valid only in a small chamber or only in

the overlaying mass boundary layer.

To consider the surface convection part, Lee et al. (2000) combined boundary layer theory with Fick's law and proposed a conjugate mass transfer model. However, the model assumed VOC concentration at the material bottom was constant and ignored the sorption factor. These assumptions are not appropriate for real building materials, since the concentration distribution inside the material is time dependent and the sorption factor cannot be ignored. Furthermore, the model developed for semi-infinite materials (Dunn, 1987) is not suitable for thin building materials.

II. Multi-phase models

Multi-phase models treat the dry material as solid and fluid overlapping porous media. VOC existing in the material are in a gas phase and a adsorbed phase. The multi-phase models consider the gas phase diffusion and ignore the adsorbed phase diffusion. The models also use Fick's second law to describe VOC gas phase diffusion within the materials (Tiffonnet, 2000; Murakami et al., 2000 and lee et al., 2002). The following equation is usually used to describe the one-dimensional problem:

$$\rho_{air} D_e \frac{\partial^2 C_{gas}}{\partial y^2} = \rho_{air} \varepsilon \frac{\partial C_{gas}}{\partial t} + \rho_{sol} \frac{\partial C_{ad}}{\partial t} \qquad (2\text{-}5)$$

Where:

C_{gas}: VOC gas phase concentration in the material, kg_{VOC}/kg_{air}

C_{ad}: VOC adsorbed phase concentration in the material, $kg_{VOC}/kg_{material}$

ρ_{air}: density of the air, kg/m^3

ρ_{sol}: density of the material, kg/m^3

D_e: VOC gas phase diffusion coefficient of the material, m^2/s

ε: porosity of the material, m^3/m^3

Substituting the relationship between VOC gas phase concentration and adsorbed phase concentration, $C_{ad} = f(C_{gas})$, into the above equation gives:

$$\rho_{air} D_e \frac{\partial^2 C_{gas}}{\partial y^2} = \left[\rho_{air} \varepsilon + \rho_{sol} \frac{\partial f}{\partial t} \right] \frac{\partial C_{gas}}{\partial t} \tag{2-6}$$

At the material/air interface, multi-phase models assume VOC gas phase concentration is continuous at the material/air interface.

$$C_{gas}(b,t) = C_{air} \tag{2-7}$$

Where,

C_{air}: VOC concentration in the air, kg_{VOC}/kg_{air}

b: thickness of the material, m

For initial VOC gas phase concentration, the mass balance gives:

$$\begin{aligned} & C_O m_{sol} = C_{gas} m_{air} + C_{ad} m_{sol} \\ & \Rightarrow C_O \rho_{sol} V_{sol} = C_{gas} \rho_{air} \varepsilon V_{sol} + f(C_{gas}) \rho_{sol} V_{sol} \\ & \Rightarrow C_O \rho_{sol} = C_{gas} \rho_{air} \varepsilon + f(C_{gas}) \rho_{sol} \end{aligned} \tag{2-8}$$

Where,

C_0: VOC initial concentration in the material, $kg_{VOC}/kg_{material}$

Compared with multi-phase models, one-phase models apply a simple simulation approach; the parameters of the one-phase models are easy to be obtained through experiments. The multi-phase models assume different VOC phases existing within the materials; thus, models need more parameters, such as the porosity of the material and the density of the material.

C) CFD models

Currently, most of the physical models did not consider air movement impact on material VOC emissions. To provide the detailed information of VOC distribution in a room and/or to overcome the drawbacks of most physical emission models, some researchers turn to CFD to study material VOC emissions. Typically, in a CFD model, one of the air flow models is integrated with a material emission model and CFD technique is applied to carry out the simulation.

For wet materials, the research concern is mainly on contaminant distribution in the air. For example, Haghighat et al. (1994) improved the VB model by coupling it with a k-ε turbulence model to predict the indoor air quality in a newly painted partitioned office. It was found that the non-uniform concentration distribution greatly influenced the decay rate of VOC emissions. Yang et al. (1998[b]) examined the VOC complete mixing assumption by using a zero-equation turbulence model. The model simulated the three dimensional air velocity profiles and VOC (from wood stain) concentration distribution

in a small chamber. Results showed that VOC distribution in the test chamber was not uniform in the early stage and the first order decay model, using the complete mixing assumption, would underestimate the total VOC emission rate in the initial time. In addition, Yang et al. (2001[b], 2001[c]) developed a more comprehensive CFD model that considered VOC transfer in the air and material/air interface, and diffusion in the material film and also in the subtract. This model can be used for detailed simulation of VOC emissions from wet coating materials.

For dry materials, Yang et al. (1998[a]) integrated a laminar air flow model with a one-phase model (diffusion controlled emission model) for short-term carpet VOC emission simulation, and proposed an analytical model for long-term carpet VOC emission prediction. The models ignored the surface sorption effect for the short-term prediction and assumed material surface concentration be zero in the long-term prediction. Those assumptions might lead models to overestimate VOC emissions in the short term and underestimate emission rates in the long term. Recently developed CFD models for dry materials considered the surface emission, sorption effect and the internal diffusion (Yang et al., 2001[a], 2001[d] and Murakami et al., 1998, 2000). Even though those CFD models did an excellent job in predicting some dry material VOC emissions in the short term, the critical problem of those models is that CFD simulation is too expensive and time consuming to be used as a routine procedure for the long term VOC emission prediction. In addition, CFD models cannot yet be applied to study the complex whole building systems.

2.4 MATERIAL SINK MODEL REVIEW

Existing sink models can be classified into two categories: statistical models and theoretical models. This classification is based on how the unknown model parameters are obtained (Zhang et al., 2000). For the statistical models, the unknown model parameters are obtained by curve fitting, while for the theoretical models by independent measurement.

2.4.1 Statistical models

The statistical models view sorption as a two way process in which adsorption and desorption processes occur simultaneously, and mass transfer at material/air interface is not always at equilibrium (Tichenor et al., 1991; Colombo et al., 1993; De Bortoli et al., 1996 and Jorgensen et al., 2000). The adsorption and desorption rates are assumed to be respectively proportional with the VOC concentration in the air and the VOC mass at the material surface. The first order reversible sink model (Tichenor et al., 1991) is probably the most widely used sorption model. The following equation is used to represent the dynamic adsorption and desorption process at the interface.

$$\frac{dM}{dt} = k_a C_a - k_d M \qquad (2\text{-}9)$$

Where:

M: adsorbed VOC mass, $\mu g/m^2$

C_a: VOC concentration in the bulk air, $\mu g/m^3$

k_a: adsorption coefficient, m/h

k_d: desorption coefficient, 1/h

The sink strength of the material at equilibrium, $\frac{dM}{dt} = 0$, is defined as $k_e = \frac{k_a}{k_d}$. Since the adsorption and desorption process occur simultaneously, it is very difficult to measure the adsorption and desorption coefficients directly. They are usually determined by fitting the models to experimental data. One limitation of the first order reversible sink model is that it considered only the relatively fast surface sorption process while ignoring the relatively slow interior sorption. To overcome this problem, the two sink model (Colombo et al., 1993 and De Bortoli et al., 1996) assumed that material was composed of a fast sink and a slow sink, and the material interior sorption part was described by the slow sink through adding more empirical parameters. The sorption-diffusion model (Dunn et al., 1993) used the Fick's second law to represent the in-material diffusion. In addition, the empirical model (Van Der Wal et al., 1998) is also called the statistical model since its model parameters were also obtained through curve fitting. The common main drawback of the statistical sink models lies in their curve fitting, which could lead to multiple solutions, and results may not be scaled up for usung in actual buildings.

2.4.2 Theoretical models

The theoretical models assume the equilibrium condition always holds at the material/air interface and adsorption and desorption are instantaneous processes (Axley, 1991; Hansson and Stymne, 1999, 2000, 2002; Little et al., 1996; Zhao et al., 1999 and Yang et al., 2001[e]). The models use the partition coefficient to describe the relationship of VOC concentration in the gas phase and VOC in the material phase.

$$C_m\big|_{y=b} = kC_g \tag{2-10}$$

Where:

$C_m|_{y=b}$: VOC concentration at material surface, $\mu g/m^3$

k: material/air partition coefficient

C_g: VOC concentration in the gas phase, $\mu g/m^3$

Review of the existing theoretical sink models for dry materials reveals some of their limitations. For example, the boundary layer diffusion controlled sink models only consider surface sorption and boundary layer advection, but ignore internal diffusion. (Axley, 1991; Hansson and Stymne, 1999). The diffusion controlled sink models only consider the surface sorption and internal diffusion, but ignore the advection in the air (Little et al., 1996 and Zhao et al., 1999). However, Hansson and Stymne (2002) showed that air concentrations were influenced by the boundary layer diffusion variations and models for the sink-effect should include the surface sorption as well as the interior sorption. Recently Yang et al. (2001[e]) developed a VOC sorption model that considered the VOC transport in the air, surface sorption and internal diffusion. This model analytically solved the VOC sorption rate at the material /air interface and can be used for detailed simulation of sorption and IAQ in buildings.

Compared to the statistical sink models, the parameters used by the theoretical sink models (partition coefficients and diffusion coefficients) have more distinct physical meanings and can be obtained independently (Cox et al., 2000; Zhao et al., 1999 and Bodalal, 1999)

2.5 INTEGRATED EMISSION AND SINK MODEL REVIEW

Indoor materials not only can emit a variety of volatile organic compounds, but also can sink pollutants. Thus, modeling source and sink effects simultaneously is more accurate for fully describing the occupant exposure than modeling them separately.

To take source, sink and ventilation effects into account, Chang and Guo (1994) proposed an empirical integrated IAQ model to evaluate the effects of VOC emissions from wood stain on indoor air quality. In this integrated IAQ model, the first order decay model (Tichenor and Guo, 1991) was used as the source model, and the first order reversible model (Tichenor et al., 1991) was adopted as the sink model. Experiments were carried out in a full-scale residential house and significant sink effects were found for three alkane species. Results also demonstrated that integrated IAQ model can describe the experimental data better than only source model. The main drawback of this IAQ model is that the input parameters were obtained from one set of experimental data (concentration vs. time).

Bodalal (1999) proposed an integrated source and sink model to study dry material source and sink behaviors. This integrated model included a 3D diffusion controlled emission model and the first order reversible sink model (Tichenor et al., 1991). Murakami et al. (2000) studied both the source and sink effects using a CFD emission model and a surface sink model (Henry, Langmuir and Polanyi RD models). The common drawback of these two models lies in the sink model, in which the material

interior sorption was ignored. Material interior sorption may be significant for porous materials.

Recently, Yang and Chen (2001[a]) coupled a turbulence air flow model with source/sink model and used CFD techniques to simulate indoor VOC exposures. Even though CFD models can provide the detailed knowledge of air flow pattern and contaminant distribution within a room, it is too complicated to be used by designers and engineers as a daily design tool to predict VOC distribution in a room. Users make great efforts in problem definitions and computations. Actually, users may not usually be interested in excessively detailed results obtained from CFD models.

2.6 PARAMETER STUDY REVIEW

A comprehensive literature review by Haghighat and De Billis (1998) showed that a number of parameters such as air velocity, temperature, and relative humidity might have influence on material VOC emissions. Many experimental works have been carried out to study the impacts of these environmental factors on VOC emissions from building materials. For example, Zhang and Haghighat (1997) studied the impact of surface air movement on VOC emissions from paint using a small air velocity-controlled test chamber. It was found that for wet materials, the emission rate increased as the air velocity over the material increased. Low et al. (1998) studied air velocity impact on VOC emissions from a carpet-adhesive assembly. Results showed that increased air velocities generally resulted in increased emission rates during the short term and no perceptible corresponding reductions of the long-term emission rates. Small chamber experiments and field study in a house were conducted by Cox et al. (2002) to determine

the effect of ventilation rates on VOC emissions from diffusion-controlled materials. Both laboratory and field results showed that an increase in the ventilation rate caused an increase in the VOC emission rate.

However, not much experimental work has been carried out to determine the impacts of other parameters, such as VOC diffusion coefficient of material and material /air partition coefficient, on VOC emissions. This is because the experimental research is very expensive and time consuming. The experimental work may take a few weeks or months. Because of this, the measurements of physical parameters impacts on entire emission life of building materials become impractical. Furthermore, it is not possible, experimentally, to simultaneously study the impacts of these parameters and their interactions on VOC emissions, especially for a long term. This could be implemented through using an appropriate VOC emission model, and simulating VOC emission characteristics under different parameter combinations. For example, Yang et al. (2001[d]) studied material/air partition coefficient effect using a CFD model and found that the partition coefficient only affected short-term emissions, and it had virtually no impact to long-term emissions. Huang and Haghighat (2002) numerically studied air velocity effect on dry building material emissions. Results showed that the impact of air velocity on the VOC emission rate increased as the VOC diffusion coefficient of the material increased. Lee et al. (2000, 2002) studied VOC diffusion coefficient of material, material thickness and air velocity effects using analytical models. It was found that the effect of the air velocity depended on the solid material properties like diffusion coefficient, porosity and sorption property and large effect of air velocity was observed at smaller diffusion resistance of solid.

Recently, The material/air partition coefficient effect was studied by Cox et al. (2002) using a diffusion controlled model and found that as material/air partition coefficient increased, diffusion controlled materials became more sensitive to ventilation rate.

The above studies investigated the effect of each parameter individually and studies were carried out by changing the parameter of interest, while maintaining other parameters fixed. Thus, in the individual parametric study, the other parameter effects were not eliminated and the parameter interaction effects were not considered. This could lead to misleading the conclusions, and the results might be valid only for some specific conditions (Keppel, 1991).

2.7 CONCLUSIONS BASED ON LITERATURE REVIEW

Experimental methods and theoretical models for characterizing building material VOC emissions and sinks have been reviewed in this chapter. The main achievements and drawbacks existing in this field have been discussed. In summary:

a) Experimental methods

- Experimental methods for measuring material VOC composition, VOC emission and sink composition employ small static laboratory studies. For measuring material emission rates and sink effects, small and large dynamic chamber measurements are the typical methods being used.
- Experimental studies are very expensive and time consuming; they are impractical for measuring long-term VOC emissions and sinks from dry materials.

b) VOC emission models

- VOC emission models can be divided into empirical models and physical models based on whether or not model parameters have distinct physical meanings.
- Empirical emission models often can be used to describe the experimental data, but they cannot be used to interpret the experimental data. The empirical models are strongly dependent on the environmental conditions. The model parameters do not have distinct physical meanings and are obtained through curve fitting, which may not be valid for a real building environment.
- Physical emission models are based on the fundamentals of mass transfer processes. Each parameter of the physical emission models has a clear physical meaning and is an independent property of the material. Compared with the empirical emission models, the physical emission models have wide applications and should be used as the prediction tools for IAQ study.
- The physical emission models for dry materials can be further divided into one-phase models and multi-phase models according to different assumptions about VOC phase within the materials.
- One-phase models treat the dry material as a single homogeneous medium. The models use Fick's second law to describe the diffusive mass transfer inside the materials.
- Multi-phase models treat the dry material as solid and fluid overlapping porous media. The models consider VOC gas phase diffusion and ignore adsorbed phase diffusion. The multi-phase models distinguish different VOC phase transport

mechanisms within the materials; thus, models need more parameters, such as the porosity of the material, the density of the material.

- Most of the physical models do not consider air movement effect on material VOC emissions except of CFD models. However, CFD models are too complicated to be used by designers and engineers as daily design tools to predict VOC distribution in a room.

c) VOC sink models

- VOC sink models can be classified as statistical sink models and theoretical sink models according to the different approaches used in describing the surface sorption.
- Statistical sink models assume surface adsorption and desorption occur simultaneously, mass transfer at material/air interface is not always at equilibrium. The statistical models have limited applications, because the adsorption and desorption coefficients are determined from the same set of experimental data by curve fitting.
- Theoretical sink models assume surface adsorption and desorption occur instantaneously, mass transfer at material/air interface is always at equilibrium. The models use material/air partition coefficient to describe the relationship of VOC concentration in the gas phase and VOC concentration in the material phase. The parameters used in the theoretical sink models are the physical properties of the materials and can be obtained by independent measurements.

- Sink models not only should consider surface sorption and boundary layer advection but also should consider internal diffusion. The theoretical sink models should be used for material sink effect study.

d) Integrated source and sink models

- Integrated source and sink models can be used to fully describe the exposure of indoor pollutants, if the coupled source and sink models can appropriately describe the material emission and sink behaviors.

e) VOC emission characteristics and parameter study

- VOC emissions from wet materials are characterized by initial high emission rates and fast decay. Surface emission usually dominates the emission process of the wet materials. When the wet materials become relatively dry, VOC emissions transit from an evaporation dominated phase to an internal diffusion controlled phase.
- The initial low VOC emission rates and the slow VOC decay rates are the main characteristics of VOC emissions from dry materials. Internal diffusion usually dominates the emission process of dry materials.
- Material parameters such as VOC diffusion coefficient, material/air partition coefficient, material thickness, environmental parameters such as air velocity, temperature, relative humidity may play important roles in VOC emissions from building materials.
- The environmental parameters effects on building material VOC emissions usually are studied experimentally. The impacts of material properties on VOC emissions can

be analyzed through model simulations. Current parametric studies are individual parameter studies: the other parameter effects are not eliminated and the parameter interaction effects are not considered.

2.8 OBJECTIVES OF THE RESEARCH

Although there are a lot of achievements in the development of mathematical models for predicting VOC emissions and sinks from building materials, a numerical and an analytical model, which could overcome the existing drawbacks, are not yet available. Moreover, the parameter effects and their interaction effects on building material VOC emissions are inconclusive. In addition, a general integrated source and sink model, which can be used as a design tool for engineers to predict VOC distribution in a room, need to be developed.

To fill those gaps, this research presents a set of new modeling approaches to predict building material VOC emissions and sinks. Modeling approaches start with a single-zone room with single-layer dry building materials; extend to a single-zone room with multi-layer source materials and sink materials; end up with a multi-zone room with source materials, sink materials and ventilation system. Furthermore, a new systematic parametric study is also presented in this research.

To achieve those objectives, this research work includes:

- Theoretically analyze building material VOC emission and VOC sink mechanisms.

- Develop a numerical and an analytical model for estimating single-layer dry building material VOC emissions and for predicting VOC concentrations in a well-mixed room.
- Systematically analyze model input parameters and their interaction effects on VOC emissions from building materials.
- Develop an integrated IAQ model to predict multi-layer material VOC emissions, to study material substrate and sink effects and to estimate VOC concentrations in a well-mixed room with complex VOC source and sink materials.
- Develop an Integrated Zonal Model for predicting transient VOC distributions in a ventilated room.
- Validate the models with experimental results and/or with CFD model results.

CHAPTER 3 MODELING OF VOC EMISSIONS FROM SINGLE-LAYER DRY BUILDING MATERIALS

3.1 INTRODUCTION

Dry building materials are usually porous materials. VOC existing in dry building materials has several phases: gas phase, absorbed phase and adsorbed phase. The quantity of VOC diffusive flux incorporates several types of microscopic effects, such as molecular diffusion, Taylor diffusion, stream splitting, tortuosity effects and adsorption effects, each of which contributes to the macroscopic spreading of VOC. The description of a transport problem at the microscopic level is impractical and, perhaps, also impossible due to the complicated geometry of the dry material structure. Therefore, VOC transport in the dry material is always described on a macroscopic level (Allen et al., 1988 and Bear et al., 1990). One of the simple approaches is using the one-phase model (Yang et al., 2001[d]; Little et al., 1994, 1996 and Cox et al., 2000), which the dry material is assumed to be a single homogeneous medium. Another approach is using the multi-phase model (Tiffonnet, 2000; Murakami et al., 2001 and lee et al., 2002), which the dry material is treated as a solid and fluid overlapping porous media. VOC existing in materials are in a gas phase and a adsorbed phase. The multi-phase models only consider the VOC gas phase diffusion by ignoring the adsorbed phase diffusion. Compared with the multi-phase models, the one-phase models are simpler, and model parameters are easier to be obtained through experiments. Thus, the one-phase model approach is

adopted here for the development of a single-layer dry building material VOC emission model. The numerical and analytical solutions of this model are presented in this chapter.

3.2 EMISSION MODEL DEVELOPMENT

The physical system considered here is a single-layer dry building material (carpet, vinyl flooring, and particleboard, etc.), which has its one surface exposed to air. The material is treated as one single homogeneous medium. VOC emissions from the material are composed of three main processes as shown in Figure 3-1.

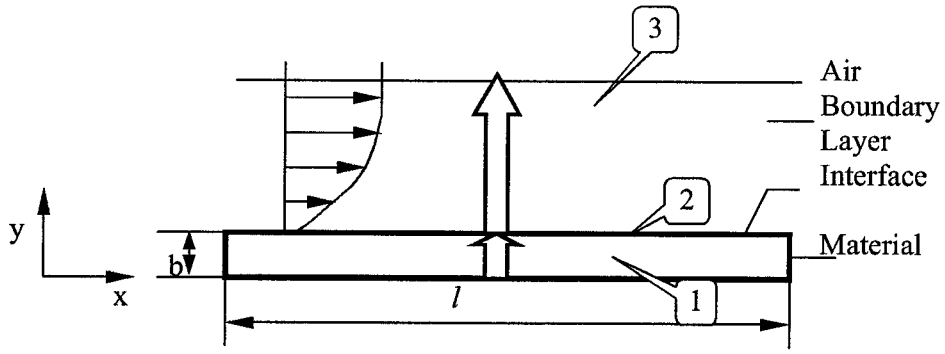

Figure 3-1 Physical configuration of VOC emissions from a single-layer dry building material. 1: Internal diffusion; 2: Material /air interface sorption; 3. External convection and diffusion.

3.2.1 Mass transfer in material

Concentration gradient is assumed to be the only driving force for VOC transport in the material, and there is no chemical reaction inside the material. For a dry material with homogeneous diffusivity, the transient VOC diffusion in the material can be described by the one-dimensional diffusion equation:

$$\frac{\partial C_m(y,t)}{\partial t} = D_m \frac{\partial^2 C_m(y,t)}{\partial y^2} \tag{3-1}$$

Where,

C_m: VOC concentration in the material, $\mu g/m^3$

D_m: VOC diffusion coefficient of the material, m^2/s

y: coordinate in which VOC diffusion in the material takes place, m

3.2.2 Material/air interface

At the material/air interface, VOC change from the material phase to the gas phase. The time scale for the surface adsorption and desorption to reach equilibrium is much smaller compared with the time scale for the VOC diffusion process within the material. Therefore, the interface adsorption and desorption can be assumed as instantaneous processes and to be always at equilibrium. Langmuir and BET are the most common isotherm models, which may be used to describe this process (Masel, 1996). At atmospheric pressure, for low VOC concentration and isothermal conditions, the equilibrium relationship between VOC concentration in the gas phase and VOC concentration in the material phase can be described by a linear isotherm (Axley, 1991 and Tiffonnet et al., 1998, 2000) :

$$C_m(b,t) = kC_{as} \tag{3-2}$$

Where,

$C_m(b,t)$: VOC concentration at the material surface, $\mu g/m^3$

C_{as}: VOC concentration in the near material surface air, $\mu g/m^3$

k: material/air partition coefficient

b: thickness of the material, m

3.2.3 Mass transfer in boundary layer

When the air passes over the material surface, a mass boundary layer exists between the surface material and the main flow. VOC mass transfer in this mass boundary layer is determined by diffusion and convection. The rate of VOC mass transfer in the boundary layer can be expressed as:

$$R(t) = h_m (C_{as} - C_a) \tag{3-3}$$

Where,

$R(t)$: VOC emission rate, μg /m^{2}s

h_m: convective mass transfer coefficient, m/s

C_a: VOC concentration in the room air, μg/m^3

3.2.4 Mass balance in a room or chamber

Assuming that VOC is completely mixed in the room air. The transient mass balance in the room or chamber can be expressed by:

$$\frac{\partial C_a}{\partial t} = NC_{in} - NC_a - LD_m \frac{\partial C_m(y,t)}{\partial y}\bigg|_{y=b} \tag{3-4}$$

Where,

C_{in}: VOC concentration in the supply air, μg/m^3

N: air exchange rate, s^{-1}

L: material loading factor, m^2/m^3

3.2.5 Initial and boundary conditions

Some initial conditions and boundary conditions are needed to close the above equations.

a) Initial conditions:

A homogeneous material with an initial VOC concentration of :

$$C_m(y,0) = C_0 \tag{3-5}$$

The initial VOC concentration in the air is VOC background concentration:

$$C_a(0) = C_{a0} \tag{3-6}$$

Where,

C_0: initial VOC concentration in the material, $\mu g/m^3$

C_{a0}: initial VOC concentration in the room air, $\mu g/m^3$

If the room inlet air is clean air, VOC concentration is zero:

$$C_{in} = 0 \tag{3-7}$$

b) Boundary conditions:

At the material bottom, it is assumed that there is no VOC passing through this surface.

$$-D_m \frac{\partial C_m(y,t)}{\partial y}\bigg|_{y=0} = 0 \tag{3-8}$$

At the material/air interface, VOC emission rate is equal to the mass transfer rate in the mass boundary layer.

$$-D_m \left.\frac{\partial C_m(y,t)}{\partial y}\right|_{y=b} = h_m(C_{as} - C_a) = h_m\left(\frac{C_m(b,t)}{k} - C_a\right) \tag{3-9}$$

3.3 SOLUTIONS

3.3.1 Numerical solution

a) The general discretization equation

To derive the general discretization equation for Eq. (3-1), the grid-point cluster shown in Figure 3-2 is employed. We focus attention on grid point P, which has the grid points S and N as its neighbors. (N denotes the north side or the positive y direction, while S stands for south side or the negative y direction.) The dashed line shows the face of the control volume. The letters n and s denote these faces. For the one-dimensional problem under consideration, A unit thickness is assumed in the x and z directions.

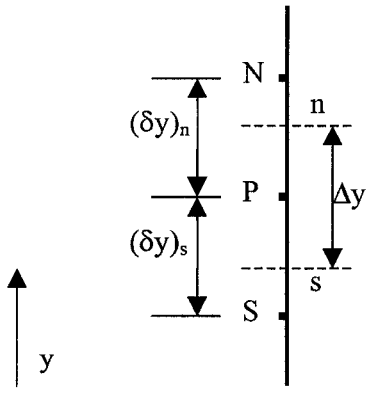

Figure 3-2 Grid-point cluster

Since time is a one-way coordinate, the solutions are obtained by marching in time from a given initial distribution of concentration. Thus, in a typical "time step" the task is this: Given the grid point values of C_m at time t, find the values of C_m at $t + \Delta t$. The "old" (given) values of C_m at the grid points are denoted as $C_{m,P}^0$, $C_{m,N}^0$, $C_{m,S}^0$, and "new" (unknown) values at the time $t + \Delta t$ by $C_{m,P}$, $C_{m,N}$, $C_{m,S}$.

The discretization equation is derived by integrating Eq. (3-1) over the control volume and over the time interval from t to t + Δt. Thus,

$$\int_s^n \int_t^{t+\Delta t} \frac{\partial C_m}{\partial t} dt dy = \int_t^{t+\Delta t} \int_s^n D_m \frac{\partial^2 C_m}{\partial y^2} dy dt \tag{3-10}$$

For the term $\frac{\partial C_m}{\partial t}$, it is assumed that the grid-point value of C_m prevails throughout the control volume. Then,

$$\int_s^n \int_t^{t+\Delta t} \frac{\partial C_m}{\partial t} dt dy = \Delta y \left(C_{m,P} - C_{m,P}^0 \right) \tag{3-11}$$

For the term $\frac{\partial^2 C_m}{\partial y^2}$, the fully implicit scheme is used (Patankar, 1980)

$$\int_t^{t+\Delta t} \int_s^n D_m \frac{\partial^2 C_m}{\partial y^2} dy dt = \left[\frac{D_m \left(C_{m,N} - C_{m,P} \right)}{(\delta y)_n} - \frac{D_m \left(C_{m,P} - C_{m,S} \right)}{(\delta y)_s} \right] \Delta t \tag{3-12}$$

Therefore,

$$\Delta y\left(C_{m,P}-C_{m,P}^{0}\right)=\left[\frac{D_m\left(C_{m,N}-C_{m,P}\right)}{(\delta y)_n}-\frac{D_m\left(C_{m,P}-C_{m,S}\right)}{(\delta y)_s}\right]\Delta t \tag{3-13}$$

Rearranging Eq. (3-13), one can have

$$a_P C_{m,P}=a_N C_{m,N}+a_S C_{m,S}+a_P^0 C_{m,P}^0 \tag{3-14}$$

Where

$$a_N=\frac{D_m}{(\delta y)_n} \tag{3-15a}$$

$$a_S=\frac{D_m}{(\delta y)_s} \tag{3-15b}$$

$$a_P^0=\frac{\Delta y}{\Delta t} \tag{3-15c}$$

$$a_P=a_N+a_S+a_P^0 \tag{3-15d}$$

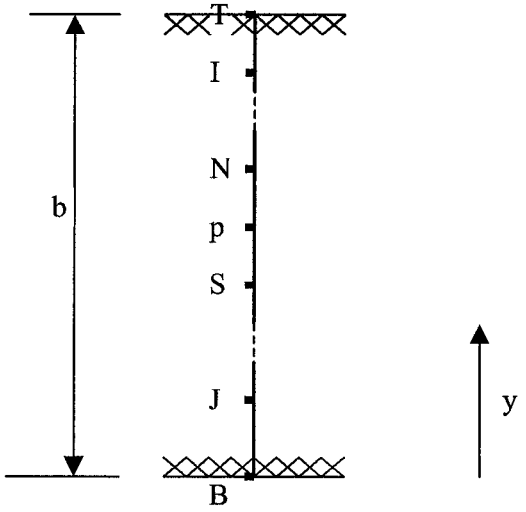

Figure 3-3 Material internal and boundary grid points

a is named as neighbor coefficient. The string of grid points for the whole material domain is shown in Figure 3-3. The grid T denotes the boundary near room air, and the

grid B denotes the boundary of material bottom. The concentration at these two grids are denoted as $C_{m,T}$ and $C_{m,B}$. The other grid points are called the internal points. The general discretization Equation (3-14) can be written for all the unknown concentrations at the internal grid points.

The discretization equation of room air VOC concentration is derived by integrating Eq.(3-4) over the time interval from t to t + Δt. The "old" value of concentration is denoted as C_a^0 and "new" value at the time t + Δt by C_a. Thus,

$$\int_t^{t+\Delta t} \frac{\partial C_a}{\partial t} dt = \int_t^{t+\Delta t} (NC_{in} - NC_a - LD_m \frac{\partial C_m}{\partial y}\Big|_{y=b}) dt \tag{3-16}$$

The room supply air is assumed to be clean air, C_{in}=0. Substituting Eq.(3-9) into Eq.(3-16), from the fully implicit procedure, one can have:

$$C_a - C_a^0 = \left[- NC_a + Lh_m \left(\frac{C_{m,T}}{k} - C_a \right) \right] \Delta t \tag{3-17}$$

Rearranging Eq. (3-17) gives VOC concentration in the room air:

$$a_a C_a = a_T C_{m,T} + a_a^0 C_a^0 \tag{3-18}$$

Where,

$$a_T = \frac{Lh_m}{k} \tag{3-19a}$$

$$a_a^0 = \frac{1}{\Delta t} \tag{3-19b}$$

$$a_a = N + Lh_m + a_a^0 \tag{3-19c}$$

b) Boundary conditions

There are two boundary conditions here: 1. There is no VOC flux passing through the bottom of the material, Eq.(3-8); 2. The material VOC emission rate is equal to the mass transfer rate in the boundary layer, Eq.(3-9).

I. First boundary condition

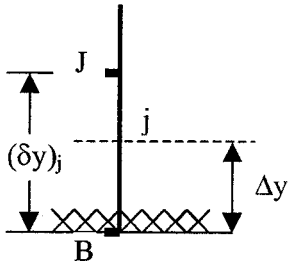

Figure 3-4 Control volume near material bottom

The control volume for the first boundary condition is shown in Figure 3-4. Integrating Equation (3-1) over the control volume gives:

$$\Delta y\left(C_{m,B} - C_{m,B}^0\right) = \left[\frac{D_m\left(C_{m,J} - C_{m,B}\right)}{(\delta y)_j} - 0\right]\Delta t \tag{3-20}$$

Rearranging Eq. (3-20) gives:

$$a_B C_{m,B} = a_J C_{m,J} + a_B^0 C_{m,B}^0 \tag{3-21}$$

Where,

$$a_J = \frac{D_m}{(\delta y)_j} \tag{3-22a}$$

$$a_B^0 = \frac{\Delta y}{\Delta t} \tag{3-22b}$$

$$a_B = a_J + a_B^0 \tag{3-22c}$$

II. Second boundary condition

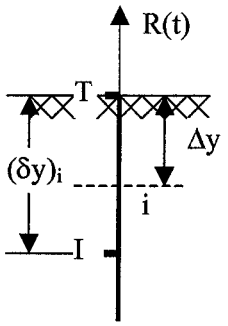

Figure 3-5 Control volume near material top surface

The control volume for the second boundary condition is shown in Figure 3-5. Integrating Eq. (3-1) over the control volume and noting the emission rate *R(t)* stands for $-D_m \left.\frac{\partial C_m}{\partial y}\right|_{y=b}$ gives:

$$\Delta y\left(C_{m,T} - C_{m,T}^0\right) = \left[-R(t) - \frac{D_m\left(C_{m,T} - C_{m,I}\right)}{(\delta y)_i}\right]\Delta t \tag{3-23}$$

Substituting Eq. (3-9) into Eq. (3-23) gives:

$$\Delta y\left(C_{m,T} - C_{m,T}^0\right) = \left[-h_m\left(\frac{C_{m,T}}{k} - C_a\right) - \frac{D_m\left(C_{m,T} - C_{m,I}\right)}{(\delta y)_i}\right]\Delta t \tag{3-24}$$

Rearranging Eq. (3-24), one can have:

$$a_T C_{m,T} = a_I C_{m,I} + a_a C_a + a_T^0 C_{m,T}^0 \tag{3-25}$$

Where,

$$a_I = \frac{D_m}{(\delta y)_i} \tag{3-26a}$$

$$a_a = h_m \tag{3-26b}$$

$$a_T^0 = \frac{\Delta y}{\Delta t} \tag{3-26c}$$

$$a_T = a_I + a_T^0 + \frac{h_m}{k} \tag{3-26d}$$

The VOC emission rate, *R(t)*, can be expressed as:

$$R(t) = h_m \left(\frac{C_{m,T}}{k} - C_a(t) \right) \tag{3-27}$$

The normalized emitted mass (M/M_0), which is the ratio of the emitted VOC mass (M) to the total VOC mass (M_0), can be described as

$$\frac{M}{M_0} = \frac{\sum_{j=1}^{m} R(t)\Delta t}{bC_0} \tag{3-28}$$

c) Solution of the linear algebraic equations

With the initial conditions, Eq. (3-5) and Eq. (3-6), the discretization equations, Eq.(3-14) (material internal grid points), Eq. (3-21), Eq. (3-25) (material boundary grid points), and Eq. (3-18) (room air), can be solved by the TriDiagnoal-Matrix Algorithm (TDMA) (Patankar, 1980).

3.3.2 Analytical solution

If the VOC concentration outside the mass boundary, C_a, is much smaller than VOC concentration in the near material surface air, C_{as}, Equation (3-9) can be rewritten as:

$$-D_m \left.\frac{\partial C_m(y,t)}{\partial y}\right|_{y=b} = h_m(C_{as} - C_a) \approx h_m\left(\frac{C_m(b,t)}{k}\right)$$

or

$$\left.\frac{\partial C_m(y,t)}{\partial y}\right|_{y=b} + \frac{h_m C_m(b,t)}{kD_m} = 0 \tag{3-29}$$

With the initial condition given by Equation (3-5) and boundary conditions given by Equations (3-8) and (3-9), Equation (3-1) can be solved by the method of separation of variables. Assume a solution of the form:

$$C_m(y,t) = Y(y)T(t) \tag{3-30}$$

Y is the function of y only and T is the function of t only.

$$\frac{\partial C_m}{\partial t} = Y(y)T'(t) \tag{3-31}$$

$$\frac{\partial^2 C_m}{\partial y^2} = Y''(y)T(t) \tag{3-32}$$

Substitution of these values in Equation (3-1) and setting it to the variable β gives:

$$\frac{T'(t)}{D_m T(t)} = \frac{Y''(y)}{Y(y)} = -\beta^2 \tag{3-33}$$

Thus:

$$Y''(y) + \beta^2 Y(y) = 0 \tag{3-34}$$

$$T'(t) + D_m \beta^2 T(t) = 0 \tag{3-35}$$

The boundary conditions for Equations (3-34) and (3-35) are:

$$\begin{cases} Y'(0) = 0 \\ Y'(b) + \dfrac{h_m}{kD_m} Y(b) = 0 \\ T(0) = C_0 \end{cases} \tag{3-36}$$

The general solution of Equation (3-34) yields:

$$Y(y) = C_1 \cos \beta y + C_2 \sin \beta y \tag{3-37}$$

$$\Rightarrow Y'(y) = -C_1 \beta \sin \beta y + C_2 \beta \cos \beta y \tag{3-38}$$

From Eq. (3-38) and the boundary condition, $Y'(0) = 0$, we have $C_2 = 0$.

From the boundary condition, $Y'(b) + \dfrac{h}{kD_m} Y(b) = 0$, we have:

$$-C_1 \beta \sin \beta b + \frac{h_m}{kD_m} C_1 \cos \beta b = 0 \tag{3-39}$$

$$\Rightarrow \frac{kD_m\beta}{h_m} = \cot \beta b \tag{3-40}$$

Now, β can be obtained by plotting each side of the equation against β, from the intersection of the two functions as many values of β can be obtained as are necessary. Therefore, $Y(y)$ has infinitely many solutions:

$$Y_n(y) = A_n \cos \beta_n y \quad n=1, 2, 3..... \tag{3-41}$$

The general solution of Equation (3-35) yields:

$$T(y) = C_3 e^{-\beta^2 D_m t} \tag{3-42}$$

For the same reason, $T(y)$ also has infinitely many solutions:

$$T_n(y) = C_n e^{-\beta_n^2 D_m t} \tag{3-43}$$

Therefore, the complete solution is:

$$C_m(y,t) = \sum_1^\infty Y_n(t) T_n(t) = \sum_1^\infty a_n e^{-\beta_n^2 D_m t} \cos \beta_n y$$
$$a_n = A_n C_n \tag{3-44}$$

From this and the initial condition, $T(0)=C_0$, gives:

$$C_0 = \sum_1^{\infty} a_n \cos \beta_n y$$

$$\Rightarrow a_n = \frac{1}{\int_0^b \cos^2 \beta_n y dy} \int_0^b C_0 \cos \beta_n y dy$$

$$\Rightarrow a_n = \frac{2C_0 \sin \beta_n b}{\beta_n b + \sin \beta_n b \cos \beta_n b} \tag{3-45}$$

So that the **concentration distribution inside the material** is:

$$C_m(y,t) = 2C_0 \sum_1^{\infty} \frac{\sin \beta_n b}{\beta_n b + \sin \beta_n b \cos \beta_n b} e^{-\beta_n^2 D_m t} \cos \beta_n y \tag{3-46}$$

Where, the eigenvalue β_n is determined by:

$$\frac{kD_m \beta_n}{h_m} = \cot \beta_n b$$

$$\Rightarrow \frac{h_m}{kD_m} = \beta_n \tan \beta_n b \tag{3-47}$$

Thus, the VOC **emission rate** is:

$$R(t) = -D_m \left(\frac{\partial C_m}{\partial y} \right)_{y=b}$$

$$\left(\frac{\partial C_m}{\partial y} \right)_{y=b} = -\sum_1^{\infty} e^{-\beta_n^2 D_m t} \frac{2C_0 \beta_n \sin^2 \beta_n b}{\beta_n b + \sin \beta_n b \cos \beta_n b}$$

$$R(t) = 2C_0 D_m \sum_1^{\infty} \frac{\beta_n \sin^2 \beta_n b}{\beta_n b + \sin \beta_n b \cos \beta_n b} e^{-\beta_n^2 D_m t} \tag{3-48}$$

The total emitted VOC mass from the material is obtained from the integration of Eq. (3-48) with the time:

$$M(t) = \int_0^t AR(t)dt = \int_0^t AD_m \sum_1^\infty e^{-\beta_n^2 D_m t} \frac{2C_0 \beta_n \sin^2 \beta_n b}{\beta_n b + \sin \beta_n b \cos \beta_n b} dt$$

$$\Rightarrow M(t) = 2C_0 A \sum_1^\infty \frac{\sin^2 \beta_n b}{\beta_n{}^2 b + \beta_n \sin \beta_n b \cos \beta_n b} (1 - e^{-\beta_n^2 D_m t}) \quad (3\text{-}49)$$

Therefore, the **normalized emitted VOC** can be determined from dividing Eq.(3-49) by initial VOC mass in the material:

$$\frac{M(t)}{M_0} = \frac{\int_0^t AR(t)dt}{AbC_0} = 2\sum_1^\infty \frac{\sin^2 \beta_n b}{\beta_n{}^2 b^2 + \beta_n b \sin \beta_n b \cos \beta_n b} (1 - e^{-\beta_n^2 D_m t}) \quad (3\text{-}50)$$

Where, A is the material surface area (m^2).

Substituting emission rate, Eq. (3-48), to Eq. (3-4) and with the initial condition, Eq. (3-7), yields:

$$C_a(t) = LD_m \sum_1^\infty \frac{1}{N - \beta^2 D_m} \frac{2C_0 \beta_n \sin^2 \beta_n b}{\beta_n b + \sin \beta_n b \cos \beta_n b} e^{-\beta^2 D_m t} + c_1 e^{-Nt} \quad (3\text{-}51)$$

Assuming the initial VOC concentration in the air is zero, $C_a(0) = 0$. Substituting it to Eq. (3-51) gives the **concentration in the room** or chamber:

$$C_a(t) = 2C_0 LD_m \sum_1^\infty \frac{\beta_n \sin^2 \beta_n b}{(N - \beta^2 D_m)(\beta_n b + \sin \beta_n b \cos \beta_n b)} \left(e^{-\beta^2 D_m t} - e^{-Nt}\right) \quad (3\text{-}52)$$

Equations (3-46), (3-48) and (3-52) indicate that VOC concentration in the material, C_m; VOC emission rate, R; and VOC concentration in the room air, C_a, are linearly proportional to the initial concentration, C_0. However, the normalized emitted VOC,

M/M_o, is not a function of the initial concentration and it is only a function of the physical properties of VOC and the material. Therefore, the normalized emitted VOC can provide a means to compare the emission rate of different VOC; compounds have a high-normalized emitted mass, it also has high emission characteristics.

3.4 PARAMETER ESTIMATION

There are four key parameters that need to be determined: the mass transfer coefficient in the air, h_m, the partition coefficient, k, the VOC diffusion coefficient of the material, D_m, and the VOC initial concentration in the material, C_0.

3.4.1 Mass transfer coefficient in the air, h_m

The average mass transfer coefficient may be measured directly or analyzed in terms of three dimensionless numbers: Sherwood number ($Sh = \frac{h_m l}{D_a}$), Reynolds number ($\mathrm{Re}_l = \frac{ul}{\nu}$) and Schmidt number ($Sc = \frac{\nu}{D_a}$). For a flow parallel to a flat plate, a flow condition that may be considered to be representative of airflow passing interior building surfaces (ref.), White (1988) provided the following corrections:

- For laminar flow, (Re_l<500,000):

$$Sh = 0.664 Sc^{\frac{1}{3}} \mathrm{Re}_l^{\frac{1}{2}} \tag{3-53}$$

- For turbulent flow, (Re_l>500,000):

$$Sh = 0.037 Sc^{\frac{1}{3}} \mathrm{Re}_l^{\frac{4}{5}}, \tag{3-54}$$

- Combined laminar /turbulent flow, ($Re_l<10^7$, Re_{tr}=500,000):

$$Sh = (0.037\,\mathrm{Re}_l^{\frac{4}{5}} - 8700)Sc^{\frac{1}{3}} \tag{3-55}$$

Where, ν is the kinematic viscosity of the air (m^2/s), u is the mean air velocity over the material (m/s), l is the characteristic length of material (m) and D_a is the VOC diffusion coefficient in the air (m^2/s).

The VOC diffusion coefficient (D_a) can be directly obtained from literature (Rafson, 1998) or can be estimated through other methods. Two main methods have been used to estimate VOC diffusion coefficient in the air (Layman, 1982): the Fuller, Schettler and Giddings (FSG) method and the Wilke and Lee (WL) method. The FSG method is the most accurate for non-polar gases at low to moderate temperatures. In this study, the FGS method was used to estimate the VOC diffusion coefficient in the air. This method is based on the following correlation:

$$D_a = \frac{10^{-7} T^{1.75} \sqrt{M_r}}{P\left(V_a^{1/3} + V_{VOC}^{1/3}\right)^2} \tag{3-56}$$

Where $M_r = \frac{(M_a + M_{VOC})}{M_a M_{VOC}}$, T is the absolute temperature (K), P is the pressure (atm), V_a is the air molar volume (m^3/mol), V_{VOC} is the VOC molar volume (cm^3/mol), M_a is the air molecular weight (g/mol) and M_{VOC} is the VOC molecular weight (g/mol).

3.4.2 Material/air partition coefficient, k

The material/air partition coefficient describes the relationship between the VOC concentration in the gas phase and the VOC concentration in the material phase. It is a material property and is obtained experimentally (Little et al., 1996; Bodalal et al., 2000 and Plett et al., 2001)

3.4.3 VOC diffusion coefficient of the material, D_m

The VOC diffusion coefficient of the material is usually a function of many factors, such as pore structure, material type, compound properties, temperature, and VOC concentration. The dependence of the diffusion coefficient on VOC concentration can be ignored considering that the VOC concentration in the dry materials is usually very low. Therefore, the dry materials can be considered as having homogeneous diffusivity. The diffusion coefficient is usually determined experimentally (Little et al., 1996; Bodalal et al., 2000; Plett et al., 2001 and Haghighat et al., 2002)

3.4.4 Initial concentration, C_0

The initial concentration in the material can be obtained through solvent extraction, high temperature thermal desorption or direct analysis (Tichenor, 1996). Recently a cryogenic grinding/fluidized bed desorption method was developed to measure the initial concentration (Cox et al., 2000). The VOC concentration in the material, the VOC emission rate and the VOC concentration in the room air, are a function of the initial concentration. Thus, a small error in the initial concentration estimation may cause a significant error in the prediction results.

3.5 MODEL VALIDATION

3.5.1 Inter-model validation

To demonstrate the accuracy of the numerical solution and to check the correctness of the exact analytical solution, the prediction results of the numerical model and the analytical model were compared with each other. In this comparison, a similar assumption made in the analytical model was made in the numerical model, that was VOC concentration outside the mass boundary, C_a, was much smaller than VOC concentration in the near material surface air, C_{as}, and it was assumed to be zero.

The numerical model and the analytical model were applied to a room with its floor furnished with a carpet. The room dimensions were 3.0×3.0×2.5 m^3 with a temperature of 23 °C, and an air exchange rate of 0.5h^{-1}. The air velocity in the room was assumed to be 0.1 m/s. Decane was chosen as the compound of interest. The Decane diffusion coefficient and the partition coefficient of the carpet were taken from literature (Bodalal, 1999). The initial decane concentration in the carpet was assumed to be 1.0×10^7 μg/m^3. All the input parameters are shown in Table 3-1.

Table 3-1 Properties of decane in the carpet

Parameter	D_a	C_0	D_m	k	b
(Unit)	(m^2/s)	(μg/m^3)	(m^2/s)	(—)	(m)
Value	5.94×10^{-6}	1.0×10^7	5.42×10^{-12}	14617	0.01

In the numerical model, around 100 nodes/cm was assigned for the emission material. The time step was 120 seconds. The prediction results of the decane concentration in the air, the decane emission rate from the carpet and the decane normalized emitted mass by the numerical model were compared with those of the analytical model, as shown in Figure 3-6, Figure 3-7 and Figure 3-8. The results clearly demonstrate that the numerical model can give as good results as the analytical model. Both models agree with each other very well, which also verifies the correctness of the analytical solution.

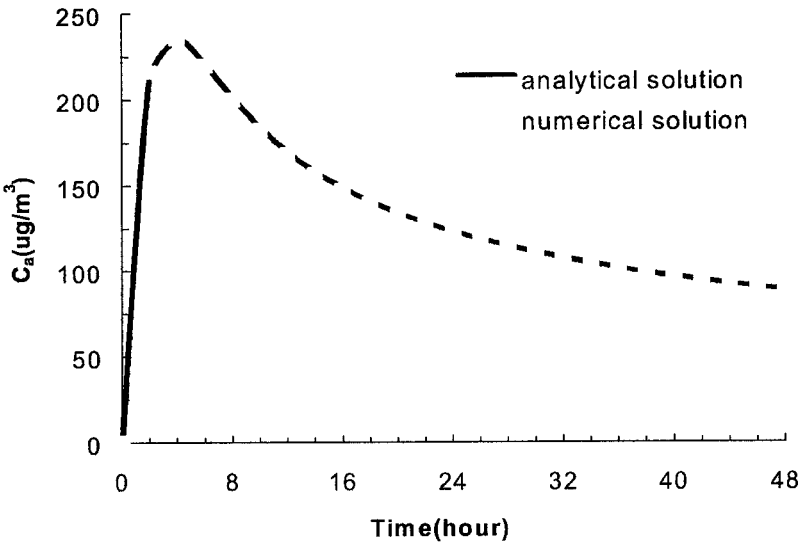

Figure 3-6 Comparison of decane concentrations in the air

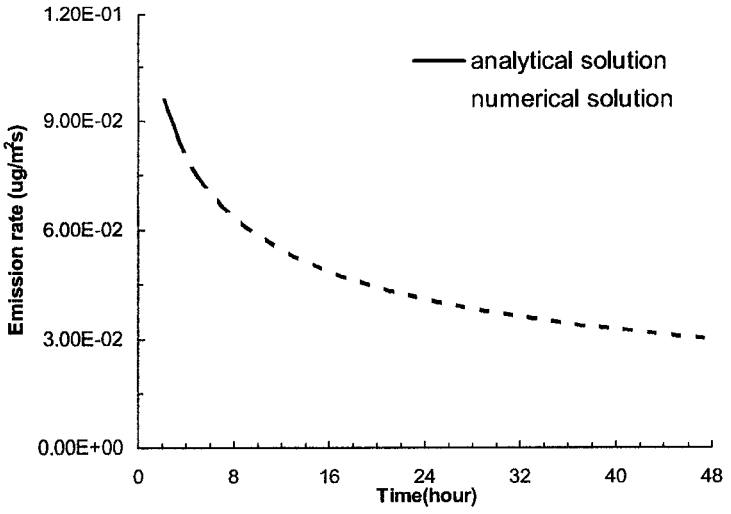

Figure 3-7 Comparison of decane emission rates

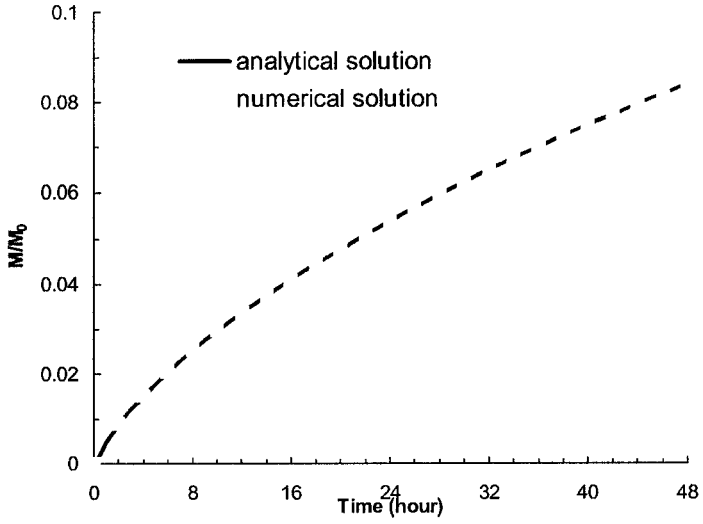

Figure 3-8 Comparison of decane normalized emitted masses

3.5.2 Validation with experimental results and CFD model

The model prediction was further compared with the experimental results of two particleboard tests and with the predictions made by a CFD model (Yang et al., 2001[d]).

The model predictions were compared with the experimental data. The experiments were carried out in a small-scale chamber of $0.5\times0.4\times0.25$ m^3 at a temperature of 23 ± 0.5 ^0C, relative humidity $50\pm0.5\%$, and an air exchange rate of $1.0\pm0.05h^{-1}$. Two different specimens of particleboard (PB1, PB2) were tested. The major compounds identified for the tested particleboards were the same: hexanal, α-pinene, camphene, and limonene. The particleboard properties: the material/air partition coefficient was estimated based on the vapor pressure of the compound (Bodalal, 1999); the diffusion coefficient of the material and the initial concentration were estimated by using the chamber emission data (concentration vs. time) to fit the CFD model (Yang et al., 2001[d]). The air flow inside the chamber was treated as a laminar flow over a flat plate. The physical properties of the particleboard are given in Table 3-2. The D_m and k of the TVOC were represented by Hexanal, which was the most abundant compound.

Table 3-2 Physical properties of particleboard emissions

Compound	TVOC	Hexanal	α-Pinene
Particleboard 1			
D_m (m^2/s)	7.65×10^{-11}	7.65×10^{-11}	1.2×10^{-10}
C_0 ($\mu g/m^3$)	5.28×10^{7}	1.15×10^{7}	3.45×10^{6}
k (—)	3289	3289	5602
Particleboard 2			
D_m (m^2/s)	7.65×10^{-11}	7.65×10^{-11}	1.2×10^{-10}
C_0 ($\mu g/m^3$)	9.86×10^{7}	2.96×10^{7}	7.89×10^{6}
k (—)	3289	3289	5602

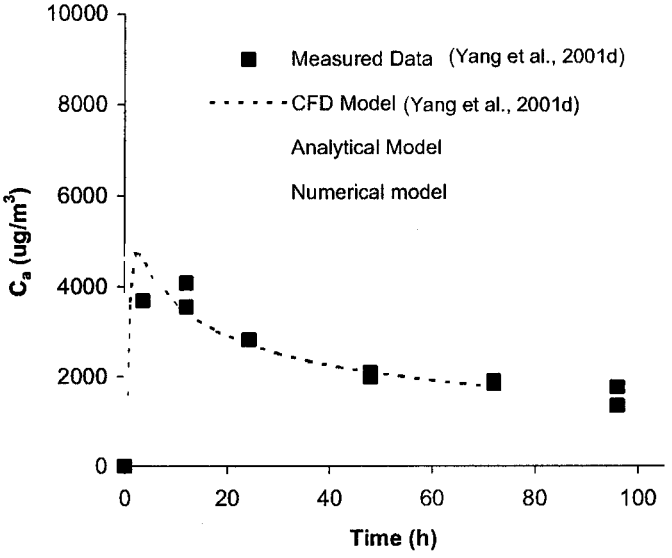

Figure 3-9 Comparison of TVOC concentrations (PB1)

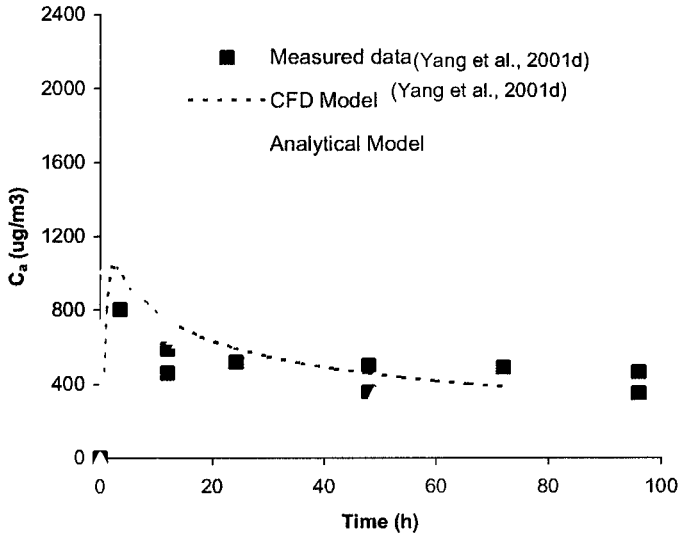

Figure 3-10 Comparison of hexanal concentrations (PB1)

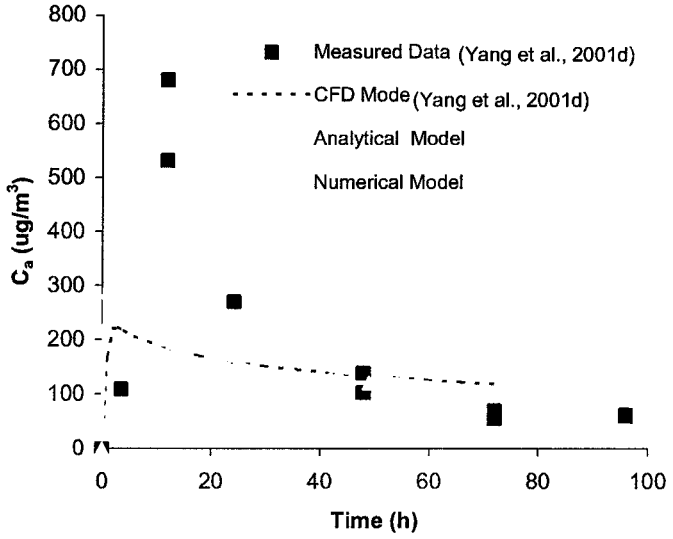

Figure 3-11 Comparison of α-pinene concentrations (PB1)

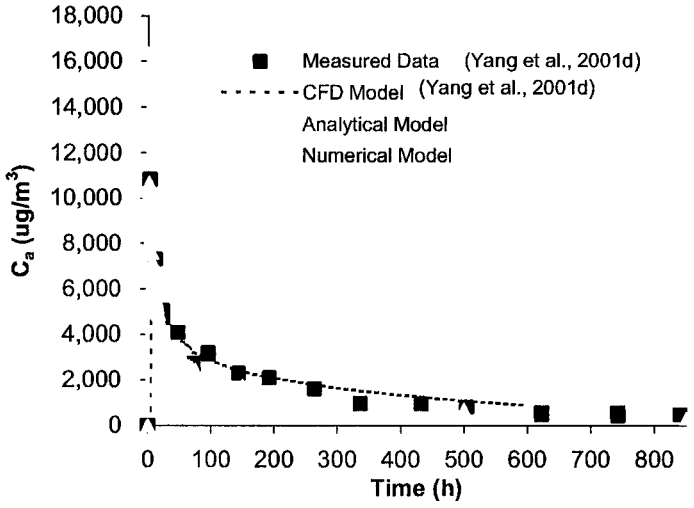

Figure 3-12 Comparison of TVOC concentrations (PB2)

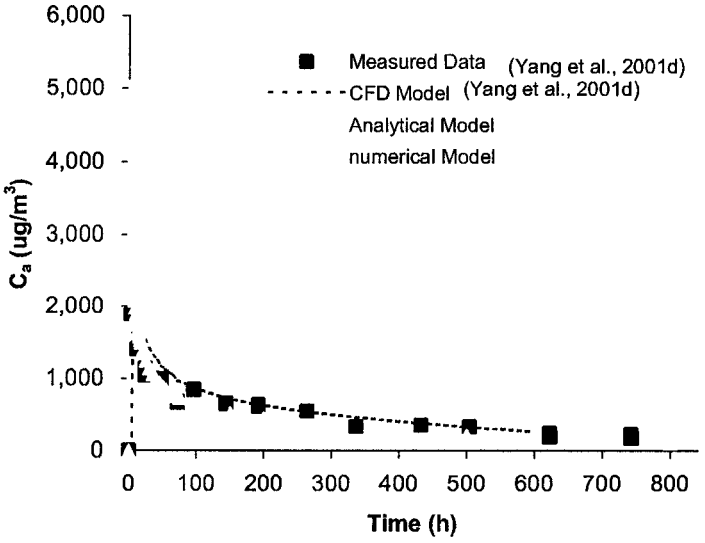

Figure 3-13 Comparison of hexanal concentrations (PB2)

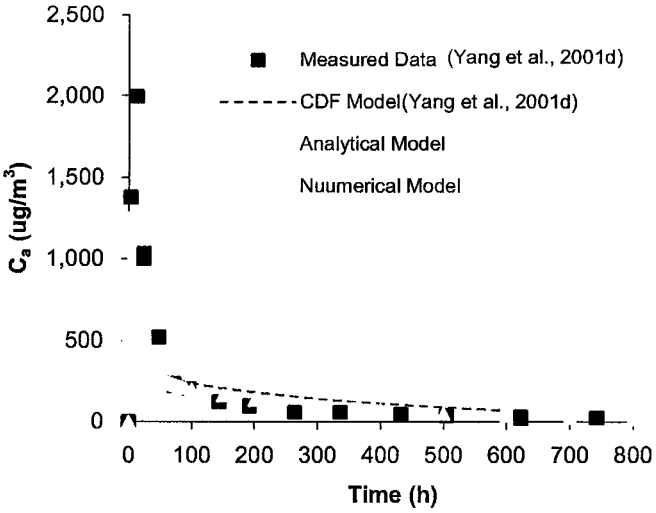

Figure 3-14 Comparison of α-pinene concentrations (PB2)

Figures 3-9 to 3-14 compare the numerical model predictions with the experimental results for concentrations of TVOC, hexanal and α-pinene for particleboard 1 and

particleboard 2. The experiments lasted 96 hours for particleboard 1 and 840 hours for particleboard 2. As shown in the figures, there is good agreement between the predicted concentrations and the experimental measurements. The predicted results and the experimental results closely follow the same trend, especially for the long term; see Figures 3-12 to 3-14. There are some minor discrepancies between the predicted results and the experimental results during the initial hours. This may be due to the total mixing assumption made in the numerical model. Actually at the early stage of the experiments, the chamber conditions were not stable and the VOC distribution in the test chamber was not uniform (Yang et al. 1998[b]). The total mixing assumption could cause model to underestimate the VOC concentration during the initial time.

The numerical model predictions were also compared with the CFD model predictions (Yang et al., 2001[d]), as shown as shown in Figures 3-9 to 3-14, for TVOC, hexanal and α-pinene concentrations. In general, there is good agreement between the predicted numerical results and the CFD predictions. Compared with the measurement data, the predictions made by the CFD model fit the experimental data better than the proposed numerical model. The predictions of the numerical model slightly underestimate the VOC concentration. The reasons may come from both the numerical model and the CFD model. The numerical model used the total mixing assumption and the convective mass transfer coefficient was estimated from the correlations of Re, Sh and Sc numbers for a constant air flow passing a flat plat, which may not represent the real flow pattern inside the chamber. On the other side, the CFD model's parameter (the VOC diffusion coefficient of the particleboard) was obtained by using the measurement data fit the CFD

model, not from directly measurement. Therefore, it is expected that the CFD model fit the experiment data better than the numerical model. However, overall, the predicted curves of the two models follow the experimental results closely.

Figures 3-9 to 3-14 also demonstrate the predictions made by the analytical model. It can be seen that during the initial period, the analytical model predicts higher concentration than the CFD or the proposed numerical model. During this period, the concentration of VOC at the surface is relatively high; this translates to the high emission rate, and consequently the high room air VOC concentration. Thus, the zero room air VOC concentration assumption can result in the analytical model overestimating the emission rate during the initial period.

These figures also show that, beyond the initial period, the surface of the material dries up and the internal diffusion starts to dominate the emission process. This results good agreement between the predictions of the analytical model, the numerical model, the CFD model and the measured data.

3.6 SUMMARY

A numerical model and an analytical model were developed to predict VOC emissions from a single-layer dry building material and VOC concentration in a well-mixed room. The models used four parameters: the diffusion coefficient of the material (D_m); the material/air partition coefficient (k); the initial concentration of the material (C_0); and the mass transfer coefficient in the air (h_m). The first three parameters are the properties of

the material and can be determined by experiments. The last parameter, h_m, can be estimated using the fundamentals of fluid dynamics.

The predictions of the models were validated at two levels: inter-model validation, and validation with the experimental results from the specially designed test and with the predictions made by a CFD model. The comparison between the numerical model and the analytical model under the same initial and boundary conditions showed that the numerical model could give as good results as the analytical model. The comparisons with the experimental results and with the predictions of the CFD model indicated that there was generally good agreement between the proposed model predictions, the experimental results, and the CFD model results.

Furthermore, the study showed that the VOC concentration in the material; the VOC emission rate and the VOC concentration in the air were linearly proportional to the initial concentration in the material. However, the normalized emitted mass was not related to the initial concentration, but was determined by the properties of the VOC and the material.

CHAPTER 4 BUILDING MATERIAL VOC EMISSIONS— A SYSTEMATIC PARAMETRIC STUDY

4.1 INTRODUCTION

For dry building materials, one-phase models (Huang and Haghighat, 2002; Yang et al., 2001[d] and Little et al., 1996) and multi-phase models (Tiffoneet, 2000; Murakami et al., 2001 and lee et al., 2002) are the most commonly used physical models. Even though in the development of those models, different assumptions have been made regarding VOC phases in the material, the basic physical processes of VOC transfer from the material to the air are the same: VOC diffusion inside the material, VOC phase change at the material/air interface, VOC diffusion and convection in the room air. To describe the VOC transfer processes, five basic parameters are required as input: the VOC diffusion coefficient of the material (D_m), the VOC partition coefficient (k), the material thickness (H), the VOC initial concentration in the material (C_0) and the air velocity over the material surface (v). The first four parameters are properties of the material, and the last one is environmentally depended. However, research found that the initial concentration does not affect the shape of the emission curve (Yang et al., 2001[d]); it only affects the magnitude of the emission. Therefore, the remaining four parameters (D_m, k, H, v) may be extremely important in determining material VOC emission characteristics.

As stated in Chapter 3, the normalized emitted mass, $M(t)/M_0$ (a ratio of the emitted VOC mass to the total VOC mass), is not a function of the initial concentration and it is only a function of the physical properties of the material and the environment. The $M(t)/M_0$ can provide a means to compare the emission characteristics of different VOC. However, $M(t)/M_0$ is time dependent. To provide an easier procedure to compare the impacts of these four parameters and their interactions on material VOC emissions, the total time of material VOC emission is used. The total time of material VOC emission is the time when 99% of the VOC is emitted from the material [$M(t)/M_0$=0.99], it is called the material VOC time.

This chapter describes a four-factor simulation design and a statistical procedure to analyze material VOC time sensitivities with respect to these four parameter variations and their interaction effects.

4.2 NUMERICAL MODEL

The numerical VOC emission model developed in Chapter 3 was used to carry out the simulations to find the material VOC time. This numerical model requires four parameters (D_m, k, H, v) as input. By using this numerical model, the four-parameter and their interaction effects on the material VOC time was studied through a four-factor simulation and statistical analysis.

4.3 FOUR-FACTOR SIMULATION DESIGN

4.3.1 Factorial design

Factorial design is mainly used in an experimental investigation, which requires a study of the effects of two or more factors on the output or response of a system. In general, factorial design is the most efficient experimental design for this type of analysis. By a factorial experiment it means that in each complete trial or replication of the experiment, all possible combinations of the levels of the factors are investigated. "The effect of a factor—*main effect* is defined to be the change in response produced by a change in the level of the factor" (Montgomery, 1976). "The *interaction between factors* refers to the effect of one factor depends on the level chosen for other factors" (Keppel, 1991). In other words, if the difference in response between the levels of one factor is not the same at all levels of the other factors, there is an interaction between the factors. Factorial designs are more efficient than one factor at a time; it is necessary when interactions may be present, to avoid misleading conclusions. Thus, factorial design allows effects of a factor to be estimated at several levels of the other factors, yielding conclusions that are valid over a range of experimental conditions (Montgomery, 1976).

The principles of factorial experiment design are adopted here for a four-factor simulation design. Detailed design and analysis procedure are described in the following sections.

4.3.2 Range of parameters

The levels of the four parameters should cover the range of the physical properties of building materials and the range of the air velocity that is usually found in an indoor environment.

The levels of diffusion coefficients and partition coefficients of materials were obtained from literatures (Bodalal et al., 2000 and Plett et al., 2001). 56 diffusion coefficients and associated partition coefficients were found for seven dry building materials (plywood, particleboard, vinyl floor tile, gypsum board, sub-floor tile, carpet and oriented strand board). Those diffusion coefficients were subdivided into three different ranges:$1.00\times10^{-10} \sim 9.99\times10^{-10}$, $1.00\times10^{-11} \sim 9.99\times10^{-11}$, and $1.00\times10^{-12} \sim 9.99\times10^{-12}$. In each range, we took the average of diffusion coefficients and associated partition coefficients to represent the levels of D_m and k. VOC source material was assumed to have three different thickness: 0.003, 0.01, and 0.03 m, which covered most of the building material thickness. Simulations were carried out at three different air velocities: 0.05, 0.1, and 0.5 m/s. The ranges of the four parameters are listed in Table 4-1.

Table 4-1 Levels of the four parameters

Parameter	**Level 1**	**Level 2**	**Level 3**
	Range Mean ($1.00\times10^{-10} \sim 9.99\times10^{-10}$)	Range Mean ($1.00\times10^{-11} \sim 9.99\times10^{-11}$)	Range Mean ($1.00\times10^{-12} \sim 9.99\times10^{-12}$)
D_m (m^2/s)	2.51×10^{-10}	3.21×10^{-11}	4.77×10^{-12}
k(—)	1095	3458	17651
H (m)	0.003	0.01	0.03
v (m/s)	0.05	0.1	0.5

A room with dimensions of 3.0×3.0×2.5 m^3, an air exchange rate of 0.5h^{-1} and a temperature of 23 °C was chosen for this parametric study. The room has only one VOC source surface, which was assumed to be the floor. The Schmidt's number was 2.63 (Sparks, et al., 1996).

4.3.3 Four-factor simulation design

a) Four factors (independent variables):

Factor A: the VOC diffusion coefficient of the material, D_m

Factor B: the VOC partition coefficient of the material, k

Factor C: the thickness of the material, H

Factor D: the air velocity over the material surface, v

b) All the possible interactions between these factors:

Two factor interaction: A×B, A×C, A×D, B×C, B×D, C×D

Three factor interaction: A×B×C, A×B×D, A×C×D, B×C×D

Four factor interaction: A×B×C×D

Where, symbol × represents interaction not multiplication

c) The dependent variable: Material VOC time (Y)

The design is the 3^4 factorial, that is, four factors each at three levels, With factor A represents D_m and has $a=3$ levels: $a_1=2.51\times10^{-10}$, $a_2=3.21\times10^{-11}$, and $a_3=4.77\times10^{-12}$ (m^2/s), factor B represents k and has $b=3$ levels: $b_1= 1095$, $b_2= 3458$, and $b_3=17651$,

factor C represents H and has $c=3$ levels: $c_1=0.003$, $c_2=0.01$, and $c_3=0.03$ (m), and factor D represents v and has $d=3$ levels: $d_1=0.05$, $d_2=0.1$, and $d_3=0.5$ (m/s). The total combinations of the levels of these four factors are $3^4 = 81$.

d) Four-way matrices

Simulations were carried out for each combination of the levels of these four factors, and the results of the material VOC time (Y) are showed in Table 4-2 (at the end of this chapter), which is called the four-way ABCD matrices. These ABCD matrices contain the *material VOC time* for each of the *(a)(b)(c)(d)* combination; they are denoted by $Y_{A_iB_jC_kD_l}$. For example, $Y_{A_1B_1C_1D_1} = 56$, $Y_{A_2B_1C_1D_1} = 173$, and $Y_{A_3B_3C_3D_3} = 96{,}074$. The grand mean of the material VOC time for all the *(a)(b)(c)(d)* combinations is:

$$\overline{Y}_T = \frac{\sum_{i=1}^{3}\sum_{j=1}^{3}\sum_{k=1}^{3}\sum_{l=1}^{3} Y_{A_iB_jC_kD_l}}{(a)(b)(c)(d)} = \frac{T_O}{(a)(b)(c)(d)} \qquad (4\text{-}1)$$

Where, $\overline{Y}_T$ is the grand mean of the material VOC time for all the *(a)(b)(c)(d)* combinations, T_O is the sum of material VOC time for all the *(a)(b)(c)(d)* combinations, $Y_{A_iB_jC_kD_l}$ is the material VOC time for factor A at level *i*, factor B at level *j*, factor C at level *k*, and factor D at level *l*, and *a, b, c, d* are factor levels associated with factor A, B, C, and D.

Substituting the values from four-away ABCD matrices (Table 4-2) into Equation (4-1), one has

$$\overline{Y}_T = \frac{56+173+976+.....+96{,}074}{(3)(3)(3)(3)} = \frac{1{,}165{,}977}{81} = 14{,}395$$

e) Three-way matrices

The three-way matrices (ABC, ABD, ACD, BCD) contain the *sum of material VOC time* for each combination of the levels of the three factors. The three-way matrices in Table 4-3 (at the end of this chapter) were formed when the levels of a fourth factor were disregarded—that is, summed across or collapsed over the four-way matrices (Table 4-2). For example, matrix ABC contains the sum of material VOC time for each of the *(a)(b)(c)* combinations, they are denoted by $A_iB_jC_k$. Any sum listed within the body of the ABC matrix was obtained by combining the corresponding material VOC time from different levels of factor D, that is:

$$A_iB_jC_k = \sum_{l=1}^{3}\left(Y_{A_iB_jC_kD_l}\right) \qquad i=1, 2, 3, j=1, 2, 3, k=1, 2, 3 \tag{4-2}$$

Where, $A_iB_jC_k$ is the sum of material VOC time for factor A at level *i*, factor B at level *j*, and factor C at level *k*. For example, from Table 4-2, one can write:

$$A_1B_1C_1 = Y_{A_1B_1C_1D_1} + Y_{A_1B_1C_1D_2} + Y_{A_1B_1C_1D_3} = 56+49+41 = 146$$

$$A_3B_2C_2 = Y_{A_3B_2C_2D_1} + Y_{A_3B_2C_2D_2} + Y_{A_3B_2C_2D_3} = 10{,}697+10{,}635+10{,}553 = 31{,}885$$

The marginal mean of the material VOC time for each of the *(a)(b)(c)* combination was obtained by averaging over, in essence, eliminating the change of the other independent variable, thus

$$\overline{Y}_{A_iB_jC_k} = \frac{A_iB_jC_k}{(d)} \quad i=1,2,3, j=1,2,3, k=1,2,3 \tag{4-3}$$

Where, $\overline{Y}_{A_iB_jC_k}$ is the marginal mean of the material VOC time for factor A at level *i*, factor B at level *j* and factor C at level *k*. For example, $\overline{Y}_{A_1B_1C_1} = \frac{A_1B_1C_1}{(d)} = \frac{146}{3} = 48.67$

The matrices ABD, ACD and BCD were formed in a similar way. The sums of the material VOC time in these three-way matrices are denoted by $A_iB_jD_l$, $A_iC_kD_l$, *and* $B_jC_kD_l$. For example,

$$A_1B_2D_3 = Y_{A_1B_2C_1D_3} + Y_{A_1B_2C_2D_3} + Y_{A_1B_2C_3D_3} = 83 + 392 + 2{,}326 = 2{,}801$$

$$B_2C_2D_2 = Y_{A_1B_2C_2D_2} + Y_{A_2B_2C_2D_2} + Y_{A_3B_2C_2D_2} = 483 + 1{,}808 + 10{,}635 = 12{,}926$$

f) Two-way matrices

The two-way matrices (AB, AC, AD, BC, BD and CD) contain the *sum of material VOC time* for each combination of the levels of the two factors, as shown in Table 4-4 (at the end of this chapter). The two-way matrices were formed when the levels of a third and a forth factor were disregarded— summed across or collapsed over the three-way matrices (Table 4-3). For example, matrix AB contains the sum of material VOC time for each of the *(a)(b)* combinations, they are denoted by A_iB_j. Any sum listed within the body of the AB matrix was obtained by combining the corresponding sums from different levels of factor C or D, that is

$$A_iB_j = \sum_{k=1}^{3}\left(A_iB_jC_k\right) = A_iB_jC_1 + A_iB_jC_2 + A_iB_jC_3 \qquad i=1,\ 2,\ 3, j=1,\ 2,\ 3 \tag{4-4}$$

$$\text{or, } A_iB_j = \sum_{l=1}^{3}\left(A_iB_jD_l\right) = A_iB_jD_1 + A_iB_jD_2 + A_iB_jD_3 \qquad i=1,\ 2,\ 3, j=1,\ 2,\ 3 \tag{4-5}$$

Where, A_iB_j is the sum of material VOC time for factor A at level *i* and factor B at level *j*. For example, from Table 4-3, one can write:

$$A_2B_2 = A_2B_2C_1 + A_2B_2C_2 + A_2B_2C_3 = 667 + 5{,}405 + 43{,}907 = 49{,}979$$

$$\text{or, } A_2B_2 = A_2B_2D_1 + A_2B_2D_2 + A_2B_2D_3 = 16{,}962 + 16{,}687 + 16{,}330 = 49{,}979$$

The marginal mean of the material VOC time for each of the *(a)(b)* combination is

$$\overline{Y}_{A_iB_j} = \frac{A_iB_j}{(c)(d)} \qquad i=1,2,3, j=1,2,3 \tag{4-6}$$

Where, $\overline{Y}_{A_iB_j}$ is the marginal mean of the material VOC time for factor A at level *i* and factor B at level *j*. For example, $\overline{Y}_{A_2B_2} = \frac{A_2B_2}{(c)(c)} = \frac{49{,}979}{(3)(3)} = 5553$.

The matrices AC, AD, BC, BD and CD were formed in a similar way. The sums of the material VOC time in these two-way matrices are denoted A_iC_k, A_iD_l, B_jC_k, B_jD_l, *and* C_kD_l. For example,

$$B_2C_2 = A_1B_2C_2 + A_2B_2C_2 + A_3B_2C_2 = 1{,}428 + 5{,}405 + 31{,}885 = 38{,}718$$

or, $B_2C_2 = B_2C_2D_1 + B_2C_2D_2 + B_2C_2D_3 = 13{,}123 + 12{,}926 + 12{,}609 = 38{,}718$

$C_1D_2 = A_1C_1D_2 + A_2C_1D_2 + A_3C_1D_2 = 639 + 977 + 3{,}327 = 4{,}943$

or, $C_1D_2 = B_1C_1D_2 + B_2C_1D_2 + B_3C_1D_2 = 1{,}177 + 1{,}350 + 2{,}416 = 4{,}943$

The marginal totals of the two-way matrices provide the A_i sums, the B_j sums, the C_k sums and the D_l sums. For example, the marginal totals of the AB matrix provide the A_i sums (column marginal totals), the B_j sums (row marginal totals) and the grand total T_o (the sum of either the row or column marginal totals):

$$A_i = \sum_{j=1}^{3}\left(A_iB_j\right) = A_iB_1 + A_iB_2 + A_iB_3 \qquad i=1,\ 2,\ 3 \tag{4-7}$$

$$B_j = \sum_{i=1}^{3}\left(A_iB_j\right) = A_1B_j + A_2B_j + A_3B_j \qquad j=1,2,3 \tag{4-8}$$

$$T_o = \sum_{i=1}^{3} A_i = \sum_{j=1}^{3} B_j \tag{4-9}$$

Where, A_i is the sum of material VOC time for factor A at level i and B_j is the sum of material VOC time for factor B at level j. For example,

$A_1 = A_1B_1 + A_1B_2 + A_1B_3 = 7{,}060 + 9{,}459 + 24{,}567 = 41{,}086$

$B_3 = A_1B_3 + A_2B_3 + A_3B_3 = 24{,}567 + 64{,}070 + 330{,}763 = 419{,}400$

$T_o = A_1 + A_2 + A_3 = B_1 + B_2 + B_3$
$= 41{,}086 + 161{,}768 + 963{,}123 = 369{,}849 + 376{,}728 + 419{,}400 = 1{,}165{,}977$

The marginal means for factor A and factor B were obtained by averaging over,

$$\overline{Y}_{A_i} = \frac{A_i}{(b)(c)(d)} \quad i=1,2,3 \tag{4-10}$$

$$\overline{Y}_{B_j} = \frac{B_j}{(a)(c)(d)} \quad j=1,2,3 \tag{4-11}$$

Where, $\overline{Y}_{A_i}$ is the marginal mean of the material VOC time for factor A at level i and $\overline{Y}_{B_i}$ is the marginal mean of the material VOC time for factor B at level j.

For example, $\overline{Y}_{A_1} = \frac{A_1}{(b)(c)(d)} = \frac{41{,}086}{(3)(3)(3)} = 1{,}522$, $\overline{Y}_{B_3} = \frac{B_3}{(b)(c)(d)} = \frac{419{,}400}{(3)(3)(3)} = 15{,}533$

The marginal totals of the C_k sums and the D_l sums were formed in a similar way. The marginal totals in any two-way matrix are duplicated in the other matrices. This redundancy can be used as a way to check the accuracy of forming a two-way matrix from the three-way matrices and a three-way matrix from the four-way matrices.

All the values in the four-way matrices ($Y_{A_iB_jC_kD_l}$), three-way matrices ($A_iB_jC_k$, $A_iB_jD_l$, $A_iC_kD_l$ *and* $B_jC_kD_l$), and two-way matrices (A_iB_j, A_iC_k, A_iD_l, B_jC_k, B_jD_l, C_kD_l, A_i, B_j, C_k, D_l *and* T) were used in the following statistical analysis.

4.4 STATISTICAL ANALYSIS

4.4.1 The analysis

Since there is only one output (material VOC time) in each simulation group, there is no variability due to the difference of output within a group. Therefore, the variability is only caused by the factor effects (no experimental error). An index Omega squared (ω^2) was applied to measure the factor effect magnitude. ω^2 is the ratio of the sum of squared deviation of a factor to the total sum of squared deviation (SS_T). It reflects the proportional amount of the total variance that is attributed to the variation among the factor effects (Keppel, 1991). It is defined as:

$$\omega^2 = \frac{SS}{SS_T} \tag{4-12}$$

Where,

$$SS_T = \sum_{i=1}^{3}\sum_{j=1}^{3}\sum_{k=1}^{3}\sum_{l=1}^{3}\left(Y_{A_iB_jC_kD_l} - \overline{Y}_T\right)^2 \tag{4-13}$$

SS is the sum of the squared deviations from the grand mean, usually shortened to sum of squares, and SS_T is the total sum of the squared deviations from the grand mean, or the total sum of squares.

Also, SS_T is equal to the total of the sum of squares for the four main effects (SS_A, SS_B, SS_C and SS_D), the sum of squares for the six two-way interactions ($SS_{A\times B}$, $SS_{A\times C}$, $SS_{A\times D}$, $SS_{B\times C}$, $SS_{B\times D}$ and $SS_{C\times D}$), the sum of squares for the four three-way interactions ($SS_{A\times B\times C}$,

$SS_{A\times B\times D}$, $SS_{A\times C\times D}$ and $SS_{B\times C\times D}$), and the sum of squares for the four-way interaction ($SS_{A\times B\times C\times D}$), it is written as:

$$SS_T = SS_A + SS_B + SS_C + SS_D + SS_{A\times B} + SS_{A\times C} + SS_{A\times D} + SS_{B\times C} + SS_{B\times D} + SS_{C\times D} + SS_{A\times B\times C} + SS_{A\times B\times D} + SS_{A\times C\times D} + SS_{B\times C\times D} + SS_{A\times B\times C\times D} \quad (4\text{-}14)$$

As examples, the following parts only illustrate how to calculate the ω^2 for factor A and for the interaction A×B.

a) ω^2 for factor A, ω_A^2

From the definition of ω^2 (Equation 4-12), we have

$$\omega_A^2 = \frac{SS_A}{SS_T} \quad (4\text{-}15)$$

Where, SS_A is sum of the squares for factor A, which is given as:

$$SS_A = (b)(c)(d)\sum_{i=1}^{3}\left(\overline{Y}_{A_i} - \overline{Y}_T\right)^2 \quad (4\text{-}16)$$

Substituting Equation (4-1), (4-9) and (4-10) into (4-16) gives

$$SS_A = (b)(c)(d)\sum_{i=1}^{3}\left(\frac{A_i}{(b)(c)(d)} - \overline{Y}_T\right)^2 = \frac{\sum_{i=1}^{3} A_i^2}{(b)(c)(d)} - \frac{T_O^2}{(a)(b)(c)(d)} = [A] - [T] \quad (4\text{-}17)$$

Where, $[A] = \frac{\sum_{i=1}^{3} A_i^2}{(b)(c)(d)}$, $\quad [T] = \frac{T_O{}^2}{(a)(b)(c)(d)}$

Substituting the relevant values from two-way matrix AB into Equation (4-17) gives

$$SS_A = \frac{41{,}086^2 + 161{,}768^2 + 963{,}123^2}{(3)(3)(3)} - \frac{1{,}165{,}977^2}{(3)(3)(3)(3)} = 18{,}603{,}533{,}463$$

Substituting the values from the four-way matrices ABCD and the value of $\overline{Y}_T$ into Equation (4-13) gives:

$$SS_T = (56 - 14{,}395)^2 + (176 - 14{,}395)^2 + (967 - 14{,}395)^2 + \ldots\ldots\ldots\ldots + (96074 - 14{,}395)^2$$
$$= 67{,}933{,}497{,}188$$

Thus, $\omega_A^2 = \frac{SS_A}{SS_T} = \frac{18{,}603{,}533{,}463}{67{,}933{,}467{,}188} = 0.274$

b) ω^2 for interaction A×B, $\omega_{A\times B}^2$

An interaction exists when the pattern of differences associated with an independent variable changes at the different levels of the other independent variable. The interaction effect A×B represents whatever is left of the deviation of the individual marginal mean ($\overline{Y}_{A_iB_j}$) from the grand mean ($\overline{Y}_T$) that cannot be accounted for by the two relevant main effects (A_i, B_j): it is not the combination effect of factor A and factor B. The interaction can be defined as a residual deviation.

Interaction effect = (deviation from $\overline{Y}_T$) –(A_i effect) – (B_j effect)

$$= \left(\overline{Y}_{A_iB_j} - \overline{Y}_T\right) - \left(\overline{Y}_{A_i} - \overline{Y}_T\right) - \left(\overline{Y}_{B_j} - \overline{Y}_T\right)$$

$$= \overline{Y}_{A_iB_j} - \overline{Y}_{A_i} - \overline{Y}_{B_j} + \overline{Y}_T \qquad (4\text{-}18)$$

Thus, the sum of squares for interaction effect A×B, $SS_{A\times B}$, is

$$SS_{A\times B} = (c)(d)\sum_{i=1}^{3}\sum_{j=1}^{3}\left(\overline{Y}_{A_iB_j} - \overline{Y}_{A_i} - \overline{Y}_{B_j} + \overline{Y}_T\right)^2 \tag{4-19}$$

Substituting Equations (4-1), (4-6), (4-10) and (4-11) into Equation (4-19) gives:

$$SS_{A\times B} = \frac{\sum_{i=1}^{3}\sum_{j=1}^{3}\left(A_iB_j\right)^2}{(c)(d)} - \frac{\sum_{i=1}^{3}A_i^2}{(b)(c)(d)} - \frac{\sum_{j=1}^{3}B_j^2}{(a)(c)(d)} + \frac{T_O{}^2}{(a)(b)(c)(d)} = [AB]-[A]-[B]+[T] \tag{4-20}$$

Where, $[AB] = \frac{\sum_{i=1}^{3}\sum_{j=1}^{3}\left(A_iB_j\right)^2}{(c)(d)}$, $\quad [B] = -\frac{\sum_{j=1}^{3}B_j^2}{(a)(c)(d)}$.

Substituting the relevant values from the two-way matrix AB into Equation (4-20) gives:

$$SS_{A\times B} = \frac{7{,}060^2 + 47{,}719^2 + \ldots\ldots + 330{,}763^2}{(3)(3)} - \frac{41{,}086^2 + 161{,}768^2 + 963{,}125^2}{(3)(3)(3)}$$
$$- \frac{369{,}849^2 + 376{,}728^2 + 419{,}400^2}{(3)(3)(3)} + \frac{1{,}165{,}977^2}{(3)(3)(3)(3)} = 113{,}609$$

Therefore, ω^2 for interaction effect A×B is:

$$\omega^2_{A\times B} = \frac{SS_{A\times B}}{SS_T} = \frac{113{,}609}{67{,}933{,}467{,}188} < 0.01$$

The basic patterns combined to calculate the sum of squares for different sources (factors and factor interactions) are listed in Table 4-5 (at the end of this chapter), and the results of ω^2 for different sources are given in the final columns of the Table 4-5.

4.4.2 Results and discussions

The significance level for a factor or factor interaction effect was measured by the criteria suggested by Cohen (1977), as listed in following:

A "small" effect is a factor that produces an ω^2 of 0.01.

A "medium" effect is a factor that produces an ω^2 of 0.06.

A "Large" effect is a factor that produces an ω^2 of 0.15 or greater.

Statistical analysis in Table 4-5 shows that three effects, namely factor A (D_m), factor C (H), and their interaction A×C ($D_m \times H$) are significant ($\omega^2>0.15$). They largely affect the VOC emission time of the material. The impacts of these three significant effects are further analyzed in the following sections. Other factors, factor B (k), factor D (v), and the interactions A×B, A×D, B×C, B×D, C×D, A×B×C, A×B×D, A×C×D, B×C×D and A×B×C×D, have minor effects on the material VOC time ($\omega^2<0.01$).

a) Diffusion Coefficient (factor A)

The VOC diffusion coefficient of the material (factor A) affects VOC internal diffusion mass transfer. Based on the Fick's law, the higher the diffusion coefficient, the greater the diffusion mass transfer.

The impact of the diffusion coefficient of the material on the material VOC time was further analyzed by using its marginal means ($\overline{Y}_{A_i}$, Equation (4-10))—*main effect*, when other independent variables (factor B, C and D) were disregarded.

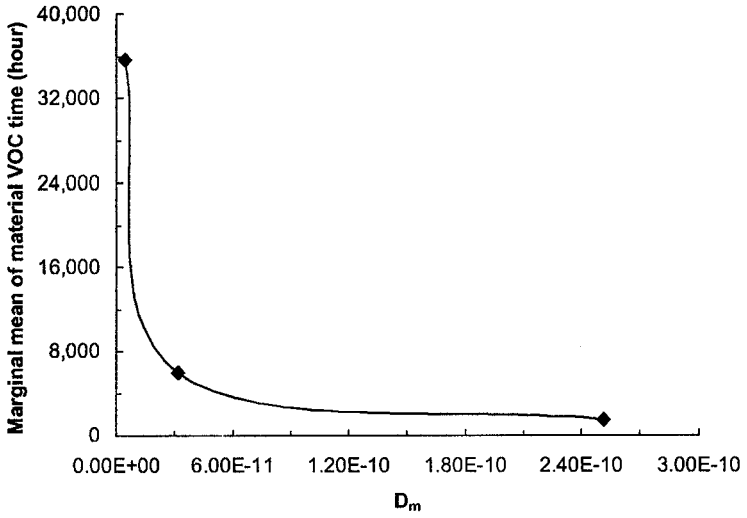

Figure 4-1 Main effect of the diffusion coefficient (factor A)

Figure 4-1 shows the main effect of the diffusion coefficient on the material VOC time. It illustrates that the material VOC time drops rapidly as the diffusion coefficient increases. The diffusion coefficient has a very significant effect in determining the material VOC time. This is due to the increase of the diffusion coefficient that significantly increases the VOC internal diffusion hence greatly decreases the material VOC time.

b) Thickness of Material (factor C)

The impact of the thickness of the material on the material VOC time was also analyzed using its marginal means—main effect, when other independent variables (factor A, B and D) were disregarded. For factor C

$$\overline{Y}_{C_k} = \frac{C_k}{(a)(b)(d)} \quad k=1,2,3 \tag{4-21}$$

Where, $\overline{Y}_{C_k}$ is the marginal mean of the material VOC time for factor C at level k and C_k is the sum of material VOC time for factor C at level k.

Figure 4-2 shows the main effect of the thickness of the material on the material VOC time. It illustrates that the material VOC time increases rapidly as the material thickness increases. It indicates that the material thickness plays an important role in determining the material VOC time. Generally, a thick material has long VOC emission time; this is for the reason that the thicker material has a higher VOC transfer resistance hence has a longer VOC emission time.

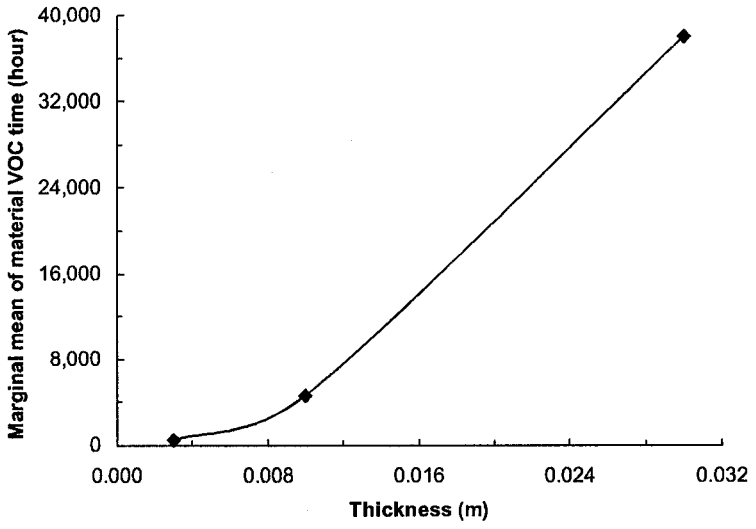

Figure 4-2 Main effect of the thickness of the material (factor C)

c) *Interaction between Diffusion Coefficient and Thickness of the Material (A×C)*

Statistical analysis shows that the interaction between the VOC diffusion coefficient and the thickness has significant effect on the material VOC time. The interaction effect can be analyzed using its marginal mean:

$$\overline{Y}_{A_iC_k} = \frac{A_iC_k}{(b)(d)} \quad i=1,2,3,\ k=1,2,3 \tag{4-22}$$

Where, $\overline{Y}_{A_iC_k}$ is the marginal mean of the material VOC time for factor A at level i, factor C at level k, and A_iC_k is the sum of material VOC time for factor A at level i and factor C at level k.

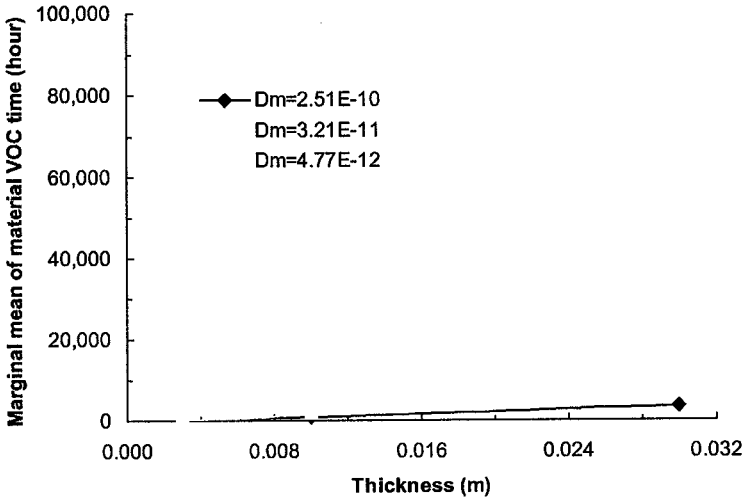

Figure 4-3 Interaction effect between the diffusion coefficient and the thickness of the material (A×C)

To illustrate, the marginal means of A×C is plotted in Figure 4-3. It exhibits a clear interaction between the diffusion coefficient (factor A) and the thickness (factor C). It appears that at three different levels of the diffusion coefficients (from high to low), the material VOC time does not appear in a similar trend and is dependent on the thickness of the material. For the high diffusion coefficient, the material VOC time increases slowly as the thickness increases. However, for the low diffusion coefficient, the material VOC time increases rapidly as the thickness increases. It illustrates that, as the thickness increases, the material VOC time increase rate is smaller at the high diffusion coefficient than at the low diffusion coefficient.

4.5 SUMMARY

Mathematical models used to predict VOC emissions from building materials require four critical parameters: the VOC diffusion coefficient of the material (D_m), the VOC partition coefficient (k), the material thickness (H), and the surface air velocity (v). A parametric study was carried out to study the impacts of these four parameters and their interactions on VOC emissions from building materials. This parametric study was accomplished by a four-factor simulation design and a statistical analysis of the material VOC time sensitivities with respect to the four parameters variations and their interaction effects. It was found that:

- D_m and H, and the interaction between them, $D_m \times H$, significantly affected the material VOC time.
- Other parameters (k, v) and interactions ($D_m \times k$, $D_m \times v$, $k \times H$, $k \times v$, $H \times v$, $D_m \times k \times H$, $D_m \times k \times v$, $D_m \times H \times v$, $k \times H \times v$, $D_m \times k \times H \times v$) had minor effects on the material VOC time.

- The material VOC time decreased rapidly as the diffusion coefficient increases.
- The material VOC time increased significantly as the thickness of the material increases.
- There was a clear interaction between the diffusion coefficient and the thickness. As the thickness of the material increased, the material VOC time increase rate was smaller at the high diffusion coefficient than at the low diffusion coefficient.

Table 4-2 Four-way matrices (ABCD) of the material VOC time $Y_{A_iB_jC_kD_l}$

$Y_{A_iB_jC_1D_1}$

d_1			
c_1			
	a_1	a_2	a_3
b_1	56	173	967
b_2	132	245	1,034
b_3	588	695	1,453

$Y_{A_iB_jC_1D_2}$

d_2			
c_1			
	a_1	a_2	a_3
b_1	49	167	961
b_2	111	224	1,015
b_3	479	586	1,351

$Y_{A_iB_jC_1D_3}$

d_3			
c_1			
	a_1	a_2	a_3
b_1	41	159	953
b_2	83	198	990
b_3	335	444	1,217

$Y_{A_iB_jC_2D_1}$

d_1			
c_2			
	a_1	a_2	a_3
b_1	307	1,646	10,478
b_2	553	1,873	10,697
b_3	2,067	3,313	12,041

$Y_{A_iB_jC_2D_2}$

d_2			
c_2			
	a_1	a_2	a_3
b_1	286	1,627	10,458
b_2	483	1,808	10,635
b_3	1,703	2,960	11,715

$Y_{A_iB_jC_2D_3}$

d_3			
c_2			
	a_1	a_2	a_3
b_1	259	1,600	10,432
b_2	392	1,724	10,553
b_3	1,223	2,499	11,286

$Y_{A_iB_jC_3D_1}$

d_1			
c_3			
	a_1	a_2	a_3
b_1	2,088	14,181	93,672
b_2	2,790	14,844	94,327
b_3	7,256	18,970	98,291

$Y_{A_iB_jC_3D_2}$

d_2			
c_3			
	a_1	a_2	a_3
b_1	2,027	14,122	93,613
b_2	2,589	14,655	94,142
b_3	6,172	17,961	97,335

$Y_{A_iB_jC_3D_3}$

d_3			
c_3			
	a_1	a_2	a_3
b_1	1,947	14,044	93,536
b_2	2,326	14,408	93,897
b_3	4,744	16,642	96,074

Note: Factor A: VOC diffusion coefficient, D_m (m^2/s), $a=3$ levels: $a_1=2.51\times10^{-10}$, $a_2=3.21\times10^{-11}$, $a_3=4.77\times10^{-12}$.
Factor B: partition coefficient of the material, k, $b=3$ levels: $b_1= 1095$, $b_2= 3458$, $b_3=17651$.
Factor C: thickness of the material, H, (m), $c=3$ levels: $c_1=0.003$, $c_2=0.01$, $c_3=0.03$.
Factor D: air velocity over material surface, v, (m/s), $d=3$ levels: $d_1=0.05$, $d_2=0.1$, $d_3=0.5$.

Table 4-3 Three-way matrices of the sum of material VOC times

ABC Matrix

	c_1			c_2			c_3		
	a_1	a_2	A_3	a_1	a_2	a_3	a_1	a_2	a_3
b_1	146	499	2,881	852	4,873	31,368	6,062	42,347	280,821
b_2	326	667	3,039	1,428	5,405	31,885	7,705	43,907	282,366
b_3	1,402	1,725	4,021	4,993	8,772	35,042	18,172	53,573	291,700

ABD Matrix

	d_1			d_2			d_3		
	a_1	a_2	a_3	a_1	a_2	a_3	a_1	a_2	a_3
b_1	2,451	16,000	105,117	2,362	15,916	105,032	2,247	15,803	104,921
b_2	3,475	16,962	106,058	3,183	16,687	105,792	2,801	16,330	105,440
b_3	9,911	22,978	111,785	8,354	21,507	110,401	6,302	19,585	108,577

ACD Matrix

	c_1			c_2			c_3		
	a_1	a_2	a_3	a_1	a_2	a_3	a_1	a_2	a_3
d_1	776	1,113	3,454	2,927	6,832	33,216	12,134	47,995	286,290
d_2	639	977	3,327	2,472	6,395	32,808	10,788	46,738	285,090
d_3	459	801	3,160	1,874	5,823	32,271	9,017	45,094	283,507

BCD Matrix

	c_1			c_2			c_3		
	d_1	d_2	d_3	d_1	d_2	d_3	d_1	d_2	d_3
b_1	1,196	1,177	1,153	12,431	12,371	12,291	109,941	109,762	109,527
b_2	1,411	1,350	1,271	13,123	12,926	12,669	111,961	111,386	110,631
b_3	2,736	2,416	1,996	17,421	16,378	15,008	124,517	121,468	117,460

Table 4-4 Two-way matrices of the sum of material VOC times

AB Matrix

	a_1	a_2	a_3	SUM	B_i
b_1	7,060	47,719	315,070	369,849	B_1
b_2	9,459	49,979	317,290	376,728	B_2
b_3	24,567	64,070	330,763	419,400	B_3
SUM	41,086	161,768	963,123	1,165,977	T_O
A_i	A_1	A_2	A_3	T_O	

AC Matrix

	a_1	a_2	a_3	SUM	C_i
c_1	1,874	2,891	9,941	14,706	C_1
c_2	7,273	19,050	98,295	124,618	C_2
c_3	31,939	139,827	854,887	1,026,653	C_3
SUM	41,086	161,768	963,123	1,165,977	T_O
A_i	A_1	A_2	A_3	T_O	

BC Matrix

	c_1	c_2	c_3	SUM	B_i
b_1	3,526	37,093	329,230	369,849	B_1
b_2	4,032	38,718	333,978	376,728	B_2
b_3	7,148	48,807	363,445	419,400	B_3
SUM	14,706	124,618	1,026,653	1,165,977	T_O
C_i	C_1	C_2	C_3	T_O	

AD Matrix

	a_1	a_2	a_3	SUM	D_i
d_1	15,837	55,940	322,960	394,737	D_1
d_2	13,899	54,110	321,225	389,234	D_2
d_3	11,350	51,718	318,938	382,006	D_3
SUM	41,086	161,768	963,123	1,165,977	T_O
A_i	A_1	A_2	A_3	T_O	

BD Matrix

	d_1	d_2	d_3	SUM	B_i
b_1	123,568	123,310	122,971	369,849	B_1
b_2	126,495	125,662	124,571	376,728	B_2
b_3	144,674	140,262	134,464	419,400	B_3
SUM	394,737	389,234	382,006	1,165,977	T_O
D_i	D_1	D_2	D_3	T_O	

CD matrix

	c_1	c_2	c_3	SUM	D_i
d_1	5,343	42,975	346,419	394,737	D_1
d_2	4,943	41,675	342,616	389,234	D_2
d_3	4,420	39,968	337,618	382,006	D_3
SUM	14,706	124,618	1,026,653	1,165,977	T_O
C_i	C_1	C_2	C_3	T_O	

Table 4-5 Summary of analysis

Source	Basic ratio		Sum of squares		ω^2
	Pattern	Quantity	Pattern	Quantity	
A	$[A]=\frac{\sum A_i^2}{(b)(c)(d)}$	35,387,513,272	$SS_A=[A]-[T]$	18,603,533,463	0.274
B	$[B]=\frac{\sum B_j^2}{(a)(c)(d)}$	16,837,356,622	$SS_B=[B]-[T]$	53,376,813	<0.01
C	$[C]=\frac{\sum C_k^2}{(a)(b)(d)}$	39,620,825,732	$SS_C=[C]-[T]$	22,836,845,923	0.336
D	$[D]=\frac{\sum D_l^2}{(a)(b)(c)}$	16,786,999,628	$SS_D=[D]-[T]$	3,019,819	<0.01
A×B	$[AB]=\frac{\sum(A_iB_j)^2}{(c)(d)}$	35,441,003,693	$SS_{A\times B}=[AB]-[A]-[B]+[T]$	113,609	<0.01
A×C	$[AC]=\frac{\sum(A_iC_k)^2}{(b)(d)}$	84,621,319,079	$SS_{A\times C}=[AC]-[A]-[C]+[T]$	26,396,959,884	0.389
A×D	$[AD]=\frac{\sum(A_iD_l)^2}{(b)(c)}$	35,390,539,174	$SS_{A\times D}=[AD]-[A]-[D]+[T]$	6,082	<0.01
B×C	$[BC]=\frac{\sum(B_jC_k)^2}{(a)(d)}$	39,706,982,937	$SS_{B\times C}=[BC]-[B]-[C]+[T]$	32,780,392	<0.01
B×D	$[BD]=\frac{\sum(B_jD_l)^2}{(a)(c)}$	16,843,410,343	$SS_{B\times D}=[BD]-[B]-[D]+[T]$	3,033,903	<0.01
C×D	$[CD]=\frac{\sum(C_kD_l)^2}{(a)(b)}$	39,625,708,390	$SS_{C\times D}=[CD]-[C]-[D]+[T]$	1,862,839	<0.01
A×B×C	$[ABC]=\frac{\sum(A_iB_jC_k)^2}{(d)}$	84,707,664,786	$SS_{A\times B\times C}=[ABC]-[AB]-[AC]-[BC]+[A]+[B]+[C]-[T]$	74,894	<0.01
A×B×D	$[ABD]=\frac{\sum(A_iB_jD_l)^2}{(c)}$	35,447,071,228	$SS_{A\times B\times D}=[ABD]-[AB]-[AD]-[BD]+[A]+[B]+[D]-[T]$	7,730	<0.01
A×C×D	$[ACD]=\frac{\sum(A_iC_kD_l)^2}{(b)}$	84,626,212,398	$SS_{A\times C\times D}=[ACD]-[AC]-[AD]-[CD]+[A]+[C]+[D]-[T]$	4,578	<0.01
B×C×D	$[BCD]=\frac{\sum(B_jC_kD_l)^2}{(a)}$	39,716,769,222	$SS_{B\times C\times D}=[BCD]-[BC]-[BD]-[CD]+[B]+[C]+[D]-[T]$	1,869,724	<0.01
A×B×C×D	$[ABCD]=\sum(Y_{A_iB_jC_kD_l})^2$	84,717,475,997	$SS_{A\times B\times C\times D}=[ABCD]-[ABC]-[ABD]-[ACD]-[BCD]+[AB]+[AC]+[AD]+[BC]+[BD]+[CD]-[A]-[B]-[C]-[D]+[T]$	6,535	<0.01
Total	$[T]=\frac{T^2}{(a)(b)(c)(d)}$	16,783,979,8091	$SS_T=$	67,933,496,188	

CHAPTER 5 AN INTEGRATED IAQ MODEL FOR PREDICTING VOC EMISSIONS FROM BUILDING MATERIALS

5.1 INTRODUCTION

Generally, building materials appear in composite forms, such as a wall assembly (paint/gypsum board/vapor barrier) or a floor assembly (wax/vinyl/adhesive/concrete). VOC emissions from wall or floor assembly have not been theoretically investigated. From the experimental studies of carpet/adhesive assembly, it has been found that the adhesive in the floor assembly is the main source of VOC: the emissions of the assembly shows a lower delayed peak and a slower decay rate compared with that of the adhesive alone (Black et al., 1991; Black et al., 1993 and Low et al., 1998). Thus, understanding of multi-layer material emission characteristics in a building is more important than single-layer material emission characteristics. Some multi-layer models were proposed (Bodadal, 1999; Yang et al., 2001[d]; Lee et al., 2002 and Kumar et al., 2002), a general multi-layer emission model that can be used to simulate wet/dry, dry/dry, dry/wet material assemblies is not yet available.

Actually, a room contains both source and sink materials. VOC emitted from source materials and VOC adsorbed by sink materials affect indoor air quality synchronically. Therefore, accurate prediction of occupants' exposure and room air VOC concentration

requires modeling of both material emissions and material sinks simultaneously rather than separately.

This chapter describes the development of an integrated IAQ model for predicting the VOC emissions from material assembly, for estimating the material sink effects, and for simulating room air VOC concentration with complex source and sink materials. The integrated IAQ model includes a multi-layer material emission model, a single-layer material sink model and a room air VOC concentration model. This model was first applied to a room with a floor assembly to simulate the multi-layer material emission characteristics, and then was applied to a room with typical walls as sink materials and with a floor assembly as source material to study the material substrate and sink effects.

5.2 INTEGRATED IAQ MODEL DEVELOPMENT

5.2.1 Multi-Layer material emission model

Multi-layer materials include three composition forms: dry/dry (e.g. composite particleboard or plywood), dry/wet (e.g. vinyl floor tile + glue + plywood, carpet + adhesive) and wet/dry (e.g. paint + gypsum board). VOC emission processes from multi-layer materials follow the same emission processes as single-layer materials. The material configuration and VOC emission processes are shown in Figure 5-1. It is assumed that only one surface of the material is exposed to the room air.

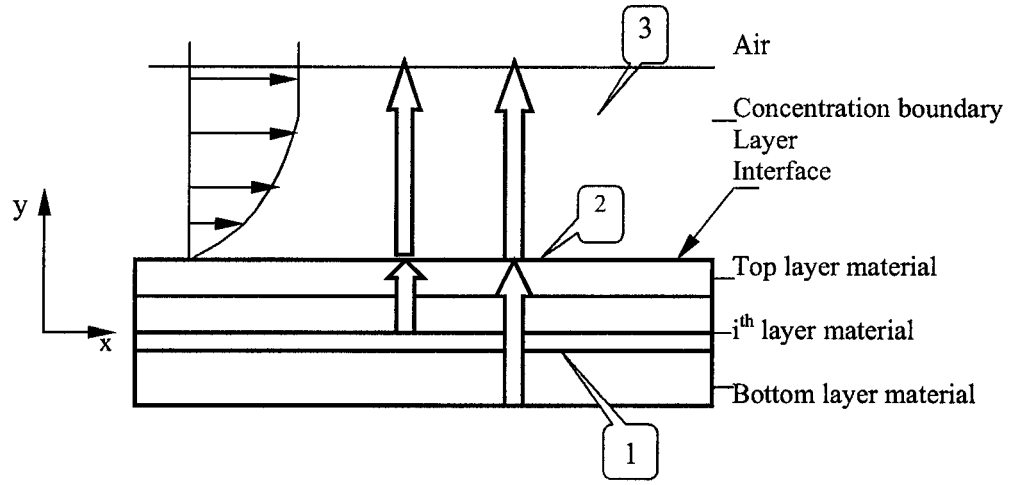

Figure 5-1 Physical configuration of VOC emissions from a multi-layer material. 1: internal diffusion; 2: material/air interface sorption; 3, external convection and diffusion

a) Mass transfer within the material

Concentration gradient is assumed to be the only driving force for VOC transport within the materials, and there is no chemical reaction inside the materials.

I. Dry/dry material assembly

For a dry material, since the VOC concentration within the material is very low, the VOC diffusion coefficient can be assumed to be independent of the VOC concentration. Therefore, each layer of the dry material can be considered as having homogeneous diffusivity. The transient VOC diffusion in the dry/dry material assembly can be described by a one-dimensional diffusion equation:

$$\frac{\partial C_{me,i}(y,t)}{\partial t} = D_{me,i}\frac{\partial^2 C_{me,i}(y,t)}{\partial y^2} \qquad (i = 1.....n) \tag{5-1}$$

Where, $C_{me,i}$ is the VOC concentration in the ith layer, ($\mu g/m^3$), $D_{me,i}$ is the VOC diffusion coefficient of the ith layer, (m^2/s), n is the total number of the material layers, y is the coordinate in which VOC diffusion in the material takes place, (m), and t is time, (s).

II. Dry/wet or wet/dry material assembly

VOC emissions from wet materials are characterized with high initial emission rates and fast decays, followed by low emission rates and slow decays. This can be explained by three emission phases from wet materials: evaporation dominant phase (wet material), transition phase (relatively wet), and internal diffusion controlled phase (completely dry). For wet materials, such as glue and wood stain, the initial VOC concentration within the materials is very high; therefore, the dependence of VOC diffusion coefficient on VOC concentration cannot be ignored, that is:

$$D_{me,wet} = f(C_{me,wet}) \tag{5-2}$$

Empirical models are usually used to express the diffusion coefficient as a function of the concentration. Yang et al. (2001[c]) studied wet coating materials applied to absorptive substrates: he used a third order empirical equation to describe the dependence of $D_{me,wet}$ on VOC concentration. This third order empirical equation is not valid when wet material is totally dry. In the numerical study that follows, we used a second order empirical equation (Eq. (5-3)) developed by Bodalal (1999) to simulate both the wet phase and the dry phase of the wet materials.

$$D_{me,wet} = D_{me0,wet}\left(\frac{C_{me,wet}}{C_{meo,wet}}\right)^2 + D_{me,dry}\left(1-\left(\frac{C_{me,wet}}{C_{meo,wet}}\right)^2\right) \tag{5-3}$$

Where, $D_{me,wet}$ is the VOC diffusion coefficient of the wet material, (m^2/s), $D_{me0,wet}$ is the initial VOC diffusion coefficient of the wet material, (m^2/s), $D_{me,dry}$ is the VOC diffusion coefficient of the dried wet material, (m^2/s), $C_{me,wet}$ is the VOC concentration in the wet material, ($\mu g/m^3$), and $C_{me0,wet}$ is the initial VOC concentration in the wet material, ($\mu g/m^3$).

Thus, the transient VOC diffusion in the wet material can be expressed as:

$$\frac{\partial C_{me,wet}(y,t)}{\partial t} = \frac{\partial}{\partial y}\left(D_{me,wet} \frac{\partial C_{me,wet}(y,t)}{\partial y} \right) \tag{5-4}$$

Combining Equations (5-1) and (5-4) gives the transient VOC diffusion expression for the dry/wet or wet/dry material assembly:

$$\frac{\partial C_{me,i}(y,t)}{\partial t} = \frac{\partial}{\partial y}\left(D_{me,i} \frac{\partial C_{me,i}(y,t)}{\partial y} \right) \qquad (i = 1.....n) \tag{5-5}$$

b) Material /air interface

At the material surface and very near surrounding, VOC adsorption and desorption occur instantaneously and always at equilibrium. When the VOC concentration at the material surface is higher than the VOC concentration in the surrounding air, the VOC will be transported to the surrounding air. At atmospheric pressure, for a low VOC concentration, the equilibrium relationship between the VOC concentration in the near surface air phase and the VOC concentration in the material phase can be described by:

$$C_{me,i}(b_e,t) = k_e C_{aes} \tag{5-6}$$

Where, $C_{me,i}\ (b_e,t)$ is the VOC concentration at the top layer material surface, ($\mu g/m^3$), C_{aes} is the VOC concentration in the near emission material surface air, ($\mu g/m^3$), k_e is the top layer material/air partition coefficient, and b_e is the thickness of the multi-layer material, (m).

c) Mass transfer in the boundary layer

The VOC mass transfer in the boundary layer is mainly through convection and diffusion. The rate of VOC mass transfer in the boundary layer can be expressed as:

$$R_e = h_e(C_{aes} - C_a) \tag{5-7}$$

Where, R_e is the VOC emission rate, ($\mu g/m^2 s$), h_e is the convective mass transfer coefficient over the emission material, (m/s), and C_a is the VOC concentration outside the boundary layer, ($\mu g/m^3$).

d) Initial and boundary conditions

I. Initial conditions:

It is assumed that each material layer is homogeneous and has a uniform initial concentration of

$$C_{me,i}(y,0) = C_{me0,i} \tag{5-8}$$

Where $C_{me0,i}$ is VOC initial concentration in the i^{th} layer, ($\mu g/m^3$).

II. Material /material interface

VOC flux through an adjacent material interface is described by:

$$-D_{me,i}\left.\frac{\partial C_{me,i}(y,t)}{\partial y}\right|_{y=b_i} = -D_{me,i+1}\left.\frac{\partial C_{me,i+1}(y,t)}{\partial y}\right|_{y=b_i} \tag{5-9}$$

Where, b_i is the height from the material bottom to the i^{th} layer top surface, (m), $C_{me,i+1}$ is the VOC concentration in the $i+1^{th}$ layer, ($\mu g/m^3$) and $D_{me,i+1}$ is the VOC diffusion coefficient of the $i+1^{th}$ layer, (m^2/s).

For each dry material /air interface, one can write:

$$C_{me,i}(b_i,t) = k_{e,i}C_{aes} \tag{5-10}$$

$$C_{me,i+1}(b_i,t) = k_{e,i+1}C_{aes} \tag{5-11}$$

Dividing Equation (5-10) by Equation (5-11) gives the expression for a dry/dry material interface:

$$C_{me,i}(b_i,t) = C_{me,i+1}(b_i,t)\frac{k_{e,i}}{k_{e,i+1}} \tag{5-12}$$

However, for a wet/dry material interface, the amount of the wet material applied is usually small, the dry material quickly absorbs the wet material after application (Yang et al. 2001[c]). Thus, VOC concentration is assumed to be continuous at the wet/dry material interface.

$$C_{me,i}(b_i,t) = C_{me,i+1}(b_i,t) \tag{5-13}$$

III. Boundary conditions:

It is assumed that there is no VOC transfer through the bottom of the multi-layer material.

$$-D_{me,i}\frac{\partial C_{me,i}(y,t))}{\partial y}\bigg|_{y=0} = 0 \tag{5-14}$$

At the material /air interface, the mass balance can be written as:

$$-D_{me,i}\frac{\partial C_{me,i}(y,t)}{\partial y}\bigg|_{y=b_e} = h_e(C_{aes} - C_a) = h_e\left(\frac{C_{me,i}(b_e,t)}{k_e} - C_a\right) \tag{5-15}$$

5.2.2 Sink model

The process of VOC sinks by a material are opposite to the process of VOC emissions from a material. That means that, the direction of the mass fluxes depends on the direction of the concentration gradient. When the VOC concentration within the material is lower than the VOC concentration in the room air, VOC pass its overlying boundary layer and transport to the material surface. At the material/air interface, the VOC change from the gas phase to the material phase. Finally, VOC at the material surface will diffuse into the material, as shown in Figure 5-2.

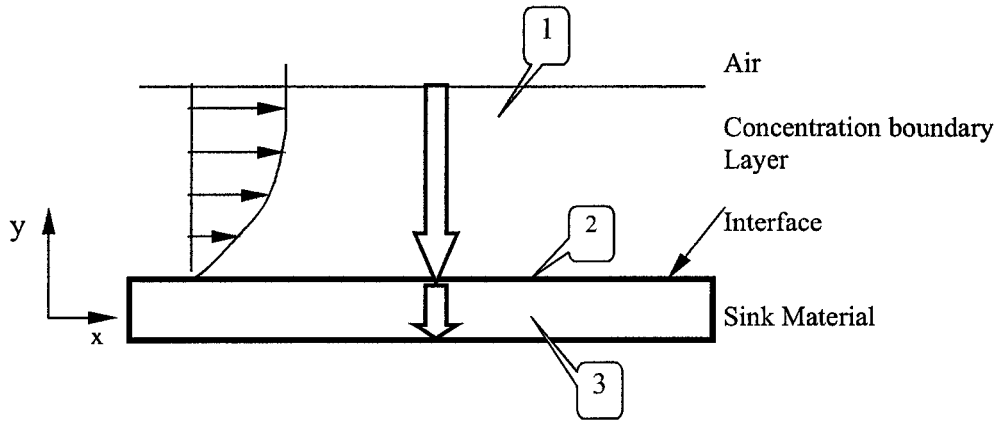

Figure 5-2 Physical configuration of VOC sinks by a building material. 1: external convection and diffusion; 2: material/air interface sorption; 3, internal diffusion.

a) Mass transfer in the boundary layer

VOC mass transfer rate in the mass boundary layer can be expressed as:

$$R_s = h_s(C_{ass} - C_a) \tag{5-16}$$

Where, R_s is the VOC sink rate, ($\mu g/m^2.s$), h_s is the convective mass transfer coefficient over the sink material, (m/s) and C_{ass} is the VOC concentration in the near sink material surface air, ($\mu g/m^3$).

b) Material /air interface

At the material/air interface, the material is the adsorbent and the VOC gas is the adsorbate. The material exerts an attractive force normal to the surface plane. Consequently, the concentration of VOC at the material phase exceeds that in the gas phase. VOC adsorption and desorption at the material/air interface are always at

equilibrium and from modeling point of view an instantaneous process. For low concentration and isotherm conditions, the VOC concentration in the gas phase and in the material phase are related through the linear isotherm:

$$C_{ms}(b_s,t) = k_s C_{ass} \tag{5-17}$$

Where, $C_{ms}(b_s,t)$ is the VOC concentration at the sink material surface, ($\mu g/m^3$), k_s is the sink material/air partition coefficient and b_s is the thickness of the sink material, (m).

c) Mass transfer within the material

For a dry material with homogeneous diffusivity, the transient VOC diffusion in the sink material can be expressed as a one-dimensional diffusion equation:

$$\frac{\partial C_{ms}(y,t)}{\partial t} = D_{ms}\frac{\partial^2 C_{ms}(y,t)}{\partial y^2} \tag{5-18}$$

Where, C_{ms} is the VOC concentration in the sink material, ($\mu g/m^3$) and D_{ms} is the VOC diffusion coefficient of the sink material, (m^2/s).

d) Initial and boundary conditions

I. Initial conditions:

It is assumed that the initial VOC concentration within the sink material is:

$$C_{ms}(y,0) = C_{s0} \tag{5-19}$$

Where, C_{s0} is the initial VOC concentration in the sink material, ($\mu g/m^3$).

II. Boundary conditions:

It is also assumed that there is no VOC transfer through material bottom.

$$-D_{ms}\left.\frac{\partial C_{ms}(y,t))}{\partial y}\right|_{y=0}=0 \tag{5-20}$$

At the material /air interface, the mass balance can be written as:

$$-D_{ms}\left.\frac{\partial C_{ms}(y,t)}{\partial y}\right|_{y=b_s}=h_s(C_{ass}-C_a)=h_s\left(\frac{C_{ms}(b_s,t)}{k_s}-C_a\right) \tag{5-21}$$

5.2.3 VOC concentration in a room

The room has multi-layer source materials and a single layer sink materials. It is assumed that VOC is well mixed within the room air. The configuration of the room is shown in Figure 5-3.

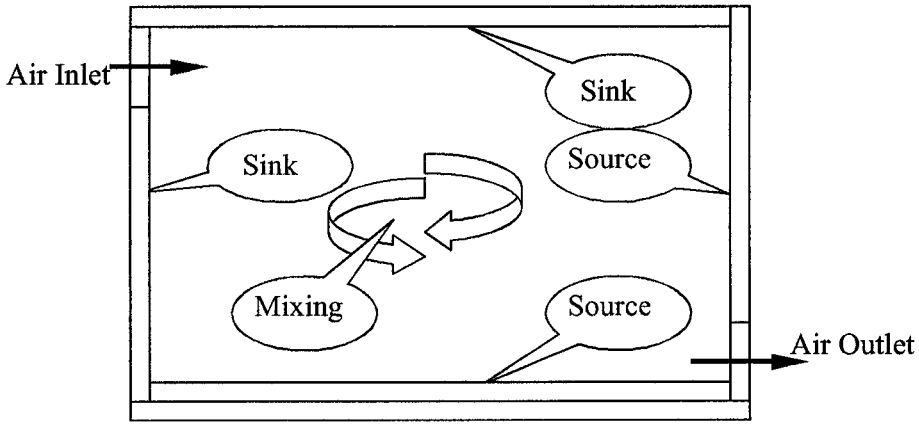

Figure 5-3 Physical configuration of the room

a) VOC mass balance

The transient VOC mass balance in the room can be expressed by:

$$V\frac{\partial C_a(t)}{\partial t} = VNC_{in} - VNC_a + \dot{m}_{source} + \dot{m}_{\sin k} \tag{5-22}$$

Where:

$$\dot{m}_{source} = -A_e D_{me,i} \left.\frac{\partial C_{me,i}(y,t))}{\partial y}\right|_{y=b_e} = A_e h_e (C_{aes} - C_a)$$

$$\Rightarrow \dot{m}_{source} = A_e h_e (\frac{C_{me,i}(b_e,t)}{k_e} - C_a) \tag{5-23}$$

$$\dot{m}_{\sin k} = -A_s D_{ms} \left.\frac{\partial C_{ms}(y,t))}{\partial y}\right|_{y=b_s} = A_s h_s (C_{aes} - C_a)$$

$$\Rightarrow \dot{m}_{\sin k} = A_s h_s (\frac{C_{ms}(b_s,t)}{k_s} - C_a) \tag{5-24}$$

Substituting Equations (5-23) and (5-24) into Equation (5-22) gives:

$$V\frac{\partial C_a(t)}{\partial t} = VNC_{in} - VNC_a + A_e h_e (\frac{C_{me,i}(b_e,t)}{k_e} - C_a) - A_s h_s (C_a - \frac{C_{ms}(b_s,t)}{k_s}) \text{ or}$$

$$\frac{\partial C_a(t)}{\partial t} = NC_{in} - NC_a + L_e h_e (\frac{C_{me,i}(b_e,t)}{k_e} - C_a) - L_s h_s (C_a - \frac{C_{ms}(b_s,t)}{k_s}) \tag{5-25}$$

Where, N is the air exchange rate, (s^{-1}), L_e is the source-material loading factor, (m^2/m^3), L_s is the sink-material loading factor, (m^2/m^3), V is volume of the room, (m^3), A_e is area of the source material, (m^2) and A_s is area of the sink material, (m^2).

b) Initial conditions

The initial room air VOC concentration is the VOC background concentration:

$$C_a(0) = C_{a0} \tag{5-26}$$

Where, C_{a0} is the initial room air VOC concentration, ($\mu g/m^3$).

It is also assumed that supply air is clean: VOC concentration is zero.

$$C_{in} = 0 \tag{5-27}$$

There are four key parameters which need to be determined in this integrated IAQ model: the diffusion coefficient of each material layer ($D_{m,i}$); the material/air partition coefficient of each material layer (k_i); the initial concentration in each material layer ($C_{0,i}$); and the convective mass transfer coefficient (h). The first three parameters are usually determined experimentally. For dry materials, the convective mass transfer coefficient can be estimated using Sherwood number, Reynolds number and Schmidt number correlations (White, 1988). The procedure for estimation of the convective mass-transfer-coefficient was discussed in chapter 3. For wet materials, the convective mass transfer coefficient can be determined using the correlations developed by Sparks et al. (1996) or Haghighat and Zhang (1999).

5.2.4 Numerical techniques

The TDMA method (Patankar, 1980) was used to simultaneously solve the discretized governing Equations (5-1) or (5-5), (5-6)~(5-7), (5-16)~(5-18), and (5-25) with their associated initial and boundary conditions. There were three main simulation domains: emission material domain, room air domain, and sink material domain. VOC mass transfers between domains through domain interface. Around 100 nodes/cm were assigned for the emission/sink materials. The room air domain was represented by one node, which was VOC concentration in the room air. The numerical simulation can provide the material VOC emission rates; the material VOC sink rates, the room air VOC concentrations, the VOC distributions inside the material and the normalized emitted mass.

5.3 MODEL VALIDATION

The integrated IAQ model predictions were compared with the experimental results of carpet-adhesive assembly VOC emissions (Low et al., 1998). The experiments were carried out in a small-scale stainless steel chamber of $1.0\times0.8\times0.5$ m^3 at a temperature 23 ± 1.3 ^0C, relative humidity $45.5\pm3\%$. The chamber consisted of an inner and an outer chamber. The outer chamber, which housed the inner chamber, was located in the test room. The inner chamber housed the test assembly. An axial fan was used to circulate the air through the inner chamber. The inner chamber had screened attachments at the air inlet and outlet to provide uniform air flow and to create several levels of turbulence, as shown in Figure 5-4. The primary test materials were carpet and adhesive. The 28 oz level-loop nylon (polypropylene) carpet was of graphic constriction, made using 100%

nylon fiber (space dyed) and synthetic jute textured back. The synthetic latex based adhesive had a 3% mineral spirit content. The concrete slab (0.25m×0.5m×0.04m) was used as the substrate. In the experiments, the concrete slab was coated with the adhesive and the carpet was placed on the adhesive. Velocities in the range of 0.01m/s to 0.25m/s were imposed along the carpet-adhesive assembly with either a low or a high turbulence level. The concentrations of TVOC, nonane decane and 4-phenylcyclohexane (4PC) were measured as a function of time.

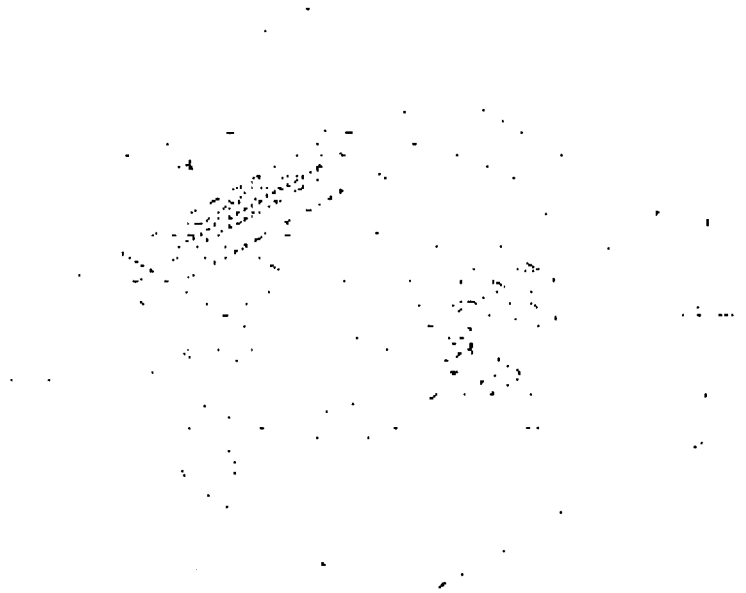

1. Outer Chamber
2. Inner Chamber
3. Flow Setting Screens
4. Perforated Plate
5. Glass Window
6. Inner Chamber Support
7. Sample Container
8. Buffer Plate
9. Fan Unit
10. Dc Motor

Figure 5-4 Schematic of the outer and inner chamber assembly (from: Low et al., 1998)

The experimental results of decane emission from carpet-adhesive assembly at air velocity of 0.04m/s (test 4), 0.1m/s (test 5) with low turbulence level were used to examine the model performance. The stainless steel chamber sink effect was ignored. For integrated IAQ model simulation, some unknown physical parameters must be determined for each test material (carpet, adhesive): the initial concentration in each material layer, the diffusion coefficient of the material, and the partition coefficient.

Decane originates from the adhesive; the initial concentration of decane in the carpet is zero. Since the initial concentration does not affect the shape of the emission curve (Yang et al., 2001[d]), it can be initially assumed as an arbitrary value in the adhesive, and later be adjusted based on the model prediction and the experimental data. The diffusion coefficient of decane in the adhesive can be obtained from literature (Bodalal 1999). Although direct measurements of diffusion coefficient and partition coefficient of decane in carpet are available (Bodalal et al., 2000), those data cannot be used because of the uncertainty in the carpet used. However, study showed that the partition coefficient only affects short-term emissions, and it has virtually no impact on long-term emissions (Yang et al., 2001[d]). Therefore, in the model simulation, the measurement data (Bodalal 1999) was used to approximately estimate the partition coefficient of decane at carpet/ air interface. The diffusion coefficient of decane in the carpet was obtained by fitting the model predictions with the experimental data. The experimental and simulation parameters are given in Table5-1.

Figures 5-5 to 5-6 show the comparison of the predicted decane emission rates with the experimental results for carpet-adhesive assembly. The experiments were carried out for 200 hours. There is a good agreement between predicted rates and experimental measurement. There are some minor discrepancies between predicted results and experimental results during the initial hours (<30 hours), Figure 5-5. This may be due to instability and partial mixing in the chamber at the beginning of the tests. In the mid term (30 hours~80 hours), the model slightly overestimates the decane emission rate, and in the long term (>80 hours), the model slightly underestimates the decane emission rate,

Figure 5-6. This may be due to the small substrate effect of concrete slab, which was not considered in the model simulations because of a lack of sufficient data. This small substrate effect delays the decane emission at the beginning, and elevates it as time progresses. Generally, the predicted results and experimental results closely follow the same trend.

Table 5-1 Experimental and simulation parameters (Temp. =23 ^{0}C).

Test Parameters					
Test	Carpet Area (m^2)	Adhesive mass (g)	Air flow (Lpm)	Average velocity (m/s)	Average Turb. (k/u^2)
4	1.24×10^{-1}	59.10	6.67	0.04	0.03×10^{-1}-L
5	1.24×10^{-1}	55.20	6.67	0.10	0.04×10^{-1}-L

Simulation Parameters					
Material	Thickness (mm)	$C_{me0,i}$ ($\mu g/m^3$)	k (—)	$D_{me,i}$ (m^2/s)	Air exchange rate (h^{-1})
Carpet (backing)	2.00	0.00	1.46×10^{4}	8.00×10^{-11}	1.00
Adhesive	Test 4: 4.37×10^{-1} Test 5: 4.08×10^{-1}	3.60×10^{9}	-	Wet: 2.92×10^{-10} Dry: 8.92×10^{-13}	1.00

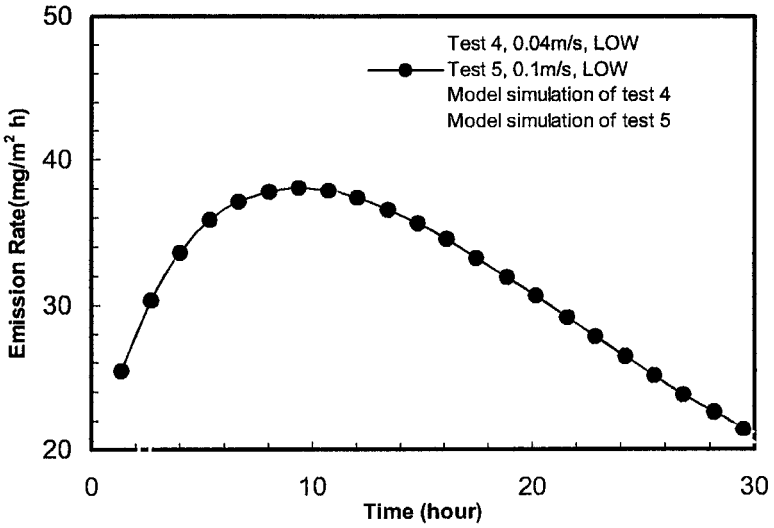

Figure 5-5 Comparison of decane emission rates (first 30 hour data)

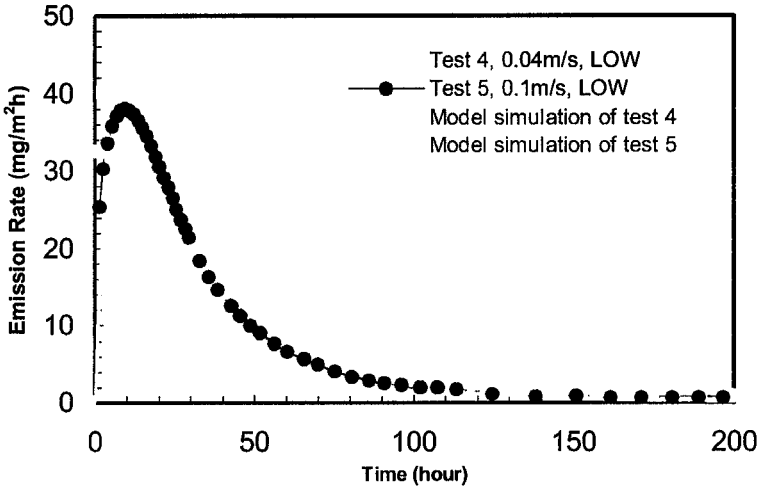

Figure 5-6 Comparison of decane emission rates (full data set)

5.4 MULTI-LAYER MATERIAL VOC EMISSION – SOURCE EFFECT

Following the validation of the integrated IAQ model, the model was applied to a room with a typical floor assembly (vinyl floor tile/glue/plywood) as the source material and with no sink materials to study the multi-layer material VOC emission characteristics. Benzene was chosen as the compound of interest, since it is commonly found both in vinyl floor tile and plywood. The dimensions of the floor assembly were 3.0×3.0×0.0197 m^3, and it was placed in a room with dimensions of 3.0×3.0×2.5 m^3. The room was kept at a temperature of 23 °C and with an air exchange rate of $0.5h^{-1}$. An air velocity of 0.1 m/s was considered over the floor assembly. The benzene diffusion coefficient and partition coefficient in the vinyl floor tile and in the plywood were taken from literature (Bodalal, 1999), and the benzene diffusion coefficient in the glue was assumed to be 1.0×10^{-11} (m^2/s). The initial benzene concentrations in the plywood and vinyl floor tile were assumed to be 1.0×10^{7} ($\mu g/m^3$). All the input parameters are shown in Table 5-2. In order to compare the multi-layer material VOC emission characteristics with the single-layer material, the simulation was first carried out for vinyl floor tile/glue/ plywood assembly, then it was carried out only for the plywood and the vinyl floor tile (VF). The simulation was carried out for 360 hours.

Table 5-2 Simulation parameters of benzene

Materials	Plywood	Glue	Vinyl floor tile
h_e (m/s)	2.45×10^{-4}	2.45×10^{-4}	2.45×10^{-4}
$D_{me,i}$ (m^2/s)	4.92×10^{-10}	1.00×10^{-11}	1.06×10^{-10}
k(—)	184	-	310
$C_{0,i}$($\mu g/m^3$)	1.00×10^{7}	0.00	1.00×10^{7}
b_i(m)	1.60×10^{-2}	0.70×10^{-3}	0.30×10^{-2}

Figure 5-7 shows the comparison of benzene concentration in the air. It demonstrates that benzene concentration in the air is initially very high and decays rapidly when the plywood or vinyl floor tile is directly exposed to the room air. However, the room air benzene concentration for the floor assembly (vinyl floor tile/glue/plywood) is initially the same as that for the vinyl floor tile and it slowly decays. This indicates that the floor assembly first shows the same emission characteristics as the top layer material vinyl floor tile, and the vinyl floor tile strongly delays benzene emission from the bottom layer material plywood. Figure 5-7 also shows, as time progressed, room air benzene concentration for the floor assembly case becomes higher than that for room air benzene concentration for the plywood or the vinyl floor case alone, which means that floor assembly has a longer emission time than its single-layer material.

Figure 5-8 shows the comparison of benzene emission rates. It indicates that benzene emission rate of the plywood directly exposed to the air is initially much higher than that of the plywood in the floor assembly. The floor assembly initially shows the same benzene emission rate as that of the vinyl floor tile. However, as time progressed benzene emission rate of the floor assembly becomes higher than that of the plywood or the vinyl floor tile alone.

This behavior is because of the slow internal diffusion of the multi-layer material. Initially, VOC concentration in the bottom layer material has not reached the top layer material. Thus, initially the multi-layer material shows the same emission characteristics as of the top (single) layer material. As time progresses, VOC from the bottom layer diffuses into the top layer(s). This causes VOC concentration in the top layer material

higher than that of single layer material case alone. The consequent higher VOC concentration of the top layer material results to a higher VOC emission rate from multi-layer material than a single-layer material as time progressed. These phenomena will result in higher room air VOC concentration for a multi-layer material than for a single-layer material. That means the room occupants will be exposed to a higher VOC concentration for a longer period of time.

These results agree very well with the normalized emitted masses, as shown in Figure 5-9. Compared with the plywood, the vinyl floor tile has a low benzene diffusion coefficient. However, it has a higher normalized emitted mass than the plywood. This is because the vinyl floor tile is much thinner than the plywood. Figure 5-9 also demonstrates that vinyl floor tile/glue/ plywood assembly has a much longer emission time than the plywood or the vinyl floor tile. This indicates that material thickness plays an important role in determining VOC emission time. Usually, for the materials, which have the same diffusivity, the thinner one has a shorter VOC emission time.

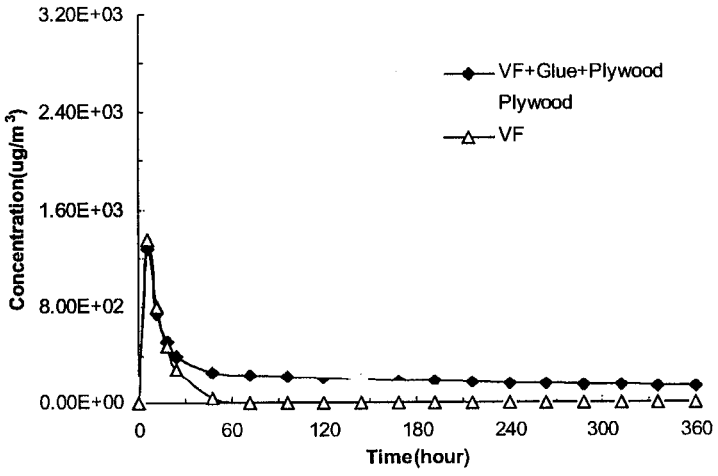

Figure 5-7 Comparison of benzene concentrations in the air

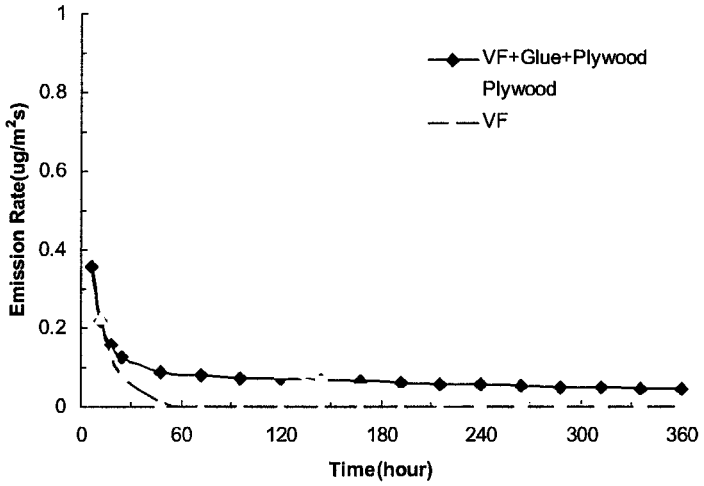

Figure 5-8 Comparison of benzene emission rates

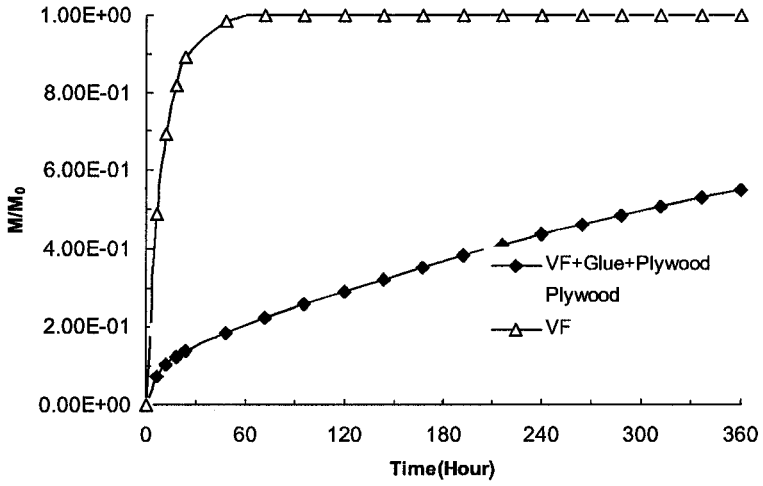

Figure 5-9 Comparison of benzene normalized emitted masses

5.5 SUBSTRATE AND SINK EFFECTS

To study the material substrate and sink effects, the integrated IAQ model was applied to a mechanically ventilated room. The room dimension was 3.0×3.0×2.5 m^3 and its floor was furnished with a floor assembly of 3.0×3.0×0.0197 m^3 and its walls were covered by

the plywood. Decane was chosen as the compound of interest, since decane is one of the major VOC compounds in glue and is not found in the plywood and vinyl floor tile. The room was kept at a temperature of 23 °C, and with an air exchange rate of $0.5h^{-1}$. The air velocity in the room was assumed to be 0.1 m/s. Decane diffusion coefficients and partition coefficient of the vinyl floor tile, glue and plywood were taken from literature (Bodalal, 1999). The initial decane concentration in the glue was assumed to be 1.0×10^{8} ($\mu g/m^3$). All input parameters are shown in Table 5-3.

Table 5-3 Simulation parameters of decane

Materials	Plywood	Glue	Vinyl floor tile
h_e (m/s)	2.45×10^{-4}	2.45×10^{-4}	2.45×10^{-4}
D_{me} (m^2/s)	1.28×10^{-11}	Wet: 2.92×10^{-10} Dry: 8.92×10^{-13}	2.09×10^{-12}
k(—)	6.95×10^{3}	-	1.31×10^{4}
C_0($\mu g/m^3$)	0.00	1.00×10^{8}	0.00

Simulation was first carried out for decane emission from the floor assembly without considering the plywood substrate effect. The simulations then were carried out for the floor assembly with the plywood and finally for the plywood walls as the sink materials and the floor assembly as the source material. The total simulation time was 60 days (1440 hours).

Figure 5-10 shows the comparison of room air decane concentrations for the cases with and without the plywood substrate effect. Room air decane concentration is much higher and decays faster for the case without plywood substrate effect than for the case with the plywood substrate effect. This agrees very well with the comparison of decane emission

rate as shown in Figure 5-11. Without the plywood substrate effect, the floor assembly shows a high decane emission rate. This is due to the reason that some of the decane in the glue diffuses to the plywood substrate initially; and as time progresses, decane concentration in the plywood increases and decane concentration in the glue decreases until they reach the equilibrium. After that, decane in the plywood starts to diffuse into the glue and vinyl floor tile. This kind of diffusion phenomena inside the floor assembly (with plywood substrate effect) makes the decane emission rate initially relatively low and decay slowly compared with the case without plywood substrate effect. This demonstrates that the plywood substrate significantly affects the decane emission from the floor assembly. Without considering the plywood substrate, the decane emission rate is largely overestimated.

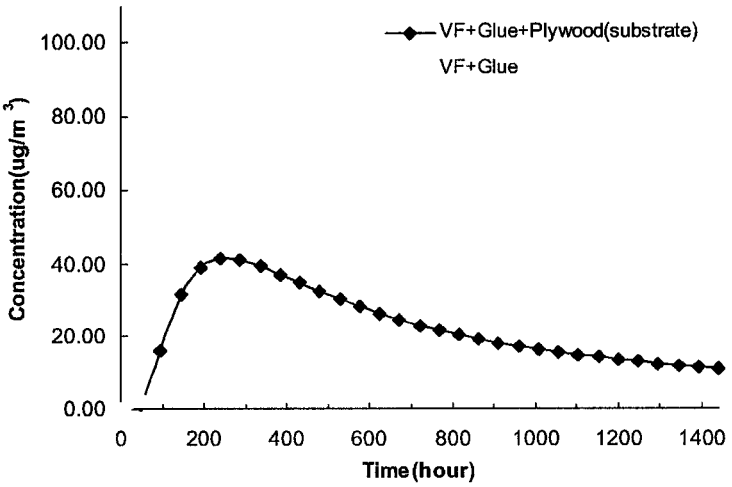

Figure 5-10 Comparison of decane concentrations in the air (substrate effect)

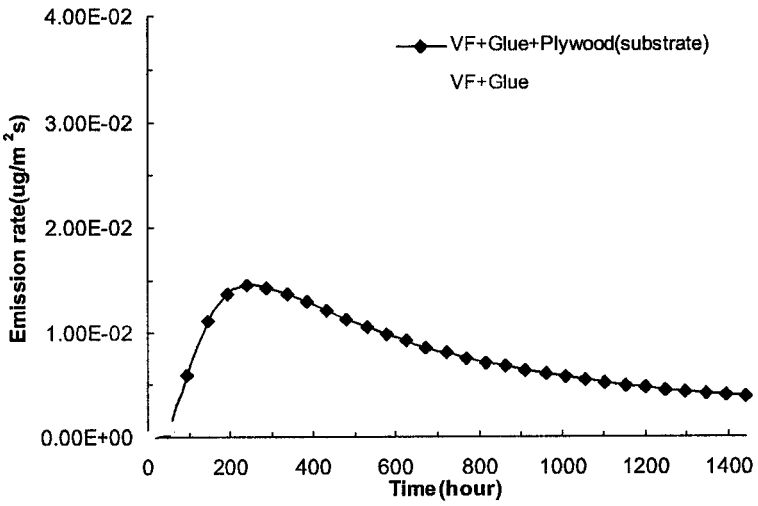

Figure 5-11 Comparison of decane emission rates (substrate effect)

Figure 5-12 shows the comparison of decane concentrations in the air for the cases with and without the plywood wall. With plywood wall, sink effect, decane peak concentration is reduced initially. As time progresses, decane concentration is elevated. However, the discrepancy between with and without considering the plywood wall sink effect is not very significant. Figure 5-13 shows the comparison of decane emission rates and sink rate. Decane emission rate from the floor assembly is almost the same with and without considering the plywood wall sink effect. Even though the simulation data shows that the decane emission rate has a small increase in the initial time and later a small decrease with considering the plywood wall sink effect. Figure 5-13 also shows the decane sink rate of the plywood walls. Decane sink rate increases as decane concentration in the air increases, and vice-versa as decane concentration in the air decreases. As the concentration decreases the sink rate decreases and eventually reaches zero. From this moment, the plywood walls act as source material and start to emit decane rather than acting as sink materials. There are two reasons, which lead to the low VOC sink rate of

the material. One reason is the low room air VOC concentration. The other reason is the low VOC diffusivity of the material. VOC transports from the air to the material is a very slow process due to the extremely low VOC diffusivity of the material, which also leads to the small sink rate of the building materials. Therefore, this low sink rate only has a marginal influence on the VOC concentration in the room air, which also has a negligible influence on VOC emissions from the source material.

Results agree very well with the normalized emitted masses, as shown in Figure 5-14. The plywood wall sink effect does not have a significant influence on the floor assembly decane emission. However, the plywood substrate effect has a significant impact on the floor assembly decane emission. Without considering the plywood substrate effect, the floor assembly decane emission time is largely underestimated.

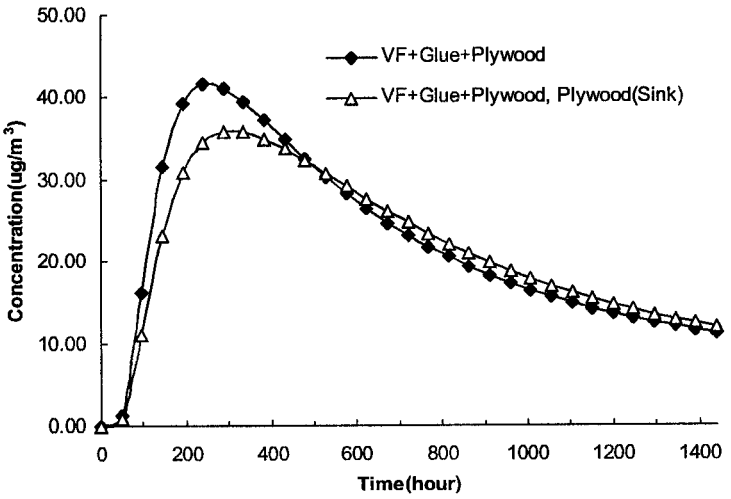

Figure 5-12 Comparison of decane concentrations in the air (sink effect)

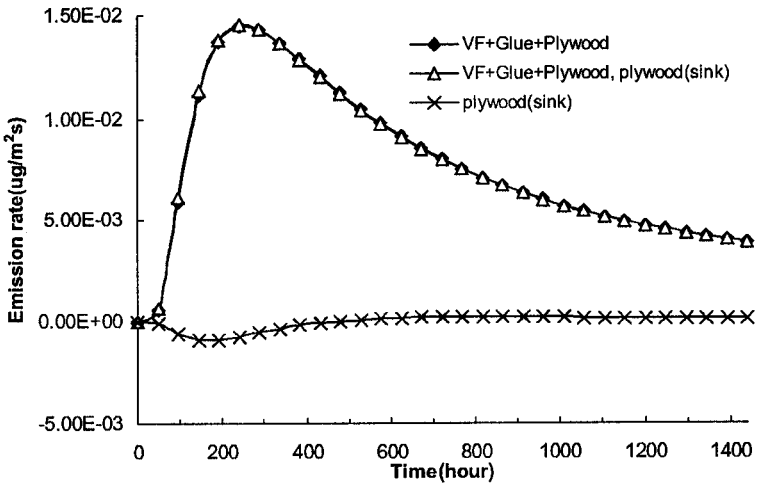

Figure 5-13 Comparison of decane emission rates (sink effect)

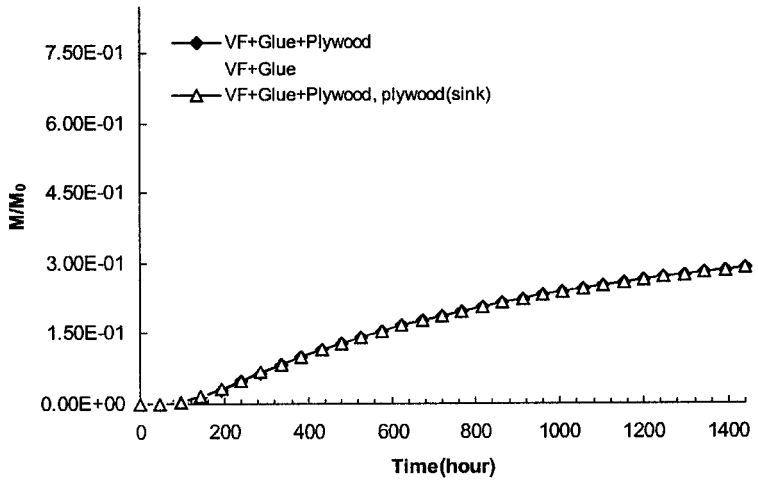

Figure 5-14 Comparison of normalized emitted masses of decane

The plywood substrate effect is also demonstrated in Figure 5-15. The Decane concentration distribution inside the floor assembly indicates that the decane concentration inside the plywood is building up as time progresses.

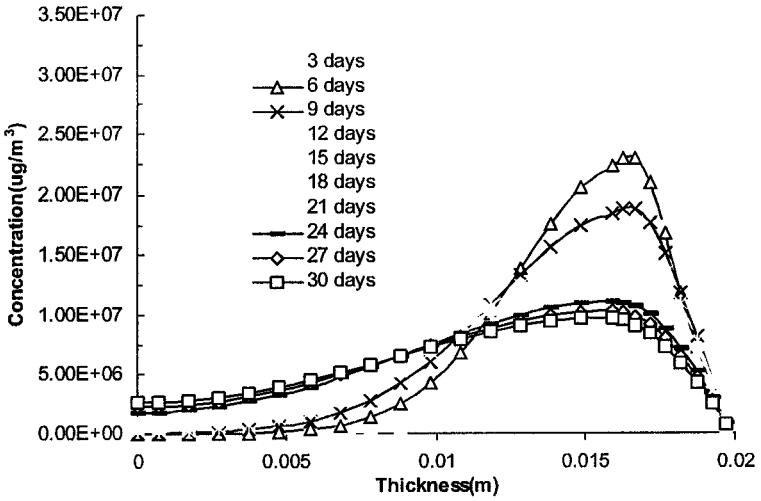

Figure 5-15 Decane concentration distribution inside the multi-layer material (VF+Glue+Plywood)

5.6 SUMMARY

An integrated IAQ model was developed to predict VOC emission rates of a multi-layer material, VOC sink rates of a material, VOC concentration in a room with both VOC source and sink materials, and VOC concentration distribution within a material. The integrated IAQ model included a multi-layer material emission model, a single-layer material sink model and a room VOC concentration model. The integrated IAQ model used four parameters: the diffusion coefficient of each material layer ($D_{m,i}$); the material/air partition coefficient of each material layer (k_i); the initial concentration in each material layer ($C_{0,i}$); and the convective mass transfer coefficient (h). The first three parameters are the property of the material and can be determined by experiments. The last parameter, h, can be estimated by using the fundamentals of fluid dynamics.

The predictions of the model were been validated with experimental results of carpet-adhesive assembly VOC emissions from the specially designed test. The results indicated that there was generally good agreement between the model predictions and the experimental results.

The integrated IAQ model was first applied to a room with a typical floor assembly (vinyl floor tile/glue/plywood), and the results were compared with single-layer material (vinyl floor tile or plywood) results. The comparisons indicated that multi-layer material first showed the same emission characteristics as the top layer material, and the top layer materials strongly delayed VOC emissions from the bottom layer materials. Compared with the single-layer material, the multi-layer material had a much longer VOC emission time and a slower VOC decay rate.

The integrated IAQ model was further applied to a room with a floor assembly (vinyl floor tile/glue/plywood) as the source material, and with plywood walls as the sink in order to study the material substrate and sink effects. Results indicated that the plywood substrate significantly affected the floor assembly decane emission. Without considering the plywood substrate effect, the decane emission rate was greatly overestimated. Results also indicated that the plywood wall sink effect reduced the peak decane concentration in the room initially and elevated decane concentration in the room as time progressed. However, The plywood sink effect on decane emission rate and decane concentration in the room was not significant.

CHAPTER 6 AN INTEGRATED ZONAL MODEL FOR PREDICTING TRANSIENT VOC DISTRIBUTION IN A VENTILATED ROOM

6.1 INTRODUCTION

The developed single-layer material emission model (Chapter 3) and the integrated IAQ model (Chapter 5) were based on the assumption that room air VOC concentration is well mixed. They are total mixing models, in which the room is treated as a mono-zone and the room air concentration is given by a single value. Therefore, it cannot provide detailed VOC concentration distribution within a room. Actually, VOC concentration varies in the space and is influenced by the characteristics of a room, such as ventilation system strategies, temperature distribution, etc. A detailed knowledge of VOC distribution is important for local pollutant control. A CFD model can provide detailed knowledge of air flow, temperature and contaminant distributions within a room, but it is too complicated to be used as a daily design tool. It is however too time consuming and expensive. Except in certain cases, users are not interested in excessively detailed results obtained from CFD models. Zonal models are intermediate models between CFD models and mono-zone models. Compared to mono-zone models, zonal models can provide users with an estimated view of airflow, temperature and contaminant distribution within a room. Zonal models have advantages over CFD models in its simple use and time saving characteristics (Haghighat et al., 2001 and Axley, 2001).

Zonal models have been widely applied in building simulations. For example, zonal models were integrated with convection, conduction and radiation heat transfer models to predict the temperature distribution within a room (Inard et al., 1996; Wurtz et al., 1999[a]; Wurtz et al., 1999[b] and Musy et al., 2001). Haghighat et al.(2001) and Rutman et al. (2002) adopted zonal model to predict thermal comfort in a room, such as PPD (Predicted Percentage of Dissatisfied). Mendonca et al. (2002) developed a zonal model to predict the moisture field in a room. While, zonal models integrated with mass transfer models to simulate the contamination distribution within a room are seldom available. Recently, Molina et al. (2000) proposed a model, which considered the air movement effect using a zonal model and the sorption effect using a sorption mass transfer model. Simple theoretical results were presented in this research by assuming that the contaminant concentration in the room was constant. Although great efforts have been made in the development of the zonal models, a zonal model that integrates with material emission model in order to predict VOC distribution in a room is not yet available.

This chapter describes the development of an Integrated Zonal Model for predicting the transient VOC distribution within a ventilated room. The model integrates a three-dimensional zonal model with air jet, thermal and material emission/sink models.

6.2 ZONAL MODEL

Different zonal models distinguish themselves in terms of modeling air flow and driving forces. The zonal model developed in this thesis follows what has become the common practice in this field (Wurtz et al., 1999[a]; Wurtz et al., 1999[b] and Haghighat et al., 2001).

The physical system considered is a room with a mechanical ventilation system. The room is at a non-isothermal condition. In zonal model, it is subdivided into a number of three-dimensional small cells. The room configuration and partition are shown in Figure 6-1.

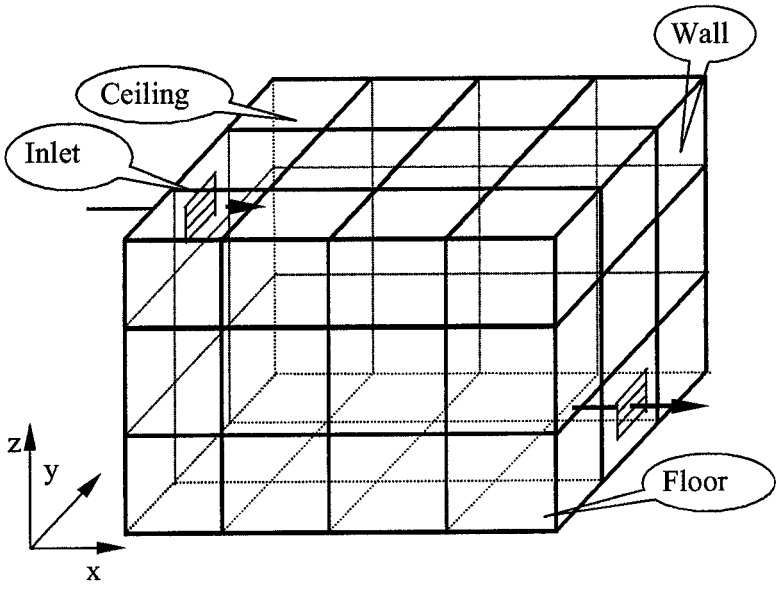

Figure 6-1 Physical configuration and partition of a room

6.2.1 Air mass conservation equations

Within each cell, pressure at the middle of each cell obeys the perfect gas law and pressure varies hydrostatically:

$$P_{m,i} = \rho_i R T_i \tag{6-1}$$

$$P_{i,h} = P_{ref,i} - \rho_i g h \tag{6-2}$$

Where,

$P_{m,i}$: pressure at the middle of cell i, Pa

ρ_i: air density of cell i, kg/m^3

R: gas constant of air, 287.055 J/kg.K

T_i: temperature of cell i, K

$P_{ref,i}$: reference pressure of the cell i, Pa, which is located at the bottom level of cell i

h: height from the bottom of cell i, m

$P_{i,h}$: pressure at the height of h in cell i, Pa

g: gravitational acceleration, m^2/s

Adjacent cells exchange mass through cell interfaces. In each cell, the general air mass balance can be written as:

$$0 = \sum_{j=1}^{6} m_{a,ij} + m_{a,source} + m_{a,\sin k} \tag{6-3}$$

Where,

$m_{a,ij}$: air flow across cell i and cell j interface, kg/s

m_{source}: air source in cell i, kg/s

m_{sink}: air sink in cell i, kg/s

Power law is applied to calculate air flow rate across the cell interface.

$$\dot{q}_{a,ij} = C_d \rho \Delta P_{ij}^n \tag{6-4}$$

Where,

$\dot{q}_{a,ij}$: air flow rate across cell i and cell j interface, kg/m^2s

ΔP_{ij} : pressure difference between cell i and cell j, Pa

C_d: coefficient of power law, m/(sPa^n), usually taken as 0.83 (Wurtz et al., 1999[a]; Wurtz et al., 1999[b] and Haghighat et al., 2001).

n: flow exponent, usually taken as 0.5 (Wurtz et al., 1999[a]; Wurtz et al., 1999[b] and Haghighat et al., 2001).

The pressure at cell bottom level is assumed to be uniform. The horizontal cell interface between two adjacent cells is shown in Figure 6-2.

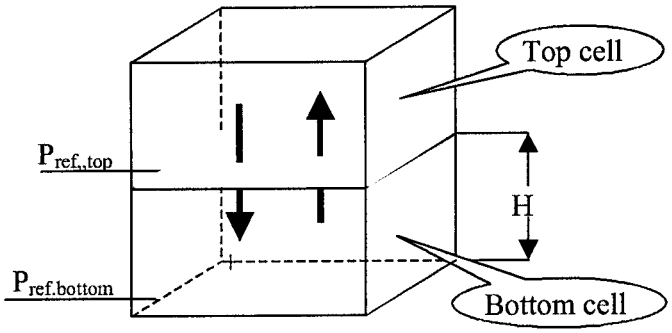

Figure 6-2 Configuration of the horizontal cell interface

For the horizontal cell interface, the air flow rate can be expressed as:

$$\dot{q}_{a,hor} = C_d \rho (P_{ref,top} - P_{ref,bottom} + \rho_{bottom} g H)^n \tag{6-5}$$

$$\Rightarrow \begin{cases} \dot{q}_{a,hor} = C_d \rho_{bottom} \left| P_{ref,top} - P_{ref,bottom} + \rho_{bottom} g H \right|^n \; if \; P_{ref,top} < P_{ref,bottom} - \rho_{bottom} g H \\ \dot{q}_{a,hor} = -C_d \rho_{top} \left| P_{ref,top} - P_{ref,bottom} + \rho_{bottom} g H \right|^n \; if \; P_{ref,top} \geq P_{ref,bottom} - \rho_{bottom} g H \end{cases} \tag{6-6}$$

Where,

$\dot{q}_{a,hor}$: air flow rate across the horizontal cell interface, kg/m^{2}s

$P_{ref,top}$: reference pressure of the top cell, Pa

$P_{ref,bottom}$: reference pressure of the bottom cell, Pa

H: height of the bottom cell, m

ρ_{bottom}: air density of the bottom cell, kg/m^3

ρ_{top}: air density of the top cell, kg/m^3

For vertical cell interface, there is a neutral plane (Z_n) where the pressure difference between the left side and the right side of the interface is zero, as shown in Figure 6-3

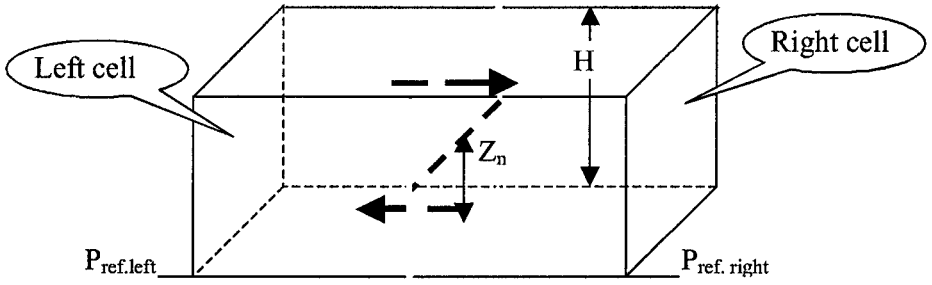

Figure 6-3 Configuration of the vertical cell interface

Therefore,

$$0 = \Delta P_{ref,LR} - \Delta\rho g Z_n \tag{6-7}$$

$$Z_n = \frac{\Delta P_{ref,LR}}{\Delta\rho g} \tag{6-8}$$

Where,

$\Delta P_{ref,LR}$: reference pressure difference between the left cell and the right cell, pa

$\Delta\rho$: density difference between the left cell and the right cell, kg/m^3

Z_n : neutral plane, m

Thus, the air flow rate below the neutral plane (0-Z_n) and above the neutral plane (Z_n-H) can be obtained by substituting Eq.(6-8) into Eq.(6-4) and integrating with respect to Z:

$$\dot{q}_{0-Z_n} = C_d \rho (\Delta\rho g)^n \frac{(Z_n)^{n+1}}{n+1} \tag{6-9}$$

$$\Rightarrow \begin{cases} \dot{q}_{0-Z_n} = C_d \rho_{left} |\Delta\rho g|^n \dfrac{|Z_n|^{n+1}}{n+1} & \text{if} \quad \rho_{left} > \rho_{right} \\ \dot{q}_{0-Z_n} = -C_d \rho_{right} |\Delta\rho g|^n \dfrac{|Z_n|^{n+1}}{n+1} & \text{if} \quad \rho_{left} < \rho_{right} \end{cases} \tag{6-10}$$

$$\dot{q}_{Z_n-H} = C_d \rho (\Delta\rho g)^n \frac{(H-Z_n)^{n+1}}{n+1} \tag{6-11}$$

$$\Rightarrow \begin{cases} \dot{q}_{Z_n-H} = -C_d \rho_{right} |\Delta\rho g|^n \dfrac{|H-Z_n|^{n+1}}{n+1} & \text{if} \quad \rho_{left} > \rho_{right} \\ \dot{q}_{Z_n-H} = C_d \rho_{left} |\Delta\rho g|^n \dfrac{|H-Z_n|^{n+1}}{n+1} & \text{if} \quad \rho_{left} < \rho_{right} \end{cases} \tag{6-12}$$

Therefore, the total air flow rate across the vertical cell interface becomes:

$$\dot{q}_{a,ver} = \dot{q}_{0-Z_n} + \dot{q}_{Z_n-H} \tag{6-13}$$

$$\Rightarrow \begin{cases} \dot{q}_{a,ver} = C_d \rho_{left} |\Delta\rho g|^n \dfrac{|Z_n|^{n+1}}{n+1} - C_d \rho_{right} |\Delta\rho g|^n \dfrac{|H-Z_n|^{n+1}}{n+1} & \text{if} \quad \rho_{left} > \rho_{right} \\ \dot{q}_{a,ver} = -C_d \rho_{right} |\Delta\rho g|^n \dfrac{|Z_n|^{n+1}}{n+1} + C_d \rho_{left} |\Delta\rho g|^n \dfrac{|H-Z_n|^{n+1}}{n+1} & \text{if} \quad \rho_{left} < \rho_{right} \\ \dot{q}_{a,ver} = C_d \rho |P_{ref.lef} - P_{ref.right}|^n & \text{if} \quad P_{ref.lef} \geq P_{ref.right} \text{ and } \rho_{left} = \rho_{right} \\ \dot{q}_{a,ver} = -C_d \rho |P_{ref.lef} - P_{ref.right}|^n & \text{if} \quad P_{ref.lef} < P_{ref.right} \text{ and } \rho_{left} = \rho_{right} \end{cases} \tag{6-14}$$

Where,

$\dot{q}_{a,0-Z_n}$: air flow rate below neutral plane, kg/m.s

$\dot{q}_{a,Z_n-H}$: air flow rate above neutral plane, kg/m.s

$\dot{q}_{a,ver}$: air flow rate across vertical cell interface, kg/m.s

$P_{ref,left}$: reference pressure of the left cell, Pa

$P_{ref,reight}$: reference pressure of the right cell, Pa

ρ_{left}: air density of the left cell, kg/m^3

ρ_{right}: air density of the right cell, kg/m^3

6.2.2 Energy conservation equations

Within each cell, temperature is assumed to be uniform. In each cell, the general energy balance can be written as:

$$0 = \sum_{j=1}^{6} Q_{T,ij} + Q_{T,source} + Q_{T,\sin k} \tag{6-15}$$

Where,

$Q_{T,ij}$: heat flow rate across cell i and cell j interface, w

$Q_{T,source}$: heat energy source in cell i, w

$Q_{T,sink}$: heat energy sink in cell i, w

Heat transfer between cells is mainly through convection:

$$Q_{T,ij} = m_{a,ij} C_p T \tag{6-16}$$

$$\Rightarrow \begin{cases} Q_{T,ij} = m_{a,ij} C_p T_j, & if\ m_{a,ij} > 0 \\ Q_{T,ij} = m_{a,ij} C_p T_i, & if\ m_{a,ij} < 0 \end{cases} \tag{6-17}$$

Heat transfer along wall surfaces is modeled by the Newton cooling law:

$$Q_{T,i-wall} = h_T A_i \Delta T_{i-wall} \tag{6-18}$$

Where,

T_i: temperature of cell i, K

T_j: temperature of cell j, K

C_p: specific heat of air, J/kgK

h_T: convective heat transfer coefficient, w/m^2 K

$\Delta T_{,i\text{-wall}}$: temperature difference between cell i and wall, K

A_i: interface area between cell i and wall i, m^2

6.3 INTEGRATING JET MODEL WITH ZONAL MODEL

6.3.1 Air jet type

Depending on the diffuser type, air jets can be classified as compact air jets, linear jets, radial air jets, incomplete radial air jets and swirling air jets (ASHRAE Fundamentals, 2001). To integrate jet models with the zonal model, the following information about the jet should be known:

- The angle of divergence of the jet boundary..
- The velocity patterns along the jet axis.
- The velocity profile at any cross section in the zone of maximum engineering importance.
- The entrainment ratios.

6.3.2 Angle of divergence

Measured angles of divergence (spread) for discharge into large open spaces usually range from 20 ^{0} to 24 ^{0} with an average of 22 ^{0}. For closely spaced multiple outlets

expand at smaller angles, average 18 ^{0}, and jet discharging into relatively small spaces show even small angles of expansion. In cases where the outlet area is small compared to the dimensions of the space normal to the jet, the jet may be considered free as long as (ASHRAE Fundamentals, 2001)

$$X \leq 1.5\sqrt{A_R} \tag{6-19}$$

Where,

X: distance from face of outlet, m

A_R: cross-sectional area of confined space normal to jet, m^2

6.3.3 Velocity patterns along the jet axis

The full length of an air jet (compact, linear, radial, or conical), in terms of the maximum of centerline velocity and temperature differential at the cross section, can be divided into four zones (ASHRAE Fundamentals, 2001), as shown in Figure 6-4.

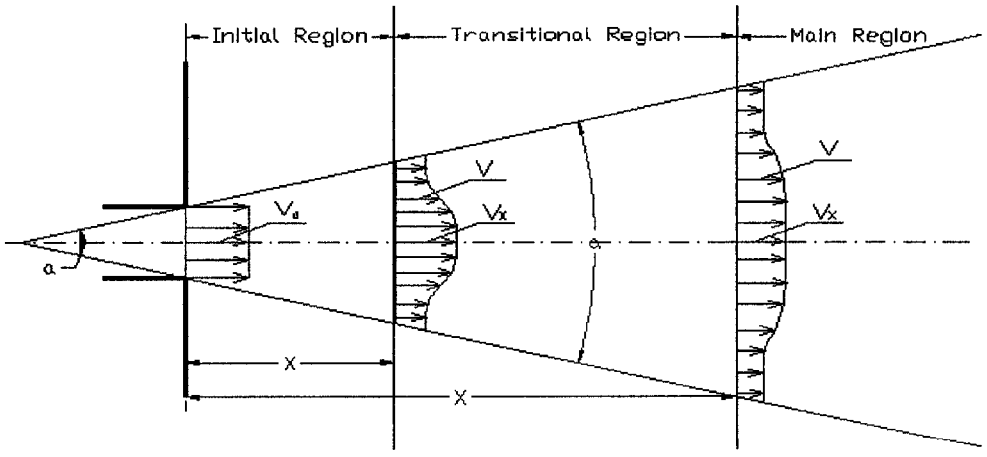

Figure 6-4 Jet expansion regions

a) Centerline velocity in zones 1

Zone 1 is a short zone, extending about four diameters or widths from the outlet face, in which the maximum velocity (temperature) of air stream remains practically unchanged. In zone 1, the ratio V_x/V_0 is constant and equal to the ratio of the center velocity of the jet at the start of expansion to the average velocity. The ratio V_x/V_0 varies from approximately 1.0 for rounded entrance nozzles to about 1.2 for straight pipe discharge. It has much higher values for diverging discharge outlets (ASHRAE Fundamentals, 2001).

b) Centerline velocity in zones 2

Zone 2 is a transition zone, the length of which depends on the type of outlet, aspect ratio of the outlet, initial air flow turbulence and so forth. Experimental evidence indicates that in zone 2 (ASHRAE Fundamentals, 2001),

$$\frac{V_x}{V_0} = \sqrt{\frac{1.13KH_0}{X}} \tag{6-20}$$

Where

V_x: centerline velocity at distance X from outlet, m/s

V_0: average velocity at discharge from outlet, m/s

H_0: width of jet at outlet, m

K: centerline velocity constant depending on outlet type and discharge pattern

X: distance from outlet to measurement of centerline velocity, m

c) Centerline velocity in zones 3

Zone 3 is a fully established turbulent flow zone that may be 25 to 100 equivalent air outlet diameters (width for slot-type air diffusers) long.

In zone 3, maximum or centerline velocities of straight flow isothermal jets can be determined with accuracy from the following equation (ASHRAE Fundamentals, 2001):

$$\frac{V_x}{V_0} = \frac{KD_0}{X} = \frac{1.13K\sqrt{A_0}}{X} \tag{6-21}$$

Where

D_0: effective or equivalent diameter of stream at discharge for open-end duct or at contracted section, m

A_0: core area or duct area, m^2

d) Centerline velocity in zones 4

In zone 4, the maximum velocity and temperature decrease rapidly. The distance to this zone and its length depend on the velocities and turbulence characteristics of the ambient air. In a few diameters of width, the air velocity becomes less than 0.25m/s. The characteristics of this zone are still not well understood (ASHRAE Fundamentals, 2001).

6.3.4 Velocity profiles of jet

Zone 1 and zone 2 are short zones. The velocities in those two zones may not change too much. Therefore, in the zonal model we use the centerline velocity to represent the velocity profile in those two regions. In zone 3 of both axial and radial jets, the velocity

distribution can be expressed by the Gauss error function or probability curve, which is approximated by the following equation (ASHRAE Fundamentals, 2001):

$$\left(\frac{r}{r_{0.5V}}\right)^2 = 3.3\log\frac{V_x}{V} \tag{6-22}$$

Where,

r: radial distance of point under consideration from centerline of jet, m

$r_{0.5V}$: radial distance in same cross-sectional plane from axis to point where velocity is one half centerline velocity, m

V: actual velocity at point being considered, m/s

6.3.5 Entrainment ratios

Entrainment is the movement of room air into the jet caused by the air stream discharged from the outlet. The following are equations for the entrainment of circular jets and jets from long slots (ASHRAE Fundamentals, 2001).

For third-zone expansion of circular jets,

$$\frac{Q_X}{Q_0} = \frac{2X}{1.13K\sqrt{A_0}} \tag{6-23}$$

For a continuous slot with active sections up to 3m and separated by 0.6m,

$$\frac{Q_X}{Q_0} = \sqrt{\frac{2}{1.13K}}\sqrt{\frac{X}{H_0}} \tag{6-24}$$

Where,

Q_x: total volumetric flow rate at distance X from face of outlet, m^3/s

Q_0: discharge from outlet, m^3/s

Therefore, in the Integrated Zonal Model, we have

- The angle of divergence: 22^0 for large open space, 18^0 for small open space.
- Centerline velocity:

$$\begin{cases} V_X = V_0 & \text{Initial Region, } X \le 4D_0 \\ V_X = V_0\sqrt{\dfrac{1.13KH_0}{X}} & \text{Transition Region, } X \le 25D_0 \\ V_X = V_0\dfrac{1.13K\sqrt{A_0}}{X} & \text{Main Region, } X > 25D_0 \end{cases} \tag{6-25}$$

- Velocity profile at the cross section:

$$\begin{cases} V = V_X = V_0 & \text{Initial Region, } X \le 4D_0 \\ V = V_X = V_0\sqrt{\dfrac{1.13KH_0}{X}} & \text{Transition Region, } X \le 25D_0 \\ V = V_X 10^{-\left(\frac{1}{3.3}\right)\left(\frac{r}{r_{0.5V}}\right)^2} & \text{Main Region, } X > 25D_0 \end{cases} \tag{6-26}$$

6.3.6 Jet cells

A jet cell contains two sub cells, one containing air belonging to the jet itself and one containing air from surrounding neighbors, as shown in Figure 6-5 for the linear jet and Figure 6-6 for the compact jet.

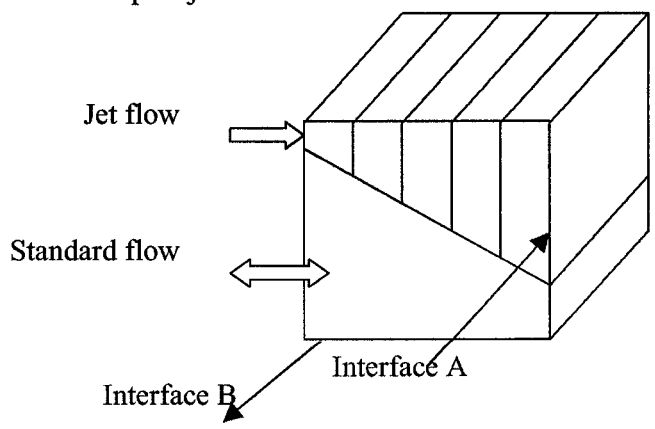

Figure 6-5 Configuration of the linear jet (2D) cell

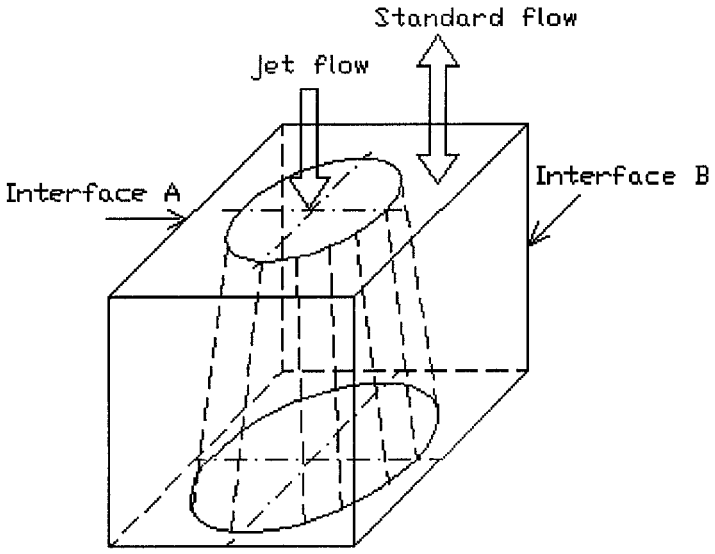

Figure 6-6 Configuration of the compact jet (3D) cell

The air flow crossing the interface A in Figures 6-5 and 6-6 includes the air from the jet and the air from the neighbors.

$$m_A = m_{jet} + m_{neighbor} \tag{6-27}$$

The air flow from the jet crossing the interface A can be modeled as:

$$m_{jet} = \iint V \rho d\left(S_{jet}\right) \tag{6-28}$$

Where,

S_{jet}: jet air flow passing area, m^2

The air flow from surrounding neighbors crossing the interface A can be modeled by:

$$m_{neighbor} = \dot{q}_{a,A}\left(S_A - S_{jet}\right) \tag{6-29}$$

Where,

S_A: total area of interface A, m^2

$\dot{q}_{a,A}$: air flow rate from surrounding neighbors crossing the interface A, $kg/m^2.s$

Therefore, the air flow crossing the interface perpendicular to the trajectory of the jet (e. g. interface A) can be modeled by substituting Equation (6-26) into (6-28) and then substituting Equation (6-28) and Equation (6-29) into Equation (6-27).

$$\begin{cases} m_A = \iint V_0 \rho d(S_{jet}) + \dot{q}_{m,A}(S_A - S_{jet}), & \text{Initial Region } X \le 4D_0 \\ m_A = \iint V_0 \sqrt{\dfrac{1.13KH_0}{X}}\ \rho d(S_{jet}) + \dot{q}_{m,A}(S_A - S_{jet}), & \text{Transion Region } X \le 25D_0 \\ m_A = \iint V_0 \dfrac{1.13K\sqrt{A_0}}{X} 10^{-\left(\frac{1}{3.3}\right)\left(\frac{r}{r_{0.5V}}\right)^2} \rho d(S_{jet}) + \dot{q}_{m,A}(S_A - S_{jet}), & \text{Main Region } X > 25D_0 \end{cases} \quad (6\text{-}30)$$

The air flow crossing the interface parallel to the trajectory of the jet (e. g. interface B) can be modeled as the air flow crossing the standard interface.

6.4 INTEGRATING MATERIAL EMISSION/SINK MODEL WITH ZONAL MODEL

6.4.1 Material emission/sink model

In previous chapters, it was suggested that VOC transport from the material to the room air through three processes: 1) VOC transport inside the material is through internal diffusion and can be described by a transient diffusion equation. 2) At the material/ air interface, VOC change from the material phase to the gas phase. At a atmospheric

pressure, for low VOC concentration and isothermal conditions, the equilibrium relationship between the VOC concentration in the gas phase and the VOC concentration in the material phase can be described by a linear isotherm, 3) the gas phase VOC pass through its overlying concentration boundary layer and transport to the room air by diffusion and convection. The convective mass transfer coefficient is used to express the mass transfer in the boundary layer. Wet building materials, such as paint and glue, are usually non-porous materials and can be treated as single homogeneous media. Therefore, one-phase models can be used to describe the VOC emissions from the wet materials. Since the VOC internal diffusion and sorption are usually considered as fully reversible phenomena and the mass fluxes depend on the direction of the concentration gradient, the sink behavior of the building materials can be modeled by setting the initial VOC concentration lower than the room air VOC concentration. Since the room considered here is partitioned into a number of three-dimensional cells; the transient VOC diffusion equation in the material should also be three-dimensional. Thus, we follow the same material emission and sink processes as described in the previous chapters and extend the one dimension multi-layer emission model and single-layer sink model to three dimensions. Therefore, the material emission/sink model becomes,

$$\frac{\partial C_{m,j}}{\partial t} = \frac{\partial}{\partial x}\left(D_{m,j} \frac{\partial C_{m,j}}{\partial x} \right) + \frac{\partial}{\partial y}\left(D_{m,j} \frac{\partial C_{m,j}}{\partial y} \right) + \frac{\partial}{\partial z}\left(D_{m,j} \frac{\partial C_{m,j}}{\partial z} \right) \tag{6-31}$$

$$C_{m,j}\Big|_{z=b} = kC_{s,i} \tag{6-32}$$

$$R = h_m\left(C_{s,i} - C_{a,i}\right) \tag{6-33}$$

Where, $C_{m,j}$ is the VOC concentration in the j^{th} layer of the material assembly ($\mu g/m^3$), $D_{m,j}$ is the VOC diffusion coefficient in the j^{th} layer of the material assembly (m^2/s), k is the top layer material/air partition coefficient, $C_{s,i}$ is the VOC concentration in the near material surface air in cell i ($\mu g/m^3$), $C_{a,i}$ is the VOC concentration in the air in cell i ($\mu g/m^3$), h_m is the convective mass transfer coefficient (m/s), b is the total material assembly thickness (m) and t is the time (s).

As stated in Chapter 3 and Chapter 5, a dry building material layer can be considered as having homogeneous diffusivity due to the VOC concentration within the material is very low. However, for a wet material layer, the initial VOC concentration within the material is usually very high and the VOC diffusion coefficient is dependent on the VOC concentration. Bodalal (1999) suggested a second order empirical equation to describe the dependence of diffusion coefficient of wet material on VOC concentration. In this study , this equation is used to simulate both the wet phase and the dry phase of the wet material layer:

$$D_{m,wet} = D_{m0,wet}\left(\frac{C_{m,wet}}{C_{mo,wet}}\right)^2 + D_{m,dry}\left(1-\left(\frac{C_{m,wet}}{C_{mo,wet}}\right)^2\right) \qquad (6\text{-}34)$$

Where, $D_{m,wet}$ is the VOC diffusion coefficient of the wet material (m^2/s), $D_{m0,wet}$ is the initial VOC diffusion coefficient of the wet material (m^2/s), $D_{m,dry}$ is the VOC diffusion coefficient of the dried wet material (m^2/s), $C_{m,wet}$ is the VOC concentration in the wet material ($\mu g/m^3$) and $C_{m0,wet}$ is the initial VOC concentration in the wet material ($\mu g/m^3$).

For the initial condition, it is assumed that each material layer is homogeneous and has a uniform initial concentration. For the boundary conditions, in the dry/dry material interface, we assume that the dry/dry materials are not perfectly contacted and the VOC concentration is not continuous at the interface. In the dry/wet material interface, the amount of the wet material applied is usually small. It can be assumed that the dry material quickly absorbs the wet material after application. Thus, the VOC concentration is assumed to be continuous at the wet/dry material interface. At the material bottom, it is assumed that there is no VOC transfer. Therefore, the initial and boundary conditions become:

$$C_{m,j}(x,y,z,0) = C_{m0,j} \tag{6-35}$$

$$-D_{m,j}\left.\frac{\partial C_{m,j}}{\partial z}\right|_{z=b_j} = -D_{m,j+1}\left.\frac{\partial C_{m,j+1}}{\partial z}\right|_{z=b_j} \tag{6-36}$$

$$C_{m,j}\Big|_{z=b_j} = \left.\frac{k_j}{k_{j+1}} C_{m,j+1}\right|_{z=b_j} \text{ (dry/dry material interface)} \tag{6-37}$$

$$C_{m,j}\Big|_{z=b_j} = C_{m,j+1}\Big|_{z=b_j} \text{ (dry/wet material interface)} \tag{6-38}$$

$$-D_{m,j}\left.\frac{\partial C_{m,j}}{\partial z}\right|_{z=b} = h_m\left(\frac{C_{m,j}\Big|_{z=b}}{k} - C_{a,i}\right) \tag{6-39}$$

$$\left.\frac{\partial C_{m,j}}{\partial z}\right|_{z=0} = 0 \tag{6-40}$$

Where, $C_{m0,j}$ is VOC initial concentration in the jth layer(μg/m^3), k_j is the j^{th} layer material/air partition coefficient and b_j is the jth layer material thickness(m).

6.4.2 VOC mass conservation in the air

Within each cell, the general VOC mass balance can be written as:

$$\frac{M_{a,i}}{\rho_i}\frac{dC_{a,i}}{dt} = \sum_{j=1}^{6} m_{VOC,ij} + m_{VOC,sorce} + m_{VOC,\sin k} \qquad (6\text{-}41)$$

Where, $C_{a,i}$ is the VOC concentration in cell i ($\mu g/m^3$), $m_{voc,ij}$ is the VOC mass flow across cell i and cell j interface ($\mu g/s$), $m_{voc,source}$ is the VOC mass source in cell i ($\mu g/s$), $m_{voc,\,sink}$ is the VOC mass sink in cell i ($\mu g/s$) and $M_{a,i}$ is the air mass in cell i (kg).

VOC mass transfer between cells is through convection and diffusion. The Hybrid scheme developed by Spalding (1972) is applied here to calculate the net flux of VOC at interfaces caused by diffusion and convection and it is dependent on its Peclet number, which denotes the strength ratio of convection to diffusion.

6.5 SOLUTION TECHNIQUES

The Newton-Raphson global convergence (Press, 1992) technique was applied to solve a set of coupled nonlinear mass and linear energy equations to get the air flow crossing each cell interface. The air flow across each cell interface was directly used in VOC mass balance equations as input. A combination of the TDMA and the Gauss-Seidel method, namely line-by-line method (Patankar, 1980), was applied to solve the set of VOC mass balance equations to get VOC distribution in the room and materials.

6.6 CASE STUDY

6.6.1 Case 1: Natural ventilation

The Integrated Zonal Model was first applied to a natural ventilation room, which was one of the MINIBAT tests in Centre de Thermique l'INSA de Lyon (Inard et al., 1996). The dimensions of the room were 3.1×3.1×2.5 m^3 and it was at a non-isothermal condition. The temperature at west wall and east wall was 14.1 °C, south wall was 6.0 °C, north wall was 13.9 °C, ceiling was 13.5 °C and floor was 11.8 °C. The convective heat transfer coefficients, h_T, were 4.1, 1.0 and 5.7 $w/m^2.K$ for the walls, floor and ceiling, respectively (Wurtz et al., 1999[b]). The temperature distribution and the air flow pattern within the room were first simulated by the Integrated Zonal Model.

The temperature distribution in the middle section of the room simulated by the Integrated Zonal Model was compared with the prediction of the POMA model (Haghighat, et al., 2001), with the prediction of the CFD model (Jiang, 1998) and the experimental results (Inard et al., 1996), as shown in Figure 6-7. Simulation and measurement results detected that there was temperature stratification within the room. The comparison showed that the tendencies of temperature distribution in the four methods were quite similar and there was a good agreement among the prediction of the Integrated Zonal Model, the POMA model, the CFD model, and the experimental results.

The air pattern inside the room predicted by the Integrated Zonal Model was compared with the prediction of the POMA model and the CFD model, as shown in Figures 6-8, 6-9 and 6-10. This also demonstrated good agreement among the Integrated Zonal Model, the

POMA model and the CFD model. The main streams of flow were always near the walls and an anti-clockwise circulation was detected in three of the models. This illustrates that the Integrated Zonal Model can provide good prediction of the temperature distribution and air flow pattern in a natural ventilation room.

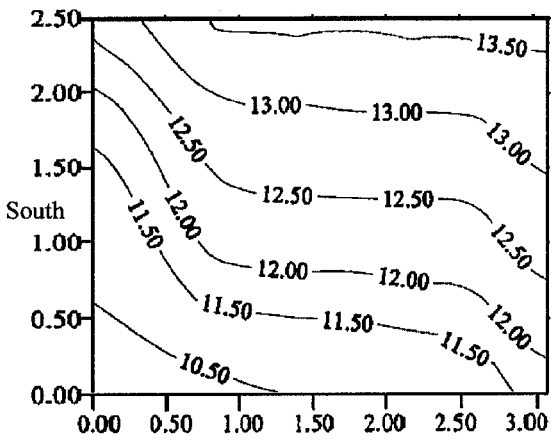

POMA (6×1×10 zones)
(Haghighat et al., 2001)

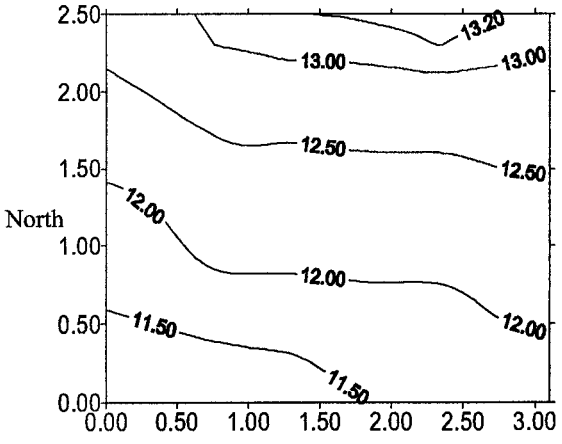

Integrated Zonal Model
(6×3×6 zones)

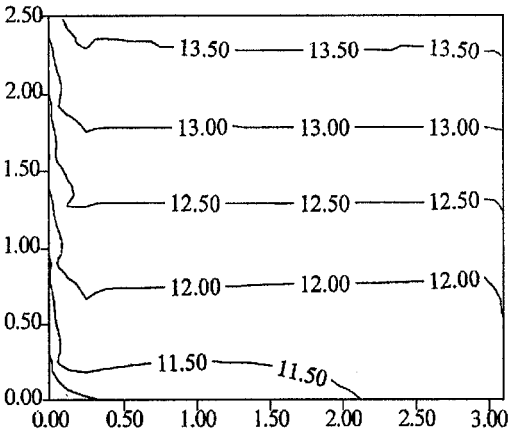

CFD Model (41×51×41 zones)
(Jiang, 1998)

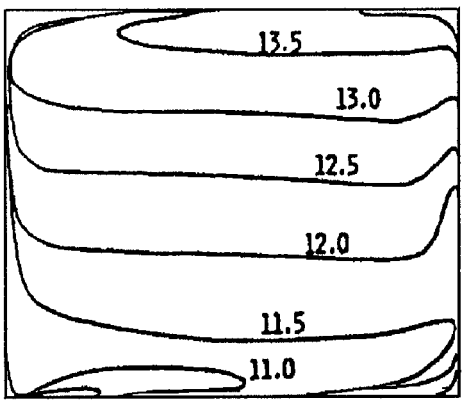

Experiment Results
(Inard, 1996)

Figure 6-7 Comparison of temperature distributions for case 1

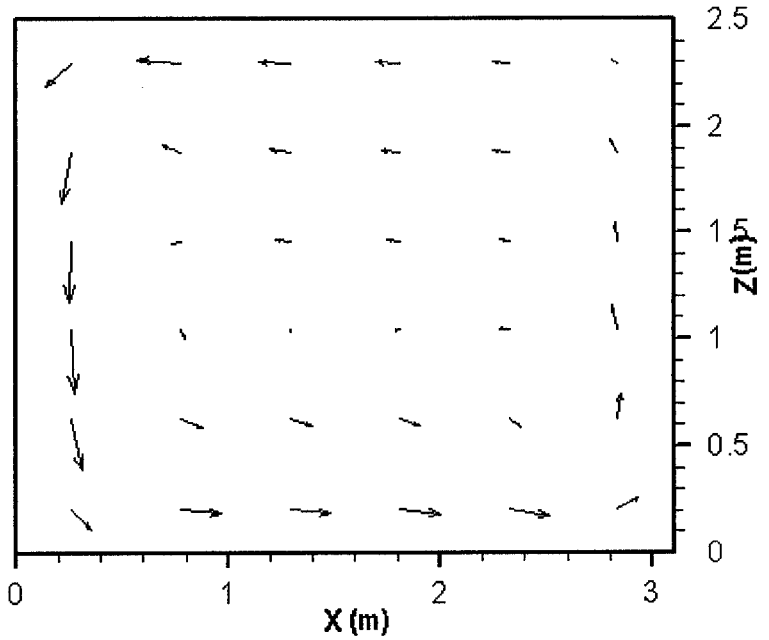

Figure 6-8 Air flow pattern predicted by the Integrated Zonal Mode for case 1 (grids: 6×3×6)

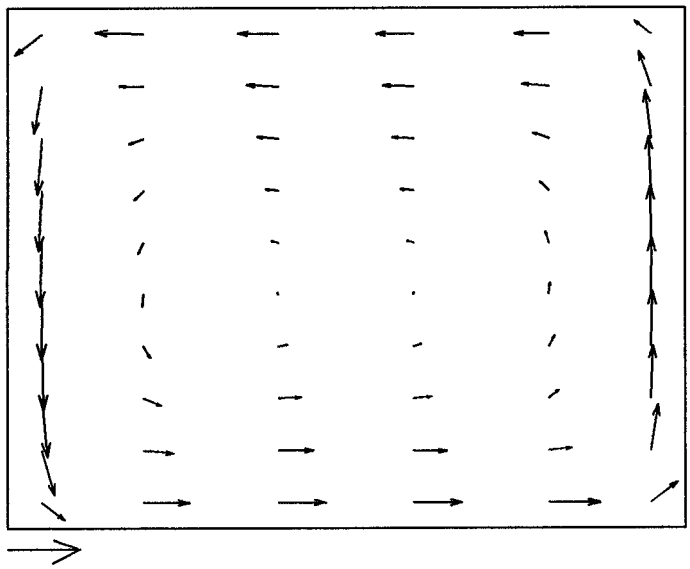

Figure 6-9 Air flow pattern predicted by the POMA model for case 1(grids: 6×1×10) (Haghighat, et al., 2001)

Figure 6-10 Air flow pattern predicted by the CFD model for case 1 (grids: 41×51×41) (Jiang, 1998)

After the validation of the Integrated Zonal Model for predicting the temperature distribution and the air flow pattern in a natural ventilation room, this Integrated Zonal Model was further used to predict VOC distribution in the room. The floor of the room was assumed to be covered with vinyl floor tile. Benzene was chosen as the compound of interest. The benzene diffusion coefficient and partition coefficient in the vinyl floor tile were taken from literature (Plett et al., 2001). The initial benzene concentrations in carpet was assumed to be 1.0×10^7 $\mu g/m^3$. All the input parameters of vinyl floor tile are shown in Table 6-1. The simulation was carried out until the benzene concentration reached steady state.

Benzene concentration distributions are graphically displayed in Figures 6-11, 6-12 and 6-13 for a section in the middle of the room after the vinyl floor tile was exposed to the air for one hour and 24 hours. The figure shows that benzene concentration was not uniform in the space at the beginning and was affected by the air flow pattern in the room, as shown for time of 1 hour after exposure. Benzene concentration was higher around the near floor and the north wall regions than the other regions. Gradually, the benzene concentration became uniform in the space, as shown for time of 24 hour after the exposure. This is because the room VOC concentration eventually reached steady state.

Table 6-1 Properties of benzene in the vinyl floor tile

Parameter	C_0	D_m	k	B
(unit)	($\mu g/m^3$)	(m^2/s)	(—)	(m)
Value	1.0×10^7	1.06×10^{-10}	310	0.003

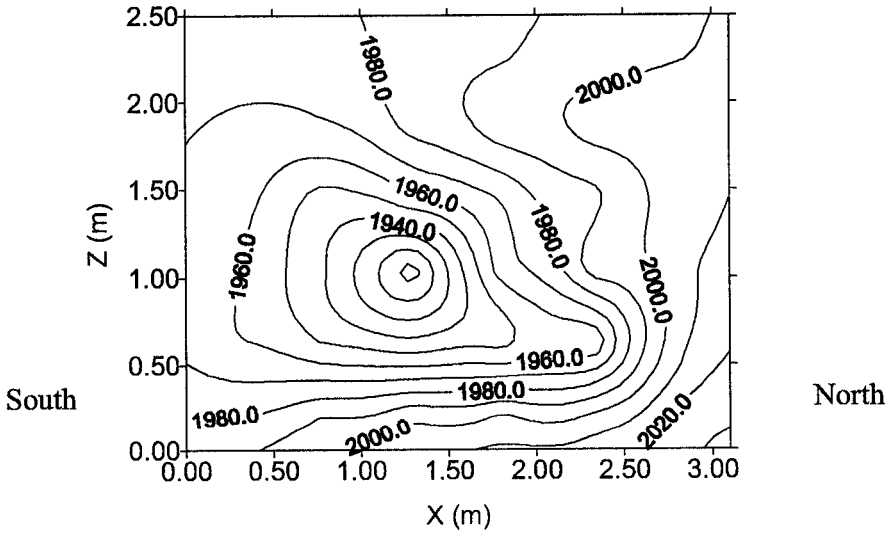

Figure 6-11 Benzene concentration distribution after 1 hour for case 1

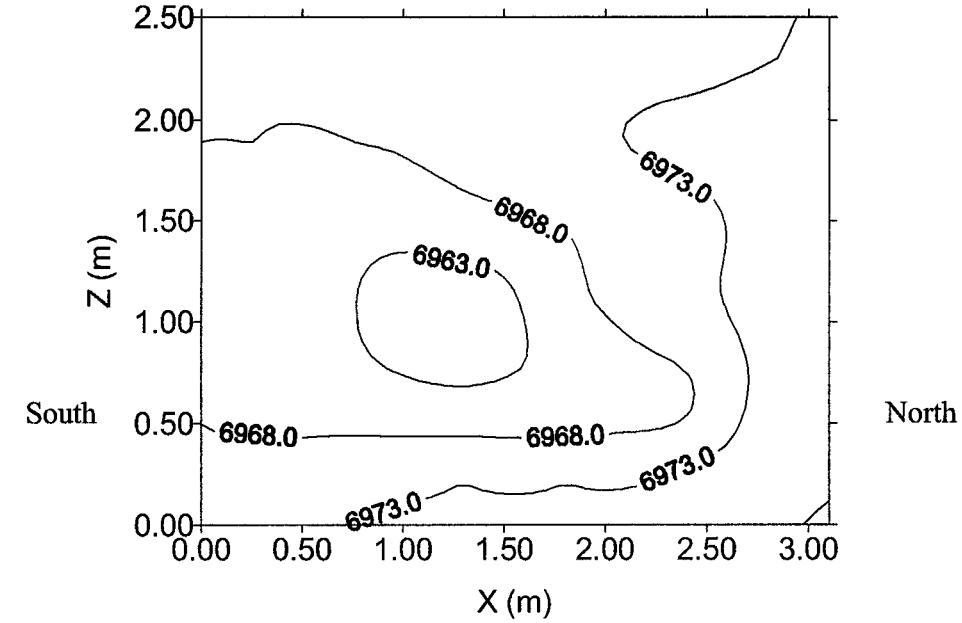

Figure 6-12 Benzene concentration distribution after 12 hours for case 1

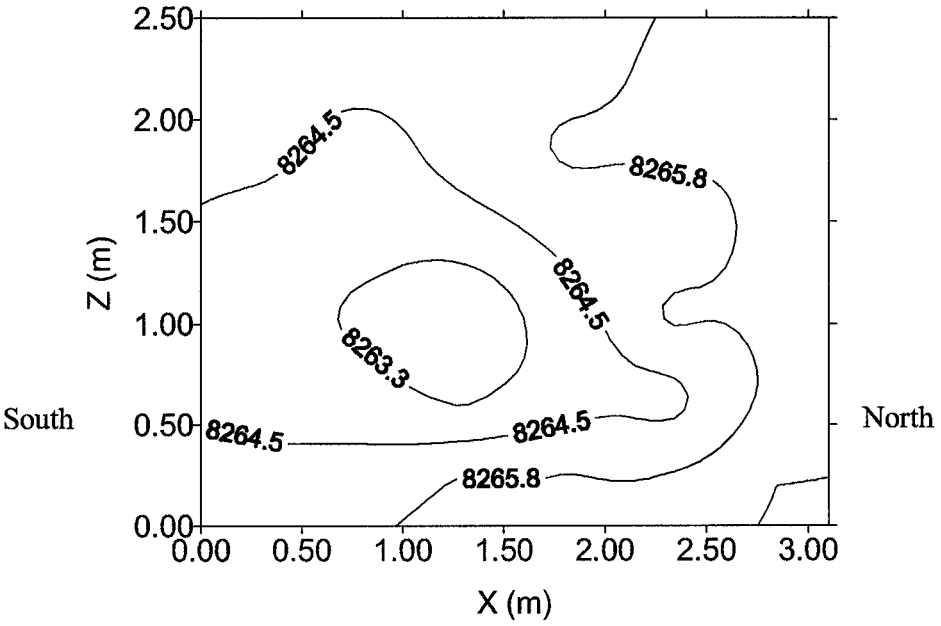

Figure 6-13 Benzene concentration distribution after 24 hours for case 1

The average room air benzene concentration, as shown in Figure 6-14, increased as time increased and gradually reached the steady state, since there was not mechanically ventilated. Figure 6-15 shows the average benzene emission rate of the vinyl floor tile. It decreased as time increased and also reached a steady state condition. This agreed very well with the normalized emitted mass, as shown in Figure 6-16. When the benzene concentration in the air reached steady state, around 75% of the benzene was emitted out from the vinyl floor tile.

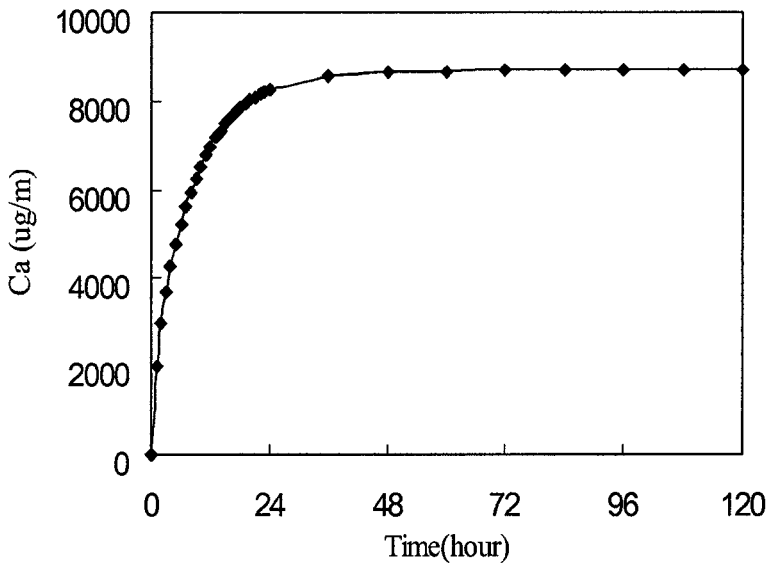

Figure 6-14 Average benzene concentration in the air for case 1

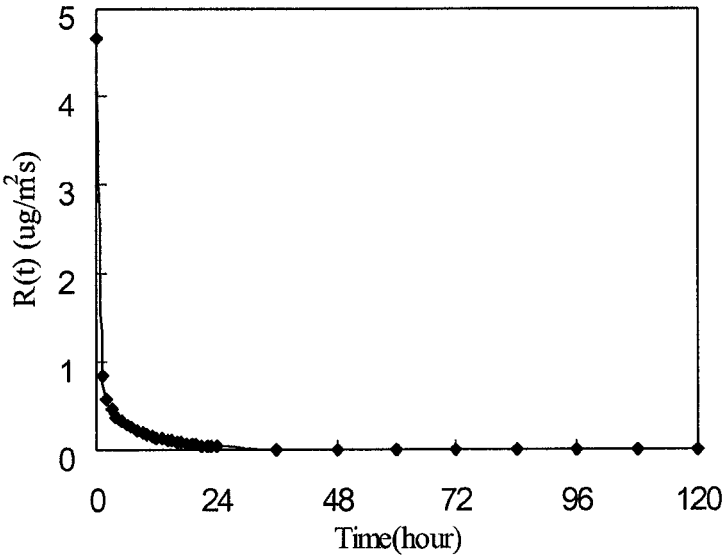

Figure 6-15 Average benzene emission rate for case 1

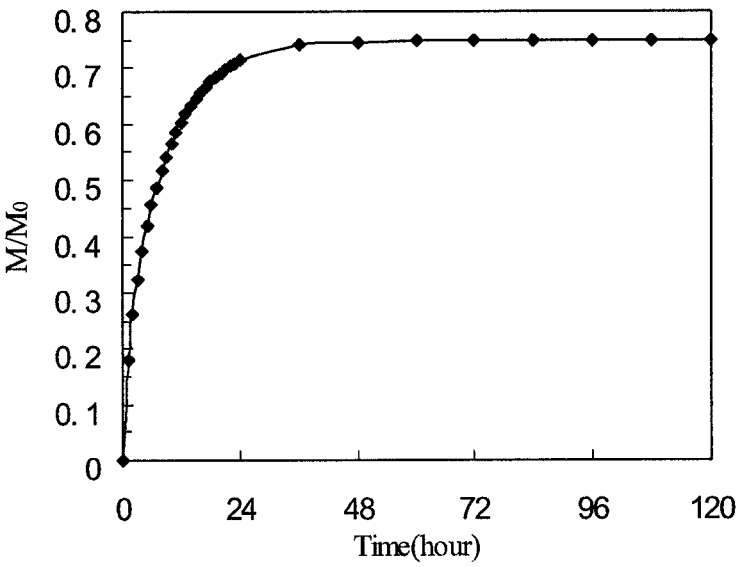

Figure 6-16 Benzene normalized emitted mass for case 1

6.6.2 Case 2: Natural and forced ventilation

In this case study, the integrated zonal model was applied to a naturally and mechanically ventilated room; its floor was covered with carpet. The dimensions of the room were $3.0\times3.0\times2.5$ m^3 with one air inlet at the top of the west wall and one air outlet at the east wall. The air exchange rate was 1.0 h^{-1} (inlet air flow rate at 0.0075 kg/s). The room was at a non-isothermal condition with temperature at the west wall 0 °C and at the other walls, ceiling and floor 21 °C. The inlet air temperature was 31 °C. The convective heat transfer coefficients, h_T, were 4.1, 1.0 and 5.7 w/m^2k for the walls, floor and ceiling, respectively (Wurtz et al., 1999[b]). Nonane was chosen as the compound of interest. The nonane diffusion coefficient and partition coefficient in the carpet were taken from literature (Bodalal, 1999). The initial nonane concentration in the carpet was assumed to be 1.0×10^7 $\mu g/m^3$. All the input parameters of carpet are shown in Table 6-2. In order to compare the ventilation system efficiency, simulations were carried out for two different ventilation layouts: for the first layout the air outlet were located at the top of the east wall and for the second layout the air outlet were located at the bottom of the east wall. Both simulation results were compared with the predictions of the total mixing model (Chapter 3), which was validated with the experimental results (Huang and Haghighat, 2002). The periods of the simulations were for both short term (1 hour) and long term (10 days).

Table 6-2 Properties of nonane in the carpet

C_0	D_m	k	B
($\mu g/m^3$)	(m^2/s)	(—)	(m)
1.0×10^7	2.83×10^{-11}	6216	0.002

Nonane concentration distributions in the middle section of the room after the carpet was exposed to the air for one hour are graphically displayed in Figure 6-17 (outlet at the bottom) and Figure 6-18 (outlet at the top). The nonane concentration was not uniform in the space and was affected by the characteristics of the room. The nonane concentration around the outlet area was around 1.4 times higher than that near the inlet area. The nonane concentration distribution for the outlet at the bottom was lower than that for the outlet at the top due to the influence of the air flow pattern. This integrated zonal model was also used to predict the temperature distribution in the room, as shown in Figure 6-19.

The room-averaged nonane concentration and the outlet nonane concentration for 1 hour and 10 days are shown in Figures 6-20 and 6-21 for the two ventilation layouts. The room-averaged concentration for the outlet at the bottom was lower than that for the outlet at the top. The outlet nonane concentrations in both ventilation layouts were higher than the room-averaged nonane concentration. Figure 6-20 and Figure 6-21 also show the predictions of the total mixing model. The prediction of average nonane concentration was slightly higher for the total mixing model than that for the Integrated Zonal Model in both ventilation patterns.

The total simulation time for 10 days VOC distribution prediction only took a few minutes, which means that the integrated zonal model is a practical tool for long-term VOC distribution prediction.

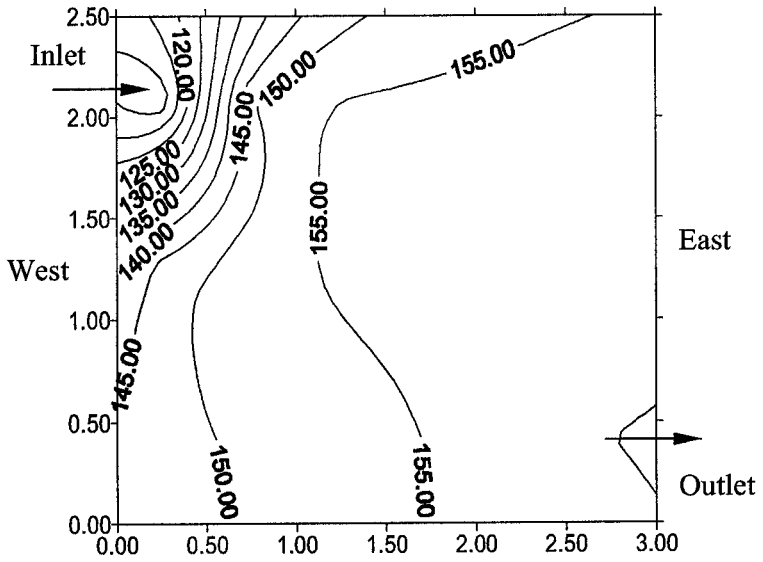

Figure 6-17 Nonane distribution for case 2 (outlet at bottom, 1hour)

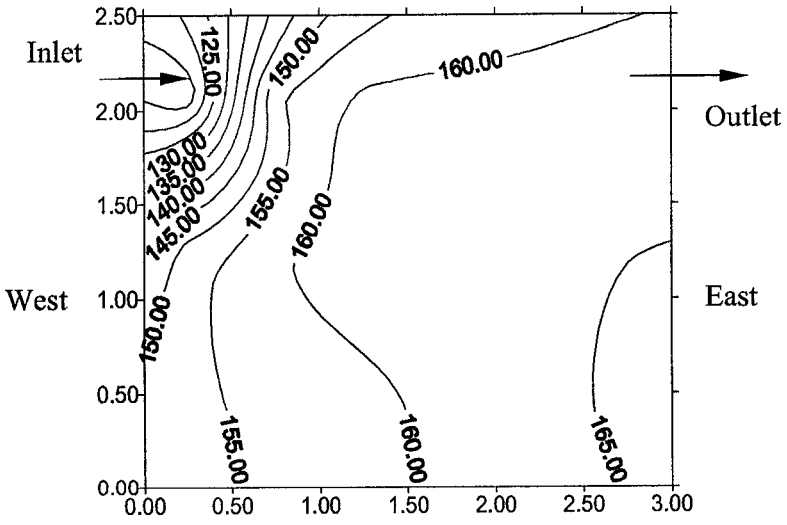

Figure 6-18 Nonane distribution for case 2 (outlet at top, 1hour)

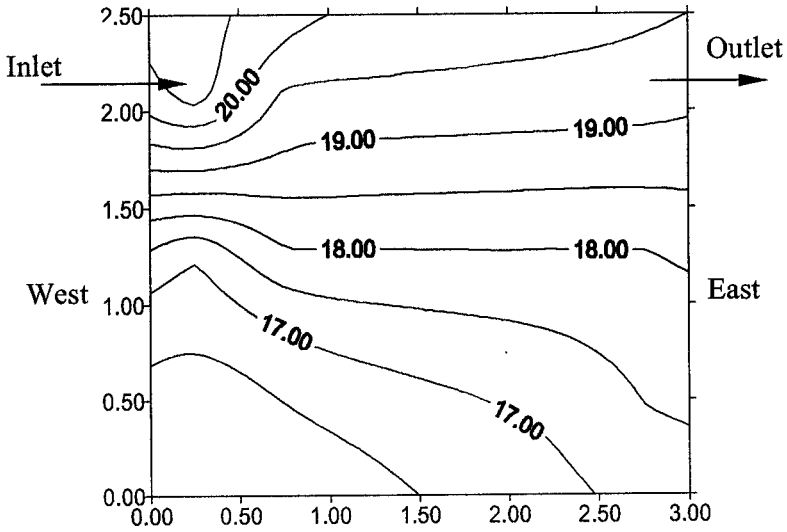

Figure 6-19 Temperature distribution in the middle section of the room for case 2 (outlet at top)

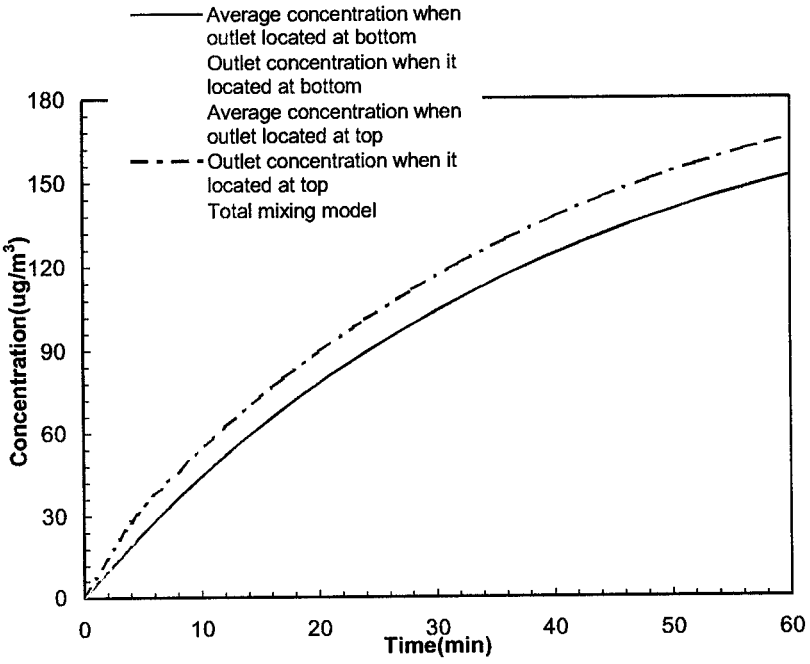

Figure 6-20 Comparison of nonane concentrations in the room for case 2

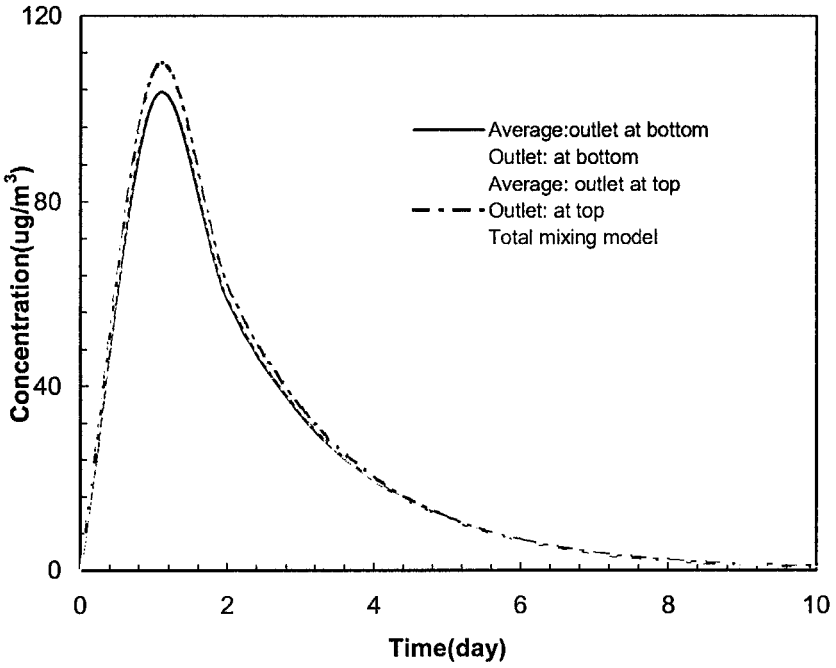

Figure 6-21 Comparison of nonane concentrations in the room air for case 2

6.6.3 Case 3: Forced ventilation with linear air jet

In this case study, a room with a two-dimensional linear air jet on the west wall and an outlet at the east wall was selected. The dimensions of the room were $3.0\times3.0\times2.7m^3$. The inlet air flow rate was 0.08 kg/s. The room was at an isothermal condition with temperature at 20 °C. The geometry of the room is shown in Figure 6-22.

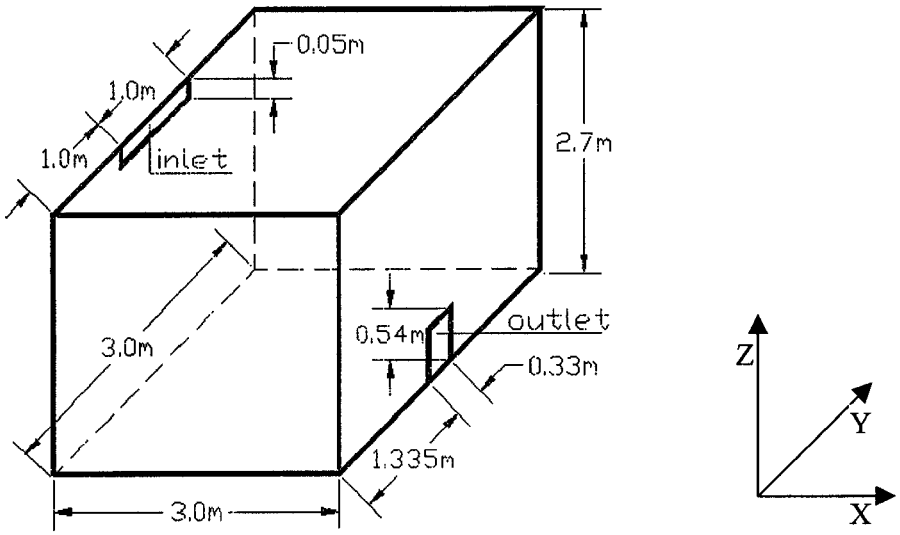

Figure 6-22 Geometry of the room with a linear jet

The Integrated Zonal Model was first applied to simulate the air flow pattern within the room. The simulation results were compared with that of the commercial CFD software FLOVENT (Jiang, 2002).

The air flow patterns in the middle section of the room, simulated by the Integrated Zonal Model and the CFD model, are graphically shown in Figures 6-23 and 6-24. Globally, a similar air flow pattern was achieved in both models. A strong air stream along the ceiling and a circulation around the middle of the room were detected in both models.

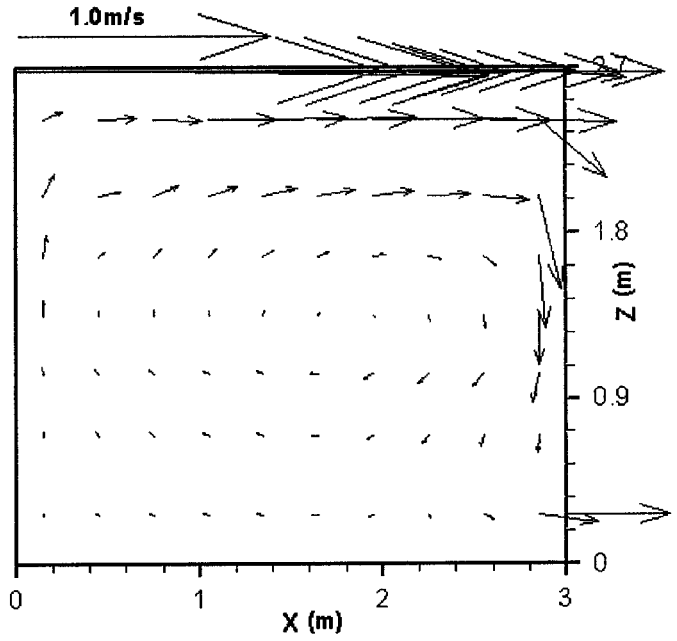

Figure 6-23 Air flow pattern predicted by the Integrated Zonal Model for case 3 (grids: 10×3×8)

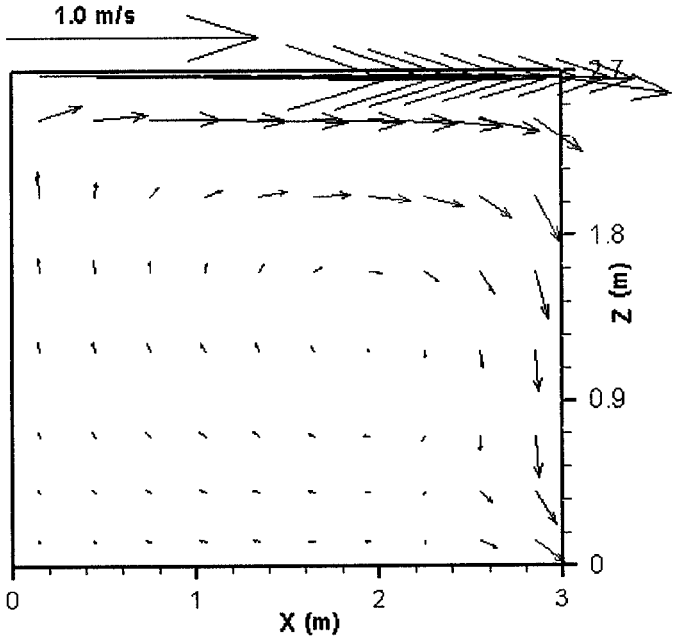

Figure 6-24 Air flow pattern predicted by FLOVENT for case 3 (grids: 10×9×8) (Jiang, 2002)

For the VOC distribution simulation, in order to be realistic, we assumed that VOC were emitted from all walls and floor. The walls of the room were decorated with plywood and the floor was covered with vinyl floor tile. Benzene is one of the common compounds that is emitted from both plywood and vinyl floor tile. The simulation parameters of plywood and vinyl floor tile were taken from literature (Plett, et al., 2001), they are listed in Table 6-3.

Table 6-3 Properties of benzene in the plywood and vinyl floor tile

Parameters	C_0	D_m	k	b
(unit)	($\mu g/m^3$)	(m^2/s)	(—)	(m)
Plywood	1.0×10^{7}	4.92×10^{-10}	184	0.016
Vinyl floor tile	1.0×10^{7}	1.06×10^{-10}	310	0.003

Benzene concentration distributions in the middle section (Y=1.5m) of the room and in the occupied zone for a seated person (Z=1.35m) are graphically displayed in Figures 6-25, 6-26, 6-27 and 6-28 after plywood walls and vinyl floor tile floor were exposed to the air for 12 hours and 24 hours. The lowest benzene concentration was detected in the near ceiling region due to the fresh air directly coming along the ceiling. The benzene concentration in the near west wall region was much higher than the other regions. Compared with the average benzene concentration in the room air (304 $\mu g/m^3$ at 12h, 204 $\mu g/m^3$ at 24h), as shown in Figure 6-29, the benzene concentration in more than half of the occupied zone was higher than the average benzene concentration. This indicated that this air distribution system could not provide good fresh air supply in order to effectively dilute contaminate in the room. Furthermore, only using the average benzene concentration could not give a good representation of benzene concentration in the whole room.

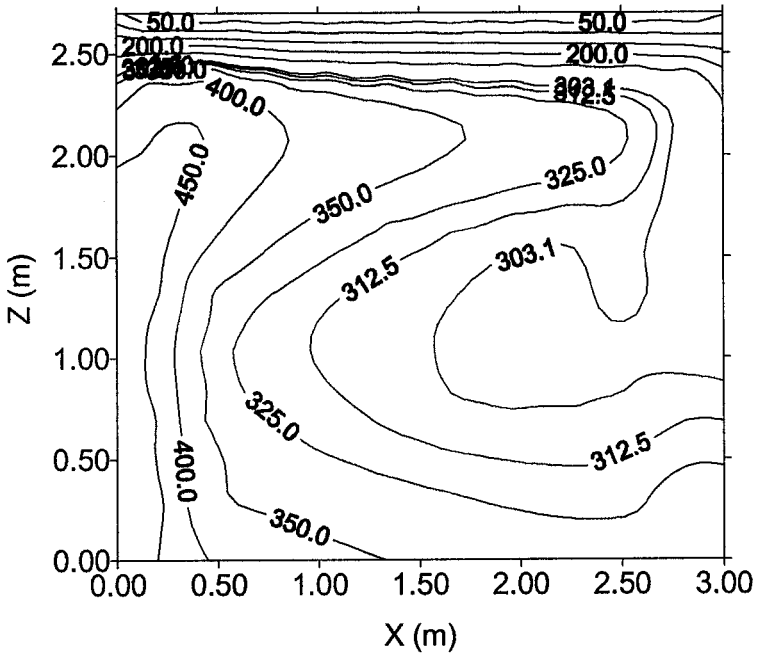

Figure 6-25 Benzene concentration distribution after 12 hours for case 3 (Y=1.5m)

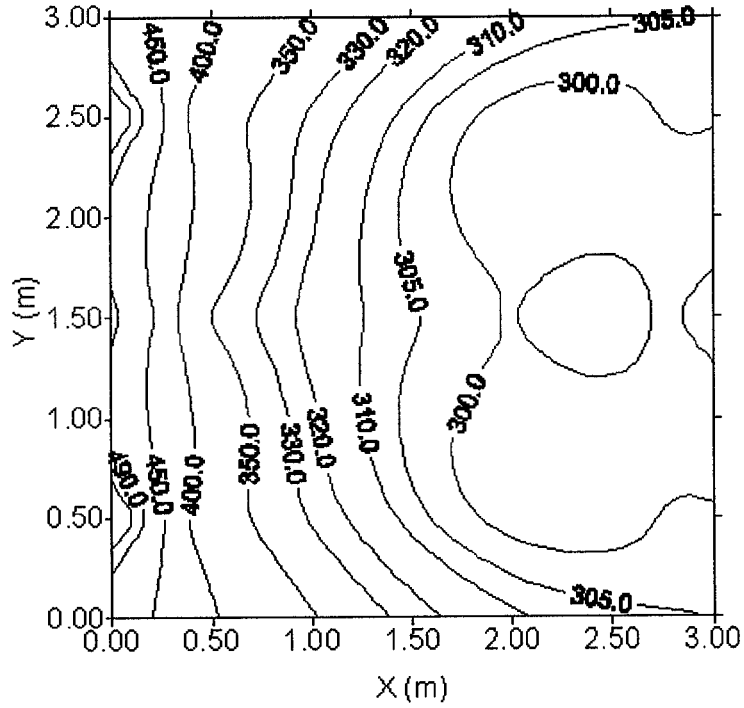

Figure 6-26 Benzene concentration distribution after 12 hours for case 3 (Z=1.35m)

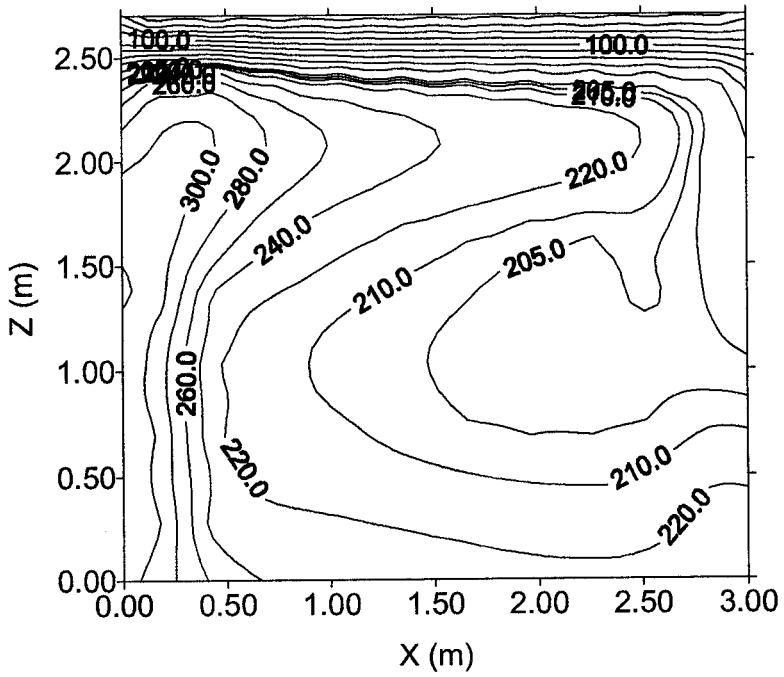

Figure 6-27 Benzene concentration distribution after 24 hours for case 3 (Y=1.5m)

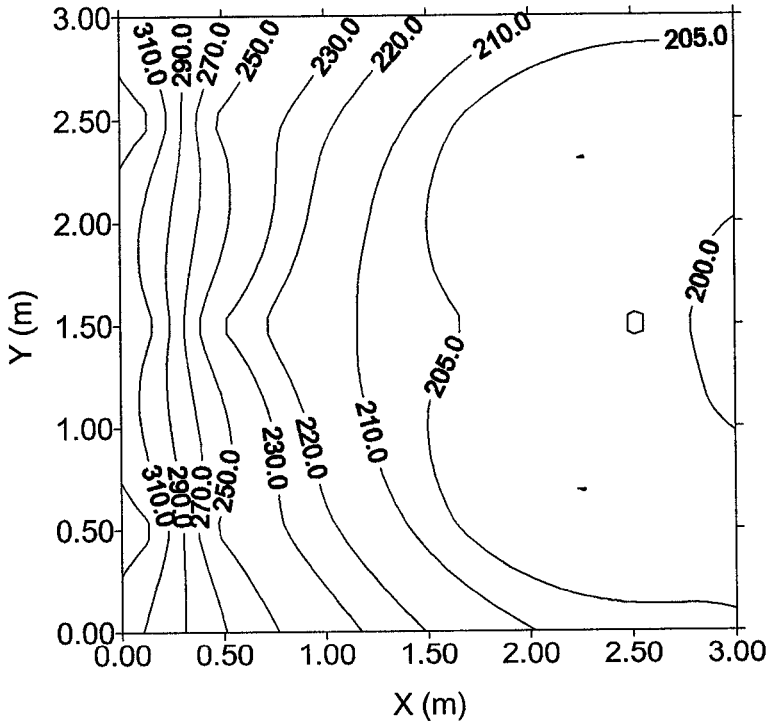

Figure 6-28 Benzene concentration distribution after 24 hours for case 3 (Z=1.35 m)

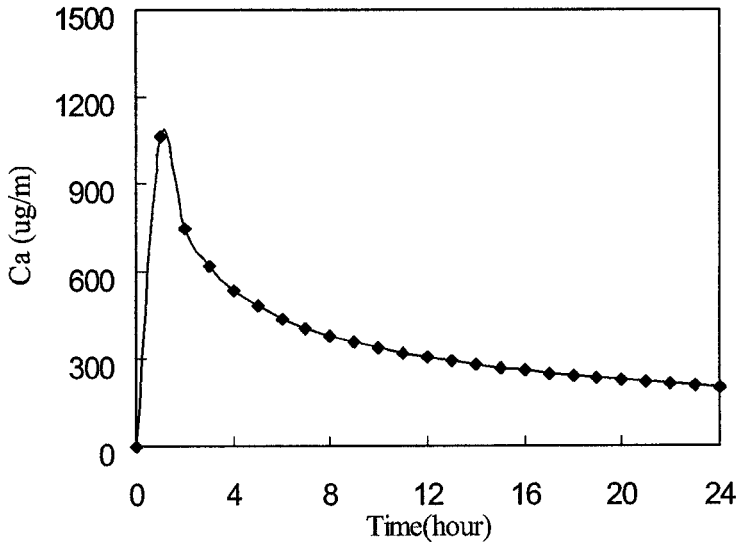

Figure 6-29 Average benzene concentration in the air for case 3

The average benzene emission rates from west, east, south and north walls and from floor for the first 2 hours are shown in Figure 6-30. Initially, the region close to the east wall had the highest benzene emission rate. It was because the air velocity along the east wall was much higher than the velocity along the other walls. Velocity had significant impact on the emission rate for the first 20 minutes. The reason was that at the beginning, the initial concentration of benzene at the plywood surface was relatively high; therefore the emission rate increased as the velocity increased. This result is in agreement with the earlier work that showed, for dry materials, the emission rate increased as the air velocity over the material increased only for short time (Huang and Haghighat, 2002). As time passed, the velocity effect diminished. The emission rates became independent of the air velocity, as shown in Figure 6-30; the emission rates from the four walls were very close to each other. This was because the internal diffusion dominates the emission process. The south wall and the north wall had the same benzene emission rate due to the

symmetry of the air flow. Compared with the walls, the floor had the lowest emission rate, which was mainly because of the low benzene diffusion coefficient.

These results agreed very well with the normalized emitted mass, as shown in Figure 6-31. Compared with the plywood, the vinyl floor tile had lower benzene diffusion coefficient. However, it had higher normalized emitted mass. This was for the reason that the vinyl floor tile was much thinner than the plywood. This agrees very well with the results of the parametric study for the thickness (Chapter 4). Usually, for the materials, which have the same diffusivity, the thinner one has the higher normalized emitted mass and hence has the shorter VOC emission time.

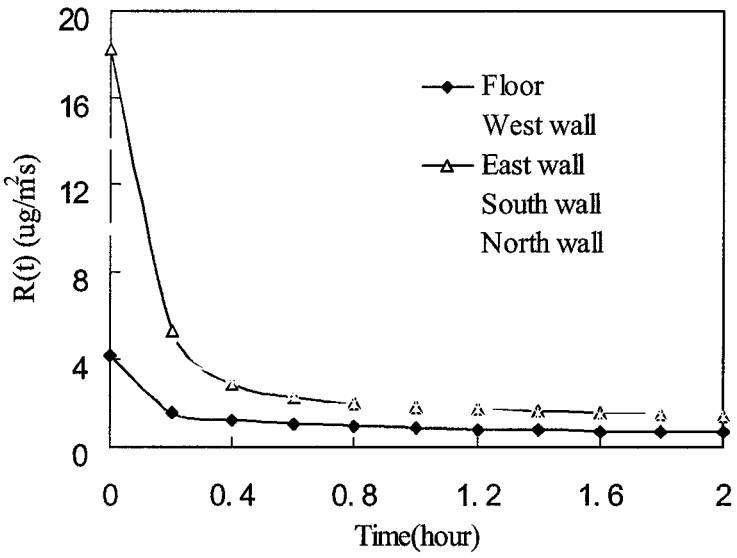

Figure 6-30 Comparison of average benzene emission rates for case 3

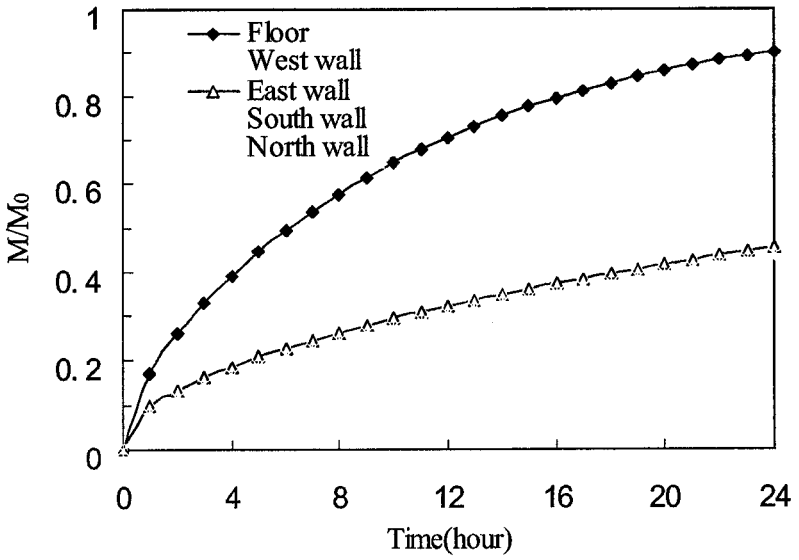

Figure 6-31 Comparison of benzene normalized emitted masses in case 3

6.6.4 Case 4: Forced ventilation with compact jet

In this case, the Integrated Zonal Model was applied to simulate a room with a three-dimensional compact jet and an outlet on the ceiling. The dimensions of the room were $3.0\times3.0\times2.7m^3$. The inlet air flow rate was 0.08 kg/s. The room was at an isothermal condition with a temperature of 20 °C. The geometries of the room and the diffuser are shown in Figures 6-32 and 6-33. The walls of this room were decorated with plywood and the floor was covered with Vinyl floor tile. The Integrated Zonal Model was used to simulate the air flow pattern within the room and the results were compared with that of FLOVENT (Jiang, 2002). 10×9×8 simulation grids were used for both models.

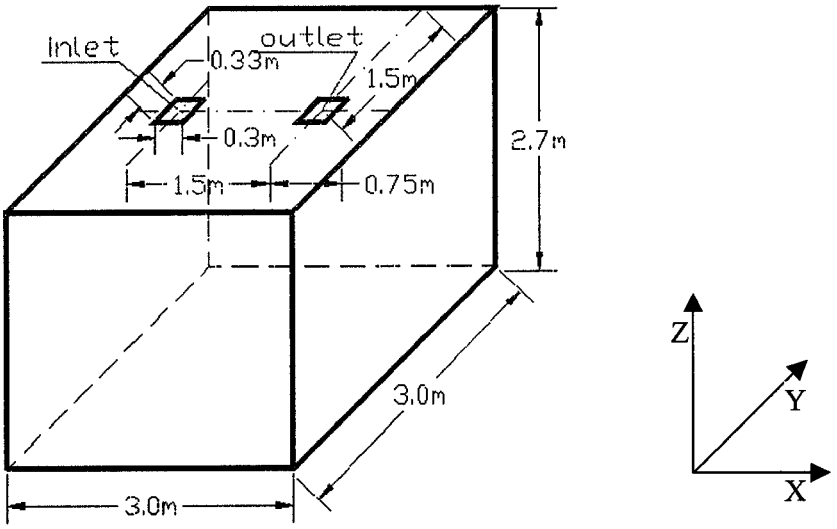

Figure 6-32 Geometry of the room with a compact jet

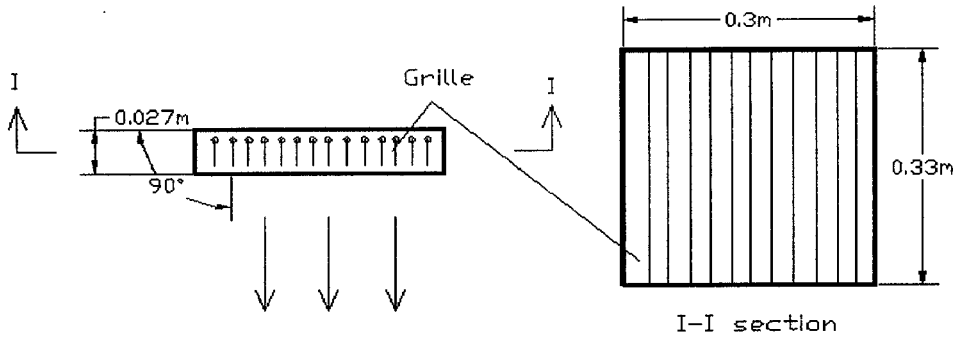

Figure 6-33 Geometry of the diffuser

Figures 6-34 and 6-35 show the air flow patterns in the middle section of the room (Y=1.5m) simulated by the Integrated Zonal Model and the CFD model. These figures show both models detected a strong air stream located around the centerline of the jet. Both models also detected a circulation on the right side of the jet centerline: there was, however a small discrepancy.

Figures 6-36 and 6-37 show the air flow patterns at jet centerline section (X=0.75m) predicted by both models. The air streams on the two sides of the jet centerline predicted by the Integrated Zonal Model were stronger than that of the CFD model. The reason is that when we integrated the compact jet model with the zonal model, we used the centerline velocity to represent the velocity profile in the jet expansion initial and transition regions. Actually, the velocity profile is not uniform in those two regions. More studies of velocity profile in those two regions are required to improve the prediction.

The air flow patterns at the outlet centerline section (X=2.25m) predicted by both models are illustrated in Figures 6-38 and 6-39. Even though there was a small discrepancy for the values of velocities, the air flow patterns at this section followed the same trend in both models. In summary, the Integrated Zonal Model could provide a reasonable prediction of the air flow pattern in the room with a compact jet.

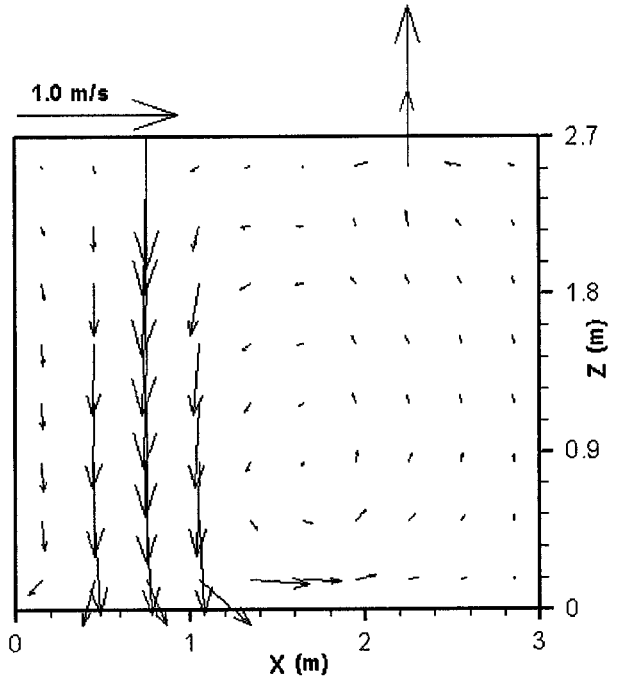

Figure 6-34 Air flow pattern predicted by the Integrated Zonal Model for case 4 (Y=1.5m)

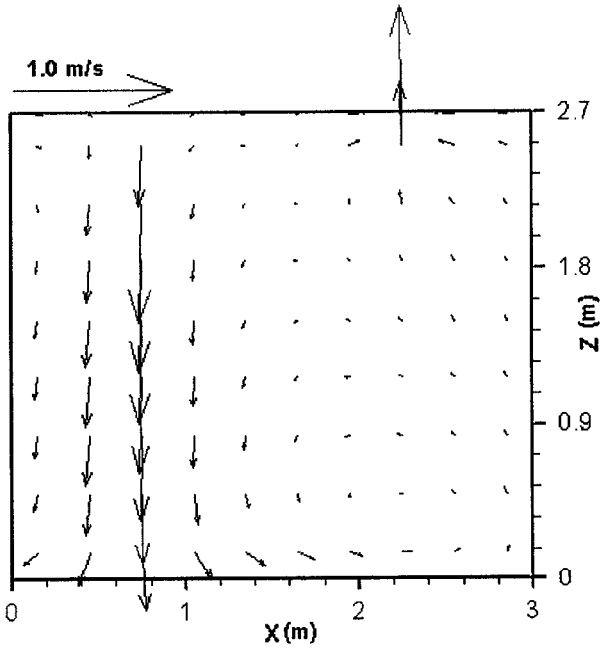

Figure 6-35 Air flow pattern predicted by FLOVENT for case 4 (Y=1.5m) (Jiang, 2002)

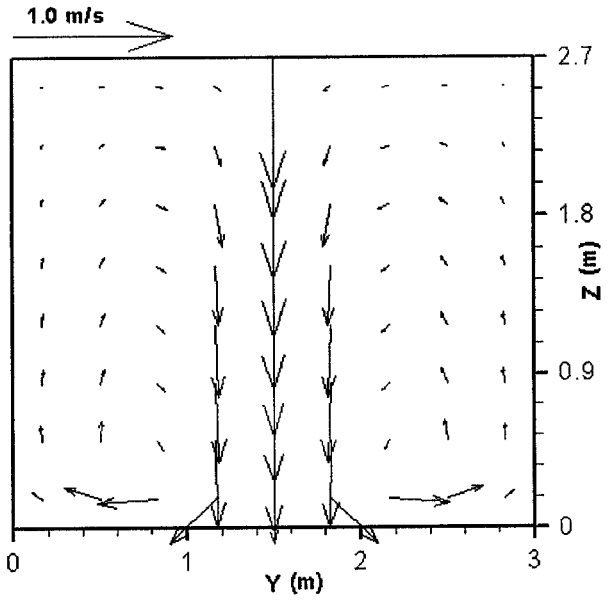

Figure 6-36 Air flow pattern predicted by the Integrated Zonal Model for case 4 (X=0.75m)

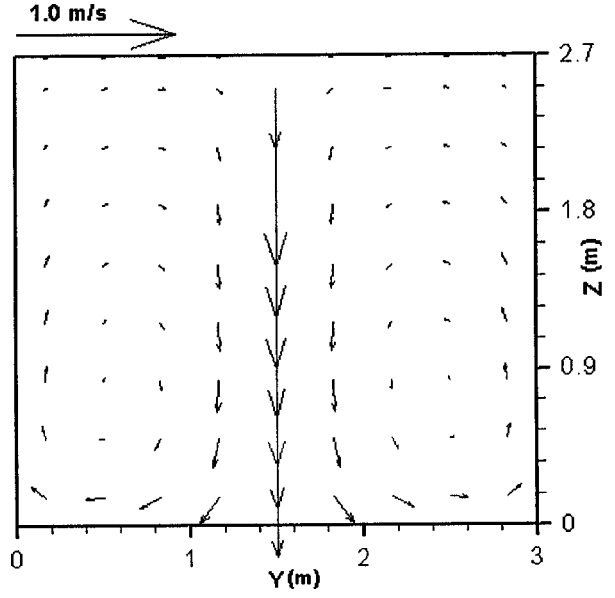

Figure 6-37 Air flow pattern predicted by FLOVENT for case 4 (X=0.75m) (Jiang, 2002)

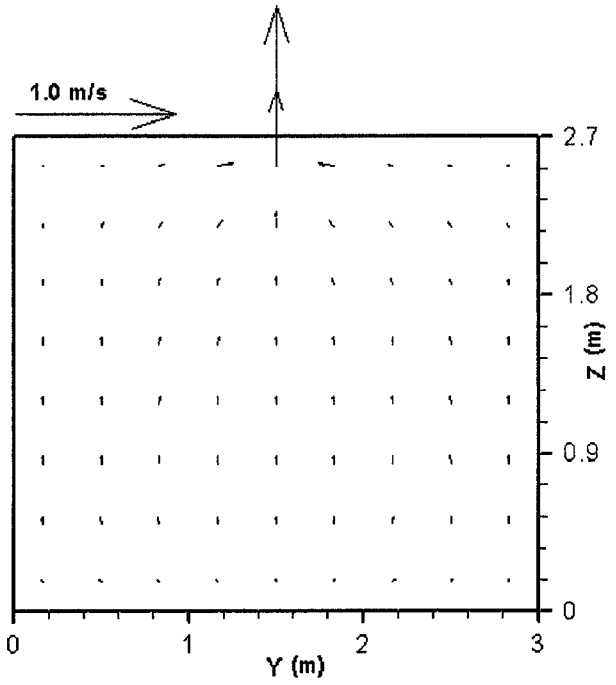

Figure 6-38 Air flow pattern predicted by the Integrated Zonal Model for case 4 (X=2.25m)

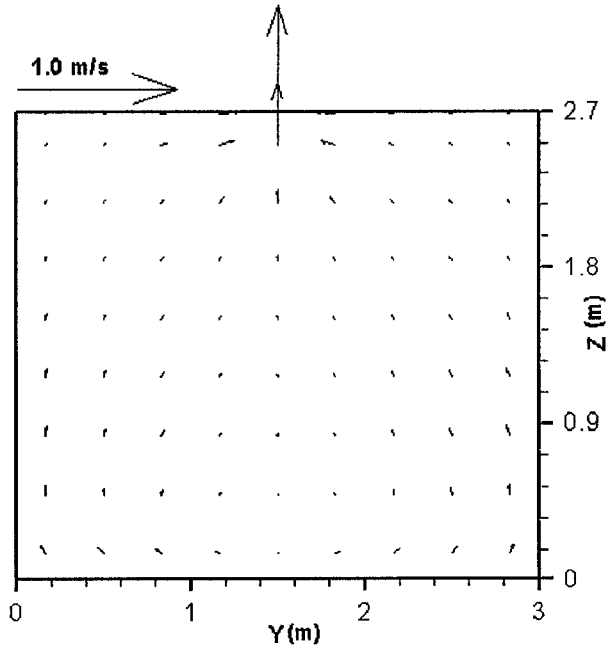

Figure 6-39 Air flow pattern predicted by FLOVENT for case 4 (X=2.25m) (Jiang, 2002)

For VOC distribution prediction, we considered that other materials may adsorb some VOC emitted from one material. VOC emitted from source materials and VOC adsorbed by sink materials affect indoor air quality synchronically. To simulate this scenario, we assumed that the vinyl floor tile as the source material and the plywood walls as the sink materials. Toluene was chosen as the compound of interest, since toluene is one of the VOC compounds in the vinyl floor tile and is not founded in the plywood. The properties of the toluene in vinyl floor tile and plywood were obtained from literature (Plett, et al., 2001), they are listed in Table 6-4.

Table 6-4 Properties of toluene in the plywood and vinyl floor tile

Parameters	C_0	D_m	k	b
(unit)	($\mu g/m^3$)	(m^2/s)	(—)	(m)
Plywood	0	1.75×10^{-10}	358	0.016
Vinyl floor tile	1.0×10^{7}	5.42×10^{-10}	539	0.003

Toluene concentration distributions in the middle section of the room (Y=1.5m) and at the height of a seated person occupied zone (Z=1.18m) are graphically displayed in Figures 6-40, 6-41, 6-42 and 6-43 after plywood walls and vinyl floor tile floor were exposed to the air for 12 hours and 24 hours. Toluene concentration around jet centerline region was much lower than the other regions due to the fresh air directly coming down from the jet (we assumed that there was no VOC in supply air). Compared with the average toluene concentration in the room air (8.3 $\mu g/m^3$ at 12h, 0.33$\mu g/m^3$ at 24 h), as shown in Figure 6-44, except in the near east wall region, toluene concentration at the height of a seated person was lower than the average concentration, which indicated that

this air distribution system could provide good air supply in most area and it was efficient in removing the contaminant from the room.

Figure 6-45 shows the comparison of toluene sink rates of the west, east, south and north walls. Initially, the east wall had the highest toluene sink rate among all the walls. However, the velocity along the east wall was the lowest. This is because the lowest air velocity cannot effectively dilute the toluene. Therefore, the toluene concentration along the east wall was much higher than toluene concentration along the other walls, which leaded to the highest sink rate on the east wall. A similar phenomenon was observed on the west wall, which had the highest air velocity along the surface hence caused the lowest sink rate. The south wall and the north wall had the same toluene sink rate due to the symmetry of the air flow. Figure 6-45 also shows, as time progressed, the sink rates of all the walls decreased as the room air toluene concentration decreased and eventually reached zero. From this moment, the plywood walls acted as a source of toluene and started emitting rather than adsorbing.

Figure 6-46 shows the toluene emission rate of the floor. The emission rate was initially very high and decayed very fast as time passed.

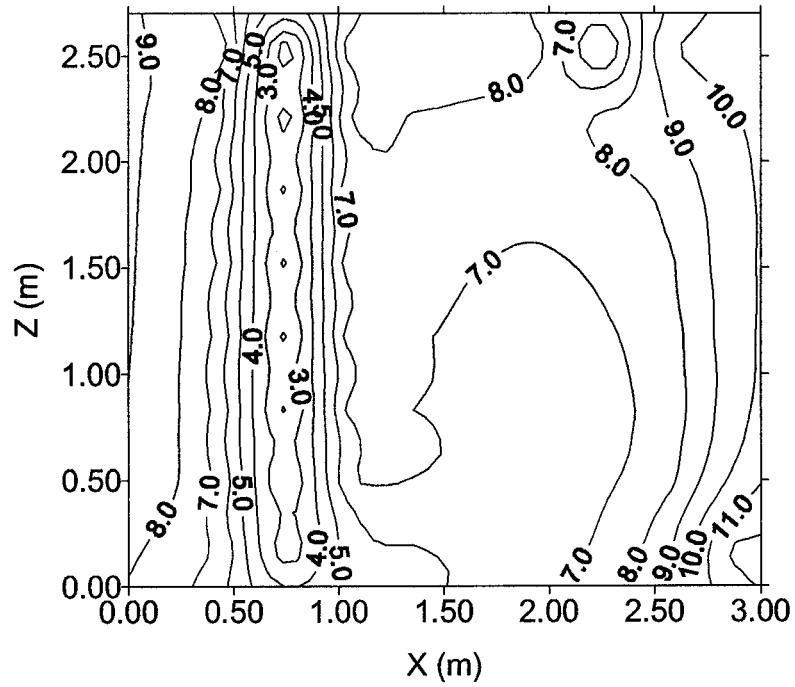

Figure 6-40 Toluene concentration distribution after 12 hours for case 4 (Y=1.5m)

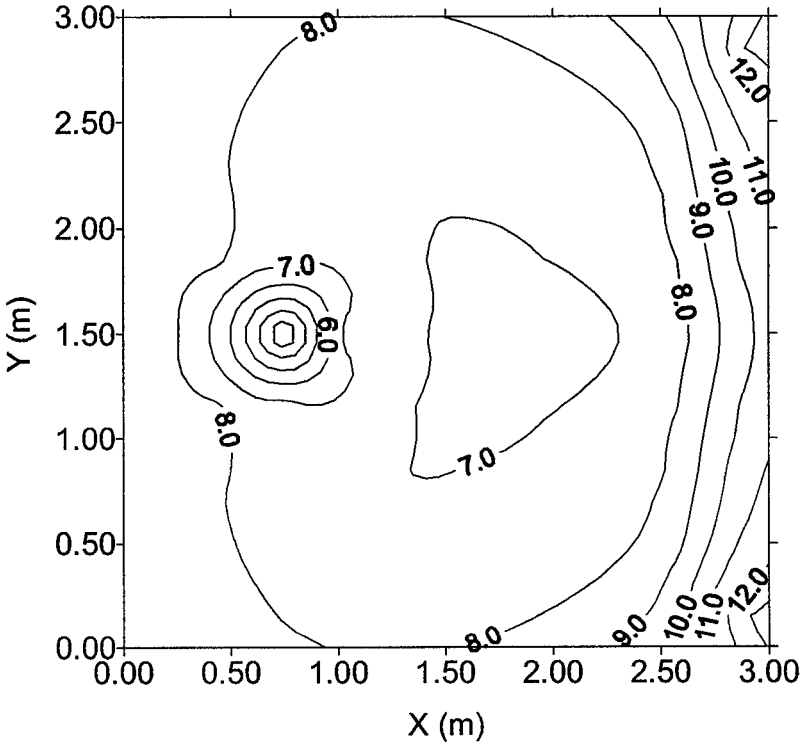

Figure 6-41 Toluene concentration distribution after 12 hours for case 4 (Z=1.18m)

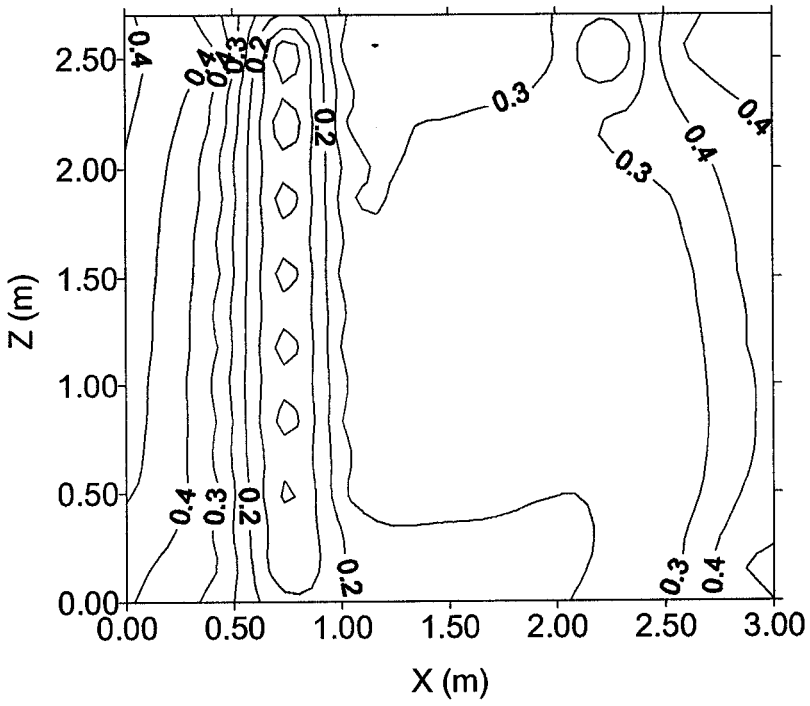

Figure 6-42 Toluene concentration distribution after 24 hours for case 4 (Y=1.5m)

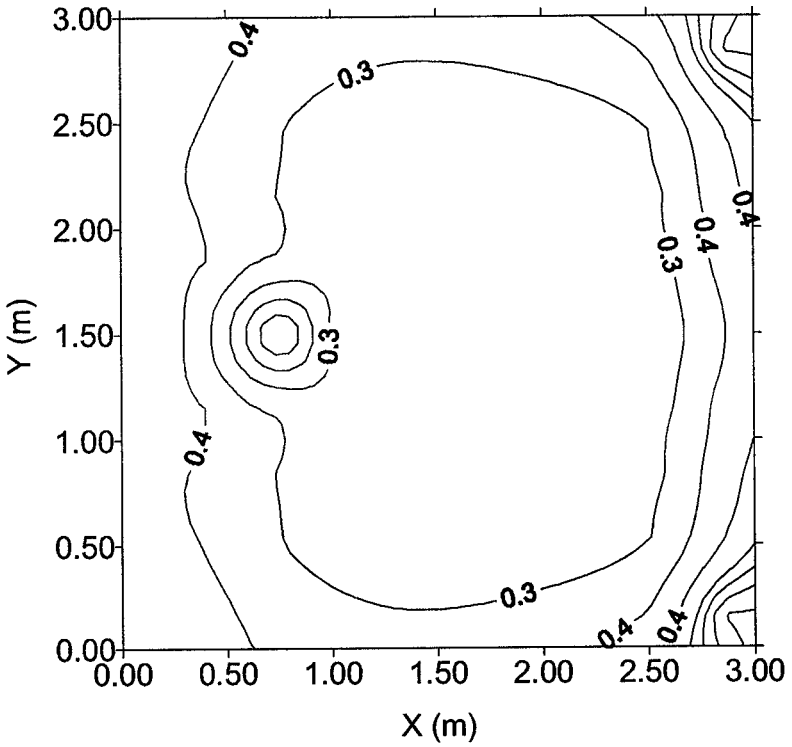

Figure 6-43 Toluene concentration distribution after 12 hours for case 4 (Z=1.18m)

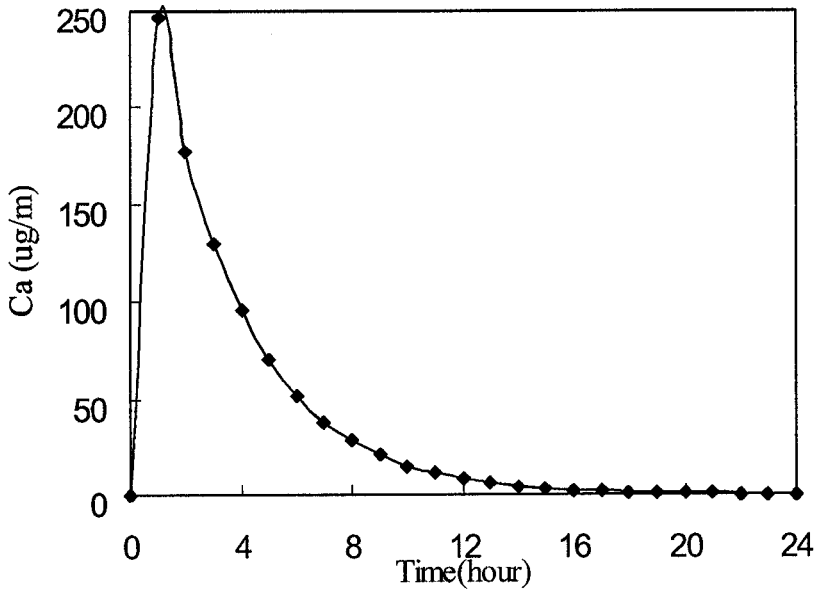

Figure 6-44 Average toluene concentration in air for case 4

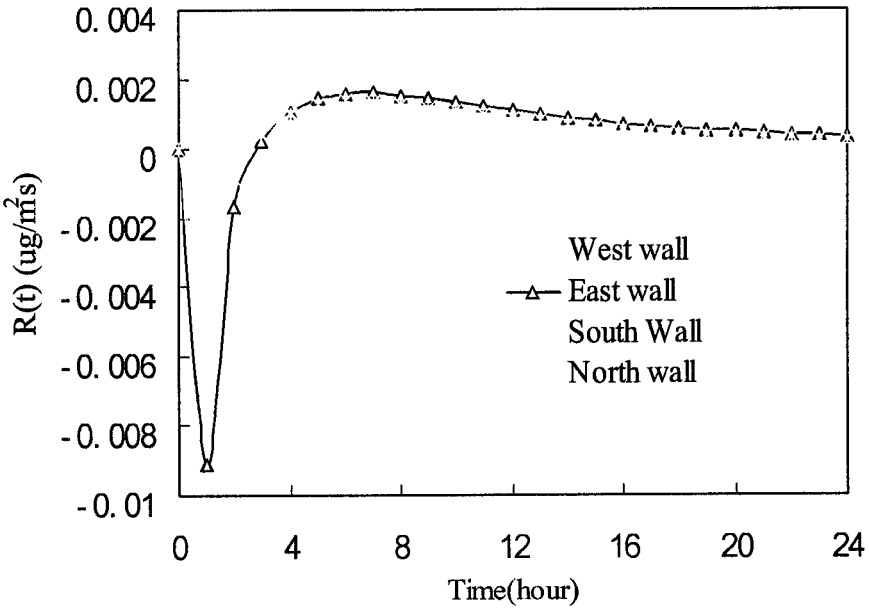

Figure 6-45 Average toluene sink rates of walls for case 4

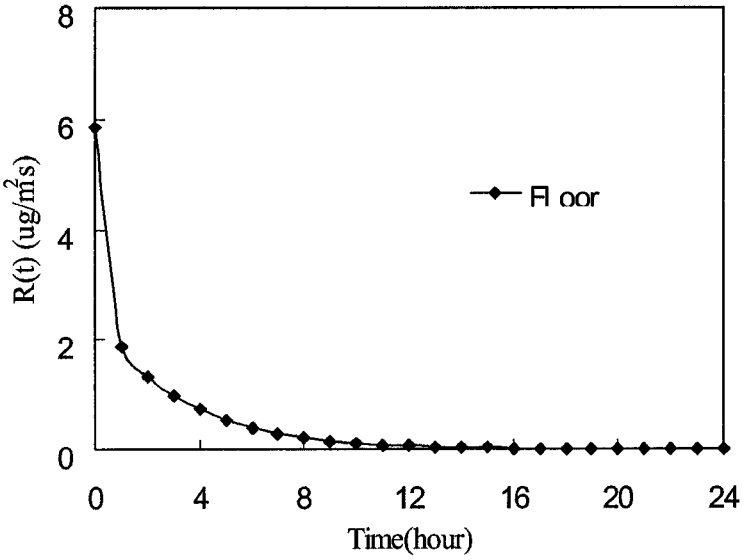

Figure 6-46 Average toluene emission rate of the floor for case 4

6.7 SUMMARY

An Integrated Zonal Model was developed to predict the three-dimensional air velocity profile, temperature distribution and VOC concentration distribution in a ventilated room. This model integrated a zonal model with a thermal model, a liner jet model, a compact jet model and a material VOC emission/sink model.

This Integrated Zonal Model was first applied to a naturally ventilated room to simulate the air flow pattern and temperature distribution. The room was at a non-isothermal condition with its floor as the VOC source material. The simulation results were compared with that of the POMA model, the CFD model and the experimental results. It was found that the Integrated Zonal Model could give a good prediction of the air flow pattern and the temperature distribution. Moreover, the model was applied to simulate

VOC distribution in the room. It was found that the VOC distribution was not uniform in space at beginning and gradually reached steady state, in which the VOC concentration became uniform.

The Integrated Zonal Model was also applied to a naturally and mechanically ventilated room to predict VOC distribution. The room was at a non-isothermal condition with different ventilation layouts. The floor was acting as the VOC source. It was found that the VOC concentration was not uniform in space and was influenced by the characteristics of the room. The average VOC concentration predicted by the Integrated Zonal Model was compared with that of the total mixing model. The prediction of average nonane concentration was slightly higher for the total mixing model than that for the Integrated Zonal Model in both ventilation layouts. Moreover, it was found that the Integrated Zonal Model was a practical tool for long-term VOC distribution prediction.

The air flow pattern and the VOC distribution of a room with a two-dimensional liner jet on the top of west wall and an outlet on the bottom of east wall were simulated by this Integrated Zonal Model. The room was at an isothermal condition with all its walls and floor acting as the VOC source materials. The air flow pattern predicted by the Integrated Zonal Model was compared with that of FLOVENT. Similar air flow patterns were detected in both models. Moreover, it was found that in most occupied zones, the VOC concentration was higher than room average VOC concentration: that indicated this ventilation strategy could not provide good air supply and effectively remove

contaminates. Furthermore, it was found that air velocity affected VOC emission only in short term when VOC concentration at material surface was relatively high.

Finally, a room with a three-dimensional compact jet and an outlet on ceiling and with its walls acting as the VOC sink materials and its floor acting as the VOC source material was simulated by this Integrated Zonal Model. The air flow pattern predicted by the Integrated Zonal Model was compared with that of FLOVENT. Globally, similar air flow patterns can be achieved in both models. For VOC concentration distribution prediction, it was found that the VOC concentration in occupied zone was lower than the room air average VOC concentration, which indicated the good efficiency of this ventilation strategy. Moreover, the sink rates of all the walls and the emission rate of the floor were also simulated by this model. It was found that for the sink material, over which the velocity was lower, had higher sink rate due to the higher VOC concentration over the material surface. Simulation results also demonstrated how a sink material could act as a source when the room air VOC concentration decreased.

Overall, the Integrated Zonal Model, with quite coarse mesh, can provide sufficiently reliable results and some global information regarding the air flow pattern, thermal and VOC distributions within a room. It is a feasible approach for long-term building material VOC emission and VOC distribution analysis from an engineering viewpoint.

CHAPTER 7 CONCLUSIONS AND RECOMMENDATIONS

7.1 CONCLUSIONS

7.1.1 Single-layer material emission model

A numerical and an analytical model were developed to predict VOC emission rates of single-layer dry building materials. These two models were based on the assumption that VOC was well mixed in the room. Both models considered the mass diffusion process within the material and the mass convection and diffusion processes in the boundary layer. The models used four parameters: the diffusion coefficient of the material (D_m); the material/air partition coefficient (k); the initial concentration of the material (C_0); and the mass transfer coefficient in the air (h_m). The first three parameters are the properties of the material and can be determined by experiments. The last parameter, h_m, can be estimated using the fundamentals of fluid dynamics.

The predictions of the models were validated at two levels: inter-model validation, and validation with the experimental results from the specially designed test and with the predictions made by a CFD model. The comparison between the numerical model and the analytical model under the same initial and boundary conditions showed that the numerical model could give as good results as the analytical model. The comparisons with the experimental results and with the predictions of the CFD model indicated that

there was generally good agreement between the proposed model predictions, the experimental results, and the CFD model results.

In addition, it was found that the VOC concentration in the material; the VOC emission rate and the VOC concentration in the air were linearly proportional to the initial VOC concentration in the material. However, the normalized emitted mass was not a function of the initial VOC concentration, but was a function of the properties of the VOC and material.

7.1.2 Parametric study

Through a four-factor simulation design and statistical analysis, a parametric study was carried out to analyze four parameters, namely VOC diffusion coefficient of the material (D_m), VOC partition coefficient (k), material thickness (H), and surface air velocity (v), and their interaction effects on VOC emissions from building materials. Simulations were carried out using the developed single-layer material emission model. The parameter effects and their interaction effects were discussed in terms of Omega Squared (ω^2). The statistical analysis involving the comparison of ω^2 of the four parameters and their interactions indicated that two parameters, D_m and H, and their interaction, $D_m \times H$, significantly affected the material VOC time. Other parameters (k, v) and interactions ($D_m \times k$, $D_m \times v$, $k \times H$, $k \times v$, $H \times v$, $D_m \times k \times H$, $D_m \times k \times v$, $D_m \times H \times v$, $k \times H \times v$, $D_m \times k \times H \times v$) had minor effects on the material VOC time. Further statistical analysis of the marginal mean values of the material VOC time for the three significant effects showed that: 1) The material VOC time decreased rapidly as the diffusion coefficient increased. 2) The

material VOC time increased significantly as the material thickness increased. 3) There was a clear interaction between the diffusion coefficient and the material thickness. As the material thickness increased, the material VOC time increase rate was smaller at the high diffusion coefficients than at the low diffusion coefficients.

7.1.3 Integrated IAQ model

An integrated IAQ model was developed to predict the VOC emission rates of a multi-layer material, the VOC sink rates of a material, the VOC concentrations in a room with both VOC source and sink materials, and VOC concentration distribution within a material. The predictions of the model were validated with the experimental results of VOC emissions from a carpet-adhesive assembly. The results indicated that there was generally good agreement between the model predictions and the experimental results.

The model was first applied to a room with a typical floor assembly (vinyl floor tile/glue/plywood) to study the multi-layer material VOC emissions. Results indicated that the multi-layer material first showed the same emission characteristics as the top layer material, and the top layer material strongly delayed VOC emission from the bottom layer material. The multi-layer material had a much longer VOC emission time and slower VOC decay rate than the single-layer material. The model was further applied to a room with a floor assembly (vinyl floor tile/glue/plywood) as the source material and with plywood walls as the sink materials. Results showed that the plywood substrate in the floor assembly significantly affected the VOC emission rate from the floor assembly. Results also showed that the plywood wall sink effect reduced the VOC concentration in the room air initially and elevated it as the time progressed. However, the plywood sink

impact on the VOC emission rate and the room air VOC concentration was not significant.

7.1.4 Integrated Zonal Model

To take air movement effect into IAQ model and predict VOC distribution in a room, a zonal model was integrated with an air jet model and an material emission/sink model. The Integrated Zonal Model bridged the gap between the simple single-zone total mixing model and the excessively complicated CFD model. This integrated zonal model was developed based on the conservation of air mass, energy and VOC mass. The Integrated Zonal Model can be used to predict the three-dimensional air velocity profile, temperature distribution and VOC concentration distribution in a ventilated room.

This Integrated Zonal Model was applied to a naturally or mechanically ventilated room to simulate air flow pattern, temperature and VOC concentration distributions. Results were compared either with measured data or with predictions made by the CFD model. It was found that the Integrated Zonal Model, with quite coarse mesh, could provide sufficiently reliable results and some global information regarding air flow pattern, thermal and VOC distributions within a room. It could be used to examine the impact of an air distribution system on the contaminant distribution within a room, and to analyze building material emission and sink behaviors. Furthermore, it was found that the Integrated Zonal Model was a feasible approach for building material VOC emission/sink and VOC distribution analysis for the viewpoint of engineering.

7.2 RECOMMENDATIONS

Mathematical models for prediction of VOC emissions/sinks from building materials require material properties and environmental parameters as input, such as diffusion coefficient, material/air partition coefficient, initial VOC concentration, air velocity, temperature et. The environmental parameters usually can be easily obtained through measurement. However, measuring material properties for different VOC are very expensive and time consuming, especially for dry building materials. Currently, only limited data of material properties are available hence limiting the model applications. Therefore, establishing a material property database and finding correlations between chemical and physical properties are critical issues in modeling building material VOC emission/sink behaviors.

Currently, the Integrated Zonal Model can only be used to predict VOC distribution in a single room with a rectangle shape. The next challenging work will be applying the Integrated Zonal Model to a complex geometry room and then to a whole building, and integrating the model with an existing building thermal analysis program, such as Esp-r, COMIS or CONTAM.

REFERENCES

- Allen III MB, Behie GA, and Trangenstein JA (1988), *Multiphase Flow in Porous Media*, New York, Berlin: Springer-Verlag.

- *ASHRAE Handbook of Fundamentals* (2001), chapter 32, 'Space air diffusion', Atlanta, U.S.A: American Society of Heating, Refrigerating and Air Conditioning Engineers, Inc.

- Axley J W (1991), 'Adsorption modeling for building contaminant dispersal analysis', *Indoor Air*, Vol. 2, p147-171.

- Axley JW (2001), 'Surface-drag flow relations for zonal modeling', *Building and Environment*, 36, p843-850.

- Bear J and Bachmat Y (1990), *Introduction to Modeling of Transport Phenomena in Porous Media*, Dordrecht, Boston : Kluwer Academic Publishers.

- Brezinski J (1989), *Manual on Determination of Volatile Organic Compounds in Paints, Inks and Related Coating Products*, MNL 4, ASTM Manual Series, American Society of Testing and Materials, Philadelphia.

- Berglund B (1985), 'Measurement of formaldehyde odor indoor', *Proceeding of the climate 2000 World Congress on Heating Ventilation, and Air Conditioning*, Copenhagen, VVS Kongres, Vol. 4, p 251-256.

- Black MS, Pearson WJ and Work LM (1991), 'A methodology for determining VOC emissions from new SBR latex-backed carpet, adhesive, cushions, and installed systems and predicting their impact on indoor air quality', *IAQ 91, Healthy Buildings*, p267-272, Atlanta, USA.

- Black MS, Work LM, Worthan AG and Pearson WJ (1993), 'Measuring the TVOC contributions of carpet using environmental chambers', *Indoor Air*

'93, 6th Int. Conf. on Indoor Air Quality and Climate, Vol. 2, p401-405, Helsinki, Finland.

- Bodalal A, Zhang JS and Plett EG (2000) 'A method for measuring internal diffusion and equilibrium partition coefficients of volatile organic compounds for building materials', *Building and Environment*, 35(2): p101-110.

- Bodalal A (1999), *Fundamental Mass Transfer Modeling of Emission of Volatile Organic Compounds from Building Materials*, PhD thesis, Carlton University, Canada.

- Brown SK (1999), 'Chamber assessment of formaldehyde and VOC emissions from wood –abased panels', *Indoor Air*, p209-215.

- Chang JCS and Guo Z (1994), 'Modeling of alkane emission from a wood stain', *Indoor Air*, Vol. 4, p35-39.

- Chang JCS and Guo Z (1992), 'Characterization of organic emission from a wood finishing product-wood stain', *Indoor Air*, Vol. 2, p146-153.

- Cohen J (1977), *Statistical Power Analysis for the Behavior Sciences*, New York: Academic Press.

- Colombo A, De Bortoli M, Pecchio E, Schauenburg H, Schlitt H and Vissers H (1990), 'Chamber testing of organic emission from building and furnishing materials', *The Science of the Total Environment*, 91, p237-249.

- Colombo A, De Bortoli M and Tichenor BA (1993), 'Adsorption of Selected Volatile Organic Compounds on a Carpet, a Wall Coating, and a Gypsum Board in a Test Chamber', *Indoor Air,* Vol. 3, p276-282.

- Colombo A and De Bortoli M (1991), 'Small chamber tests and headspace analysis of volatile organic compounds emitted from household products', *Indoor Air*, Vol. 1, p13-21.

- Colombo A and De Bortoli M (1992), 'Comparison of models used to estimate parameters of organic emissions from materials tested in small environmental chambers', *Indoor Air,* Vol. 2, p49-57.

- Cox SS, Little JC and Hodgson AT (2000), 'A new method to predict emission rates of volatile compounds from vinyl flooring', *Proceeding of Healthy Building 2000*, Vol. 4, p169-174.

- Cox SS, Hodgson AT and Little JC (2002), 'Effect of ventilation rate on contaminant emission rates from diffusion-controlled materials', *Proceedings: 9th International Conference on Indoor Air Quality and Climate*, Monterey, California, Vol. 3, p196-201.

- Dunn JE (1987), 'Models and statistical methods for gaseous emission testing of finite sources in well-mixed chambers' *Atmospheric Environment*, Vol. 21(2), p425-430.

- Guo Z, Fortman R, Marfiak S, Tichenor B, Sparks L, Chang J and Mason M (1996), 'Modeling the VOC emissions from interior latex paint applied to gypsum board" *Proceeding of indoor air 96*, Nagoya, 7th international conference on indoor air quality and climate, Vol. 1, p 987-991.

- Haghighat F and De Bellis L (1998), 'Material emission rates: literature review, and the impact of indoor air temperature and relative humidity', *Building and Environment*, Vol. 33(5), p 261-277.

- Haghighat F, Lee CS and Ghaly WS (2002), 'Measurement of diffusion coefficients of VOCs for building materials: review and development of a calculation procedure', *Indoor air*, 12, p81-91.

- Haghighat F, Lin Y and Megri AC (2001), 'Development and validation of a zonal model-POMA', *Building and Environment*, Vol. 36, p1039-1047.

- Haghighat F and Zhang Y (1999), 'Modeling of emission of volatile organic compounds from building materials-estimation of gas-phase mass transfer coefficient', *Building and Environment*, Vol. 34, p 377-389.

- Haghighat F, Jiang Z and Zhang Y (1994), 'The impact of ventilation rate and partition layout on the VOC emission rate: time dependent contaminant removal', *Indoor Air*, Vol. 4, 276-283.

- Hansson P and Stymne H (1999), 'On the sink effect of VOCs on indoor materials-- consequences of repeated adsorption', *Proceeding of the 8th International Conference on Indoor Air Quality and Climate,* Vol. 5, p223-228.

- Hansson P and Stymne H (2002), 'VOC sorption of activity related contaminants-influence of boundary layer diffusion', *Proceedings: 9th International Conference on Indoor Air Quality and Climate*, Monterey, California, Vol. 3, p546-551.

- Hansson P (2000), 'VOC diffusion and absorption properties of indoor materials-consequences for indoor air quality', *Proceeding of Healthy Building 2000*, Vol. 4, p 151-155.

- Holmberg B (1977), *Some ideas on chemically induced cancer, from a toxicologic view*, Swedish Board of Occupational Health, report 1977:37.

- Huang H and Haghighat F (2002), 'Modeling of volatile organic compounds emission from dry building materials', *Building and Environment*, Vol. 37, p1127-1138.

- Inard C, Bouia H and Dalicieux P (1996), 'Prediction of air temperature distribution in buildings with a zonal model' *Energy and Building*, Vol. 24, p125-132.

- ITS (1996), *Residential indoor air quality-A guide to understanding*, Information Technology Specialists Inc.

- Jiang Z (1998), private communication.
- Jiang Z (2002), 'FLOVENT', Flomerics Inc.
- Jorgensen RB, Dokka TH and Bjorseth O (2000), 'Introduction of a sink – diffusion model to describe the interaction between Volatile Organic Compounds (VOCs) and Material Surfaces', *Indoor Air*, Vol. 10, p27-38.
- Keppel G (1991), *Design and Analysis: a Researcher's Handbook*, Prentice-Hall, Inc.
- Kumar D and Little JC (2002), 'Barriers to reduce emission rates from diffusion-controlled materials', *Proceedings: 9th International Conference on Indoor Air Quality and Climate*, Monterey, California, Vol. 3, p570-575.
- Layman WJ (1982), *Handbook of Chemical Property Estimation Methods*, New York.
- Lee CS, Ghaly W and Haghighat F (2000), 'VOC emission from diffusion controlled building material: analogy with conjugate heat transfer', *Proceeding of Healthy Building 2000,* Espoo, Finland; SIY Indoor Air Information Oy, Helsinki, Finland; Vol. 4: p163-168.
- Lee CS, Haghighat F and Ghaly W (2002), 'Modeling the VOC emissions of solid/wet building material assembly and its assessment', *Proceedings: 9th International Conference on Indoor Air Quality and Climate*, Monterey, California, Vol. 3, p238-243.
- Little JC, Hodgson AT and Gadgil A (1994), 'Modeling emissions of volatile organic compounds from new carpets', *Atmospheric Environment,* Vol. 28(2), p27-234.
- Little JC and Hodgson AT (1996), 'A Strategy for Characterizing Homogeneous, Diffusion-Controlled, Indoor Source and Sinks', *ASTM STP 1287*, p294-304.

- Low JM, Zhang JS, Plett EG and Shaw CY (1998), 'Effects of air flow on emissions of volatile organic compounds from carpet adhesive assemblies', *ASHRAE Transactions*; 104, part 2: 1281-1283.

- Masel RI (1996), *Principles of Adsorption and Reaction on Solid Surfaces,* John Wiley & Sons, Inc.

- De Bortoli M, Knoppel H, Columbo A and Kefalopoulos S (1996), 'Attemption to characterize the sink effect in a small stainless steel test chamber', *ASTM STP 1287*, p307-320.

- Mendonca KC, Inard C, Wurtz E, Winkelmann FC and Allard F (2002), ' A zonal model for predicting simultaneous heat and moisture transfer in buildings', *Proceedings: 9th International Conference on Indoor Air Quality and Climate*, Monterey, California, Vol. 4, p518-523.

- Molina JL, Musy M, Blondeau P and Blanco A (2000), 'Modeling the IAQ of single zone buildings taking into account air movement and sorption effects', *Proceeding of Healthy Building 2000*, Vol.4, p139-144.

- Montgomery DC (1976), *Design and Analysis of Experiments*, John Wiley and Sons, Inc. Canada.

- Murakami S, Kato S, Kondo Y, Ito K, and Yamamoto A (2000), 'VOC distribution in a room based on CFD simulation coupled with emission/ sorption analysis', *Proceedings of the 7th International Conference on Air Distribution in Rooms;* Reading, UK; Elsevier Science Ltd.; Vol.1, p473-478.

- Murakami S, Kato S and Ito K (1998), 'Coupled analysis of TVOC emission and diffusion in a ventilated room by CFD', 2nd European Conference on Energy Performance and Indoor Climate in Buildings and 3rd International Conference on Indoor Air Quality, Ventilation and Energy Conservation in Buildings. *EPIC'98*, Vol.1, p19-26. France, Lyon.

- Musy M, Wurtz E, Winkelmann F and Allard F (2001), 'Generation of a zonal model to simulate natural convection in a room with a radiative/ convective heater' *Building and Environment*, Vol 36, p589-596.

- Pantankar SV (1980), *Numerical heat transfer and fluid flow*, McGraw-Hill Book Company, p64-68.

- Pliel J and Whiton R (1990), 'Determination of organic emissions from new carpeting', *Applications of Occupational Environmental Hygiene*, Vol.5(10), p693-699.

- Press WH (1992), *Numerical Recipes in FORTRAN 90*, Cambridge (England); New York, NY, USA: Cambridge University Press.

- Plett EG, Bodalal A and Zhang JS (2001), 'Internal diffusion of volatile organic compounds in building materials', *Proceedings of the 4th international conference on Indoor Air Quality, Ventilation and Energy Conservation In Buildings*, Changsha, China. Vol. 1, p357-365.

- Rafson HJ (1998), *Odor and VOC control handbook*, McGraw-Hill.

- Ruthven DM (1984), *Principles of Adsorption and Absorption Processes*, John Wiley & Sons.

- Rutman E, Inard C, Bailly A and Allard F (2002), ' Prediction of global comfort in air conditioned building with a zonal model', *Proceedings: 9th International Conference on Indoor Air Quality and Climate*, Monterey, California, Vol. 3, p724-729.

- Spalding DB (1972), 'A novel finite-difference formulation for differential expression involving both first and second derivatives', *Int. J. Num. Methods Eng.*, Vol.4, p.551

- Sparks LE, Tichenor BA, Chang JCS and Guo Z (1996), 'Gas-phase mass transfer model for predicting volatile organic compound emission rates from indoor pollutant sources', *Indoor Air*, Vol.6, p31-40.

- Sparks LE, Guo Z, Chang JCS and Tichenor BA (2000[a]), 'Volatile organic compound emissions from latex paint- part2. Test house studies and indoor air quality (IAQ) modeling', *Indoor Air,* Vol.9, p18-25.

- Sparks LE, Guo, Z, Chang JCS and Tichenor BA (2000[b]), 'Volatile organic compound emissions from latex paint- part1. Chamber experiments and source model development' *Indoor Air,* Vol. 9, p10-17.

- Tichenor BA (1995), 'Evaluation of emissions from latex paint', *low and No-VOC Coating Technologies 2nd Biennial International Conference*, March 13-15, Duham, NC.

- Tichenor BA (1996) 'Overview of source/sink characterization methods', *ASTM STP1287*, p9-19.

- Tichenor BA and Sparks LE (1996), 'Managing exposure to indoor air pollutants in residential and office environment', *Indoor Air*, p259-270.

- Tichenor BA, Guo Z and Sparks LE (1993), 'Fundamental mass transfer model for indoor air emissions from surface coatings', *Indoor Air*, Vol.3, 263-268.

- Tichenor BA and Guo Z (1991), 'The effect of ventilation on emission rates of wood finishing materials', *Environment International,* Vol.17, p317-323.

- Tichenor BA, Guo Z, Dunn JE, Sparks LE and Mason MA (1991), 'The Interaction of vapor phase organic compounds with indoor sink', *Indoor Air,* Vol.1, p23-35.

- Tiffonnet AL (2000), *Contribution à l'analyse de la qualité de l'air intérieur-Influence des transports de composés organiques volatils (COV) entre les*

parois et l'ambiance, Thése de doctorat: Université de La Rochelle, 2000. 300p.

- Tiffonnet AL, Blondeau P and Allard F (2000), 'Adsorption isotherms of acetone on building materials', *Proceedings of Healthy Buildings 2000*, Vol.4, p205-210.

- Tiffonnet AL, Blondeau P and Allard F (1998), 'Experimental characterization of sorption phenomena of VOCs on building materials' *Proceeding of EPIC'98,* Vol.1, p13-18.

- Van Der Wal JF, Hoogeveen AW and Van Leeuwen L (1998), 'A Quick Screening Method for Sorption Effects of Volatile Organic Compounds on Indoor Materials', *Indoor Air*, Vol. 8, p103-112.

- White FM (1988), *Heat and Mass Transfer*, Addison Wesley Series Publishing Company, Inc.

- Wurtz E, Musy M and Mora L (1999[a]), ' Introduction of specific law in zonal model to describe temperature fields and air flow patterns in ventilated buildings', *Journal of Human- Environment System*, Vol. 3(1), p43-59.

- Wurtz E, Nataf J-M and Winkelmann F (1999[b]), 'Two and three dimensional natural and mixed convection simulation using zonal models in buildings', *International Journal of Heat and Mass Transfer*, Vol. 40, p923-940.

- Yang X and Chen Q (2001[a]), 'A coupled air flow and source/sink model for simulating indoor VOC exposures', *Indoor Air*, Vol.11, p257-269.

- Yang X, Chen Q, Zeng J, Zhang JS, Nong G and Shaw CY (2001[b]), 'Effects of air flow on VOC emission from wet coating materials: experimental measurements and numerical simulation', *ASHRAE Transaction*, 107(1), p801-811.

- Yang X, Chen Q, Zeng J, Zhang JS and Shaw CY (2001[c]), 'A mass transfer model for simulating volatile organic compound emissions from 'wet' coating materials applied to absorptive substrates', *Internal Journal of Heat and Mass Transfer,* p1803-1815.

- Yang X, Chen Q, Zhang JS, Magee R, Zeng J, Shaw CY. (2001[d]), 'Numerical simulation of VOC emission from dry materials', *Building and Environment,* Vol. 36(10): 1099-1107.

- Yang X, Chen Q and Bluyssen PM (1998[a]), 'Prediction of short term and long term VOC emission from SBR bitumen backed carpet under different temperature', *ASHRAE Transactions*, p1297-1308.

- Yang X, Chen Q and Zhang JS (1998[b]), 'Impact of early stage incomplete mixing on estimating emission in small test chambers', *Indoor Air*, Vol. 8, p180-189.

- Yang X, Chen Q, Zhang JS, An Y, Zeng J and Shaw CY (2001[e]), 'Mass transfer model for simulating VOC sorption on building materials', *Atmospheric Environment*, Vol. 35 (7), p1291-1299.

- Yu C, Crump D and Squire R (1997), 'The indoor air concentration and the emission of VOCs and formaldehyde from materials installed in BRE low energy test house', *Indoor and Building Environment*, Vol. 6, p45-55.

- Yu C and Crump D (1998), 'A review of the emission of VOCs from polymeric materials used in buildings', *Building and Environment*, p357-374.

- Zhang Y and Haghighat F (1997), 'The Impact of Surface Air Movement on Material Emissions', *Building and Environment,* Vol. 32(6), p551-556.

- Zhang Y (1996), *A study of the mechanisms of contaminant emissions from building materials*, Ph.D. thesis, Concordia University, Canada

- Zhang JS, Kanabus-Kaminska JM, Shaw CY (1996), 'Full-scale test chamber for material emission studies and indoor air quality modeling', *ASTM Special Technical Publication*, n1287, p58-66.

- Zhang JS, Herrmann TJ, Zhang Z and Noble K (2002), 'Development of a unique ultra-clean full scale thermal and air quality research facility', *Proceedings: 9th International Conference on Indoor Air Quality and Climate*, Monterey, California, Vol. 3, p184-189.

- Zhang J, Zhang JS, Chen Q and Yang X (2000), 'A critical review on VOC sorption models' *Proceeding of Healthy Building 2000*, Vol. 4, p 187-192.

- Zhao DY, Rouques J, Little JC, and Hodgson AT (1999) 'Effect of reversible, diffusion-controlled sinks on VOC concentrations in buildings', *Proceeding of the 8th International Conference on Indoor Air Quality and Climate*, Vol. 5, p264-269.

- Zhao DY, Cox SS and Little JC (1999), 'Source/ sink characterization of diffusion controlled building materials', *Proceeding of 8th international conference on indoor air quality and climate,* Vol 1, p408-413.